แบบจำลองอย่างง่ายสำหรับประมาณค่ามิวชวลคัปปลิงในสายอากาศแถวลำดับ

นายมางเสียง ฮอ

วิทยานิพนธ์นี้เป็นส่วนหนึ่งของการศึกษาตามหลักสูตรปริญญาวิศวกรรมศาสตรมหาบัณฑิต
สาขาวิชาวิศวกรรมไฟฟ้า ภาควิชาวิศวกรรมไฟฟ้า
คณะวิศวกรรมศาสตร์ จุฬาลงกรณ์มหาวิทยาลัย
ปีการศึกษา 2559

SIMPLE MODEL FOR APPROXIMATION OF MUTUAL COUPLING IN MICROSTRIP PATCH ARRAY

Mr. Mangseang Hor

A Thesis Submitted in Partial Fulfillment of the Requirements

for the Degree of Master of Engineering Program in Electrical Engineering

Department of Electrical Engineering

Faculty of Engineering

Chulalongkorn University

Academic Year 2016

Thesis Title	SIMPLE MODEL FOR APPROXIMATION OF MUTUAL COUPLING IN MICROSTRIP PATCH ARRAY
By	Mr. Mangseang Hor
Field of Study	Electrical Engineering
Thesis Advisor	Panuwat Janpugdee, Ph.D.

Accepted by the Faculty of Engineering, Chulalongkorn University in Partial Fulfillment of the Requirements for the Master's Degree

.....Dean of the Faculty of Engineering

(Associate Professor Supot Teachavorasinskun, D.Eng.)

THESIS COMMITTEE

.....Chairman

(Assistant Professor Tuptim Angkaew, Ph.D.)

.....Thesis Advisor

(Panuwat Janpugdee, Ph.D.)

.....External Examiner

(Associate Professor Titipong Lertwiriyaprapa, Ph.D.)

มางเสียง ฮอ : แบบจำลองอย่างง่ายสำหรับประมาณค่ามิวชวลคัปปลิงในสายอากาศแถวลำดับ (SIMPLE MODEL FOR APPROXIMATION OF MUTUAL COUPLING IN MICROSTRIP PATCH ARRAY) อ.ที่ปรึกษาวิทยานิพนธ์หลัก: ดร.ภาณุวัฒน์ จันทร์ภักดี, 85 หน้า.

วิทยานิพนธ์ฉบับนี้นำเสนอแบบจำลองอย่างง่ายและมีประสิทธิภาพสำหรับประมาณค่ามิวชวลคัปปลิงระหว่างสายอากาศไมโครสตริป แบบจำลองนี้ถูกพัฒนาจากพฤติกรรมเชิงเส้นกำกับของคลื่นแม่เหล็กไฟฟ้าที่เกิดจากกระแสไฟฟ้าบนวัสดุฐานรองบนแผ่นกราวนด์ โดยแสดงอยู่ในรูปของอนุกรมจำนวนไม่กี่พจน์ของฟังก์ชันคลื่นทรงกระบอกของตัวแปร 2 ตัว ได้แก่ ระยะเชิงเส้นและระยะเชิงมุมระหว่างสายอากาศทั้งสอง นิพจน์ดังกล่าวประกอบด้วยสัมประสิทธิ์ที่ต้องคำนวณหาค่าเพียงครั้งเดียวในตอนแรกสำหรับสายอากาศรูปแบบหนึ่งๆ ที่ความถี่ใดความถี่หนึ่ง โดยการเปรียบเทียบค่ามิวชวลคัปปลิงที่คำนวณจากแบบจำลองที่นำเสนอกับค่าอ้างอิงโดยใช้ระเบียบวิธีกำลังสองน้อยที่สุด ค่ามิวชวลคัปปลิงอ้างอิงดังกล่าวคำนวณโดยการวิเคราะห์เชิงคลื่นเต็มรูปแบบซึ่งมีความแม่นยำสูงโดยใช้ซอฟต์แวร์เชิงพาณิชย์ หลังจากหาค่าสัมประสิทธิ์ได้แล้ว แบบจำลองที่ได้สามารถใช้ประมาณค่ามิวชวลคัปปลิงระหว่างสายอากาศไมโครสตริปแบบเดียวกันที่ความถี่นั้นๆ สำหรับระยะเชิงเส้นและระยะเชิงมุมระหว่างสายอากาศที่ค่าใดๆ เนื่องจากแบบจำลองที่นำเสนออยู่ในรูปแบบปิดอย่างง่ายจึงคาดได้ว่าใช้เวลาในการคำนวณน้อยกว่าการวิเคราะห์เชิงคลื่นเต็มรูปแบบ แบบจำลองที่นำเสนอสามารถนำไปประยุกต์ใช้ประมาณค่ามิวชวลคัปปลิงระหว่างองค์ประกอบของสายอากาศแถวลำดับแบบไมโครสตริปได้อย่างมีประสิทธิภาพ ตัวอย่างการประมาณค่ามิวชวลคัปปลิงระหว่างสายอากาศไมโครสตริปโดยใช้แบบจำลองที่นำเสนอเปรียบเทียบกับค่าที่คำนวณด้วยการวิเคราะห์เชิงคลื่นเต็มรูปแบบโดยใช้ซอฟต์แวร์เชิงพาณิชย์ ได้แสดงไว้ในวิทยานิพนธ์ฉบับนี้ โดยผลที่ได้พบว่าค่าที่คำนวณจากทั้งสองวิธีมีค่าใกล้เคียงกันและแบบจำลองที่นำเสนอใช้เวลาในการคำนวณน้อยกว่า ซึ่งแสดงให้เห็นถึงความถูกต้องและประสิทธิภาพของแบบจำลองที่นำเสนอในวิทยานิพนธ์ฉบับนี้

ภาควิชา วิศวกรรมไฟฟ้า ลายมือชื่อนิสิต .....

สาขาวิชา วิศวกรรมไฟฟ้า ลายมือชื่อ อ.ที่ปรึกษาหลัก .....

ปีการศึกษา 2559

5770526321 : MAJOR ELECTRICAL ENGINEERING
KEYWORDS: EMPIRICAL MODEL / MICROSTRIP PATCH ARRAY / MUTUAL COUPLING / MUTUAL IMPEDANCE / LEAST SQUARE METHOD

MANGSEANG HOR: SIMPLE MODEL FOR APPROXIMATION OF MUTUAL COUPLING IN MICROSTRIP PATCH ARRAY. ADVISOR: PANUWAT JANPUGDEE, Ph.D., 85 pp.

A relatively simple and efficient empirical formulation for the estimation of mutual coupling between two microstrip patch antennas has been proposed in this thesis. The formulation is constructed based on the asymptotic behavior of the electromagnetic wave excited by an electric current on a grounded substrate. It is expressed by a few terms of cylindrical wave functions of two variables, which are center-to-center spacing and azimuthal angular separation between two antennas. The formulation contains coefficients which need to be determined *at once*, for any given antenna geometry and operating frequency, by matching with few sample values of mutual impedance for several antenna separations using the least square method. The latter are calculated by a rigorous full-wave analysis using a commercial software. The formulation with the obtained coefficients can then be used to estimate the mutual coupling between two similar antennas for any arbitrary separations. The proposed formulation is expected to be far more efficient than the exact solution due to its simple closed form. The proposed approach can be employed to efficiently estimate the mutual coupling between any elements of a microstrip patch array antenna. Some numerical examples are given to illustrate the applicability, validity, and efficiency of the proposed approach. The good agreement of the mutual impedance estimated by the present approach and that obtained by a rigorous full-wave solution has been demonstrated.

Department:	Electrical Engineering	Student's Signature	.....
Field of Study:	Electrical Engineering	Advisor's Signature	.....
Academic Year:	2016		

ACKNOWLEDGEMENTS

This work has been conducted at Telecommunication Research Laboratory, Department of Electrical Engineering, Faculty of Engineering, Chulalongkorn University. I gratefully appreciate Graduate School of Chulalongkorn University who has supported the funding for this research under the Program of ASEAN Scholarship.

I would like to take this opportunity to express my deepest gratitude to my thesis advisor, Dr. Panuwat Janpugdee, for his advises, patient guidance, and his caring throughout my studying period in Chulalongkorn University. All his inspirational talks have truly motivated me to go through the long term of doing research and to succeed many problems which I had thought that I was not able to solve. Without his enthusiastic encouragement and support, this thesis would not have been completed.

I would like to express my sincere appreciation to my thesis committee members, including Assistant Professor Dr. Tuptim Angkaew from Chulalongkorn University, and Associate Professor Dr. Titipong Lertwiriyaprapa from King Mongkut's University of Technology North Bangkok, for their valuable time and technical suggestions to complete my work. I would like to thank all professors and lecturers at Electrical Engineering Department Chulalongkorn University who have provided me great knowledge in their classes that help me to get a fundamental background of Communication Engineering, especially Microwave and Lightwave Communications. I would like to extend my thanks to all student members at Telecommunication Research Laboratory for their encouragement and their kind helps during my study in Chulalongkorn University.

Finally, I also would like to express my grateful thanks to my beloved parents and my two beloved sisters for their support and unconditional love throughout my whole life.

CONTENTS

Page

Page

Page

LIST OF FIGURES

Chapter 1 INTRODUCTION

1.1. Motivation

In the wireless communication, antenna is an important part of the communication systems. The communication cannot be made wirelessly without an antenna. Antenna system has been developed continually in accordance with the new generation of the wireless communication technology. Phase array antenna has been found as an important role in many applications of wireless communications, and radar systems [1], for instant; aerospace, satellite, and shipboard application and so on. In addition phase array antenna has been popularly used with smart antenna systems and multiple input and multiple output (MIMO) antenna systems. All of the systems which are described above require antennas with relatively high gain, low profile, and electronic beam steering capability.

Therefore, microstrip antenna can be considered as a good candidate for the systems above. Microstrip antenna has a simple configuration which is combination of a thin metallic radiating patch bonded to a thin grounded dielectric substrate. The radiating element normally has some regular shapes; rectangular, square, circular or elliptical. Moreover, microstrip antenna has typical properties which are suitable with the systems above: a) micropstrip antenna has light weight, small size and low profile planar configurations which can conform to any pattern; b) microstrip antenna is not expensive to fabricate and easy for large scale production by printed circuit techniques; c) microstrip antenna is compatible with modular designs (solid state device such as oscillator, amplifiers, phase shifters, etc., and can be attached directly to the antenna substrate board); d) the feed lines of microstrip antenna can be manufactured at the same time with antenna structure, so that discontinuities due to connectors can be eliminated. However, there are also some disadvantages of the microstrip antenna; a) simple microstrip antennas have narrow bandwidths; their gain are low; c) they have a small power handling capability; d) dielectric losses reduce the radiation efficiency; e) unwanted surface waves may cause spurious radiation at the edge of the microstrip patch.

In array antenna, closely-space antenna elements unavoidably lead to mutual coupling. In array antennas and MIMO antenna systems, antenna mutual coupling is also a main problem to be concerned, since mutual coupling does affect the array performance and radiation pattern of the antenna [1].

1.2. Problem Statement

Due to the scarcity of the frequency, millimeter wave is likely interested and favorable in the future. Therefore, the high frequency is needed for future generation of wireless communications. In the high frequency applications, the substrates are often thicker and have higher dielectric constant than at lower frequencies. Consequently the electric performance of the antenna will be severely degraded due to the mutual coupling. This shows that the analysis of mutual coupling is important in the design of antenna arrays, typically if the tight pattern control or low side-lobes are needed. The mutual impedance of microstrip patch antenna can be realized by various methods; a) simplified models: transmission line and cavity models; b) method of moment; c) integral equation formulation; and so on.

The mutual impedance between two rectangular patch antennas is commonly determined by using full-wave analysis which is a popular method for researchers as well as antenna design engineer. However, using full-wave analysis requires long time and more resources to do it. Moreover, the researchers who want to use the full-wave must have an in-depth knowledge about it. In addition to full-wave analysis methods, some EM simulation commercial software can be used to calculate the mutual impedance between two rectangular patch antennas. When a parameter (element spacing, etc.) is changed, the software needs to be re-run, and it takes some time to obtain another value of mutual impedance. To reduce time and resource consumption and complexity of calculating the mutual impedance, the approximation model will be proposed in this research. Some data points from full-wave analysis or EM simulation software are required to fine the proposed model. After obtaining the proposed model, it can be used to approximate the mutual impedance at any points of an interval within which the element spacing is changed.

1.3. Research Objective

The objectives of this research are described as follows:

1. To find an approximation formula to calculate the mutual impedance between two microstrip patch antennas.
2. To investigate the applicability of the approximation formulation.
3. To investigate results from the formulation with the existing results.
4. To investigate the effect of orientation of patch on the mutual impedance between two microstrip antennas.
5. To use the approximation to find the mutual impedance in the array antennas and compare with results from simulation software.

1.4. Scope of this research

The scope of this research is limited to the following issues:

1. Find an approximation model as a function of two variables, which are center-center spacing (ρ) and azimuthal angle separation (ϕ).
2. Mutual Impedance between two rectangular microstrip antenna can be approximate by the proposed model whose coefficients can be re-determine when parameters of patch antenna are different from the following:
    - Frequency f = 2.98GHz
    - Dimension of microstrip patch: $0.3\lambda_0 \times 0.27\lambda_0$
    - Substrate thickness: $\varepsilon_r = 2.3$
    - Two antenna are alike
3. Element spacing (ρ) is within interval of $[0.5\lambda_0 , 2.48\lambda_0]$ and the azimuthal angle (ϕ) is with interval of [0 , π/2 rad].

1.5. Methodology

1. Reviewing literature on background knowledge relevant to microstrip antenna and mutual coupling between two microstrip patch antennas.

2. Model the microstrip antenna on in a simulation program.
3. Use the model to simulate the mutual coupling between two microstrip patch antennas.
4. Proposing the approximation model with some unknown coefficients.
5. Use least-square optimization technique to find the unknown coefficients.
6. Investigate the applicability of the proposed formulation.
7. Compare the results from proposed formulation with the existing results.

1.6. Expected Contributions

This research is anticipated to provide an analytical formulation that can be used to calculate the mutual impedance between two patch antennas. Instead of using the full wave analysis to calculate the mutual coupling between two patch antennas, the formula can be used for saving time. Although the formulation can be used to facilitate the calculation, there are a lot of limitations regarding to parameters of the microstrip patch antenna.

Chapter 2 LITERATURE REVIEW

2.1. Microstrip Antenna

The concept of microstrip antenna was originally introduced in [2] and [3]. Deschamps has proposed that feeding of an array printed antenna elements can be made by the microsrtip feed lines. Nevertheless, until the development of printed circuit board technology in 1970s, the concept of microstrip antenna has been realized as importance. Since then, microstrip antenna technology has been researched extensively by academic researchers. In the last decades, the patch antenna has been famously studied due to its advantages such as: light weight, small size, low cost, conformability, and facilitation of integration with active devices. In the last decade, Microstrip antenna has been widely used for the civilian and military purpose such as radio frequency identification (RFID), broadcast radio, mobile communication systems, global position system (GPS), television, multiple input multiple output systems, satellite communications, surveillance system, guiding systems, radar systems, remote sensing, missile guidance and several other application [4] [5] [6].

Microstrip antennas can be used as a transmitter or a receiver. Microstrip antenna has three main parts which are radiating patch, dielectric substrate and ground plan (See Figure 2.1).

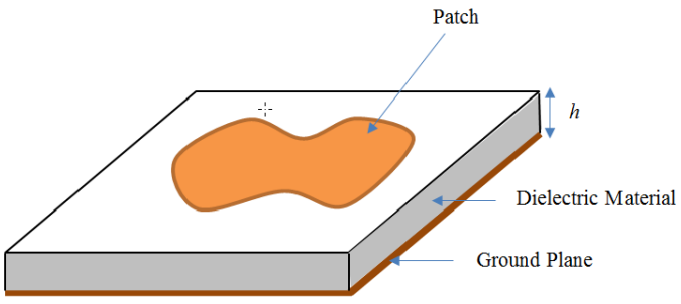

Figure 2.1 General Geometry of Microstrip Patch Antenna

The materials, which are generally used to fabricate the patch antenna, are copper or metal. The shape of radiating patch can be arbitrary selected; however,

the generally used shapes are rectangular, square and circular. The substrate thickness (h) is very thin comparing to free-space wavelength (λ_0); ($h << \lambda_0$).

There are various types of substrate material which can be used for the design of microstrip antennas, and their relative permittivity (dielectric constants) is usually within the interval of $2.2 \leq \varepsilon_r \leq 12$. Typically, the lower dielectric constant and thick substrates have better efficiency and larger bandwidth, whereas the thin substrate is good for microwave application [7] [8]. Due to their performance and robust characteristic, microstrip antennas are favorably used in various applications [9] [10] [11]. In mobile communication, the antennas are required to be small and low profile. Microstrip patch antennas have all the requirements above. Moreover, microstrip antennas are also low cost for fabrication. In global positioning system (GPS) for vehicles, microstrip antennas are good candidate due to their high value of permittivity substrate material. To fulfill the demand for precise and reliable of the GPS applications, the circular microstrip antenna has been developed. In addition, microstrip antennas are also used for radar application which is for detecting moving targets such as vehicles and people. Finally, microstrip antennas can be considered as a crucial novel technology for human being.

2.2. Analysis Techniques For Microstrip Patch Antenna

There are many methods which are used to analyze the microstrip element. The commonly used models are the transmission-line, cavity, and full wave (which are mainly integral equation/Moment Method) [1]. The transmission-line model is the simplest of all, it gives good physical insight, but the accuracy of the model is not good and it is more complicated and difficult to model coupling [12]. Cavity gives a better physical insight than the transmission-line model, and it is more accurate than transmission-line model; however the cavity model is even more complicated than transmission-line to model the coupling. To properly apply analysis models for microstrip antennas, the full-wave models are very accurate, very versatile, and can treat single elements, finite and infinite arrays, stacked elements, arbitrary shaped and coupling; however, the full-wave models are the most complicated and they usually give less physical insight.

2.2.1. Transmission-Line Model

Transmission-line model is described above that it is the simplest and easiest model of all, but it gives the least accurate results and it has a shortage of versatility. In transmission-line model, rectangular microstrip antennas are models as an array of two parallel radiating narrow apertures (slots) [13] [14] as shown in Figure 2.2.

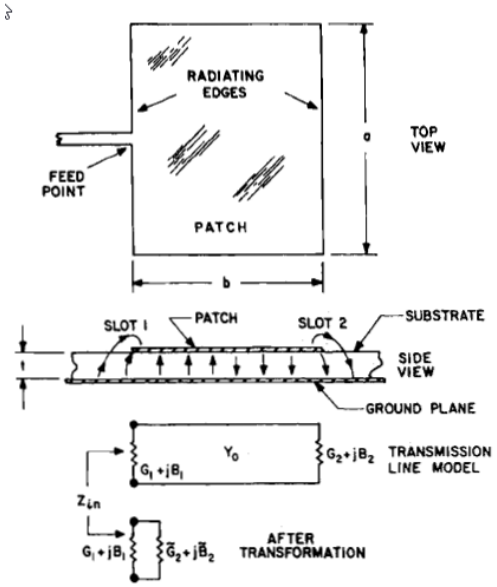

Figure 2.2 Transmission-line model of rectangular microstrip antenna [9, 13].

Each patch edge of length a is modeled as a narrow slot radiating into a half-space, with a slot admittance given by [13, 15]:

$$G_1 + jB_1 \cong \frac{\pi a}{\lambda_0 z_0}\left[1 + j\left(1 - 0.636\ln\left(k_0 w\right)\right)\right] \tag{2.1}$$

Where λ_0 is the free-space wavelength

z_0 is the free-space wave impedance $Z_0 = \sqrt{\frac{\mu_0}{\varepsilon_0}}$

$$k_0 = \frac{2\pi}{\lambda_0}$$

w is the slot width, approximately equal to the substrate thickness t

For the slot 2, the expression of admittance is the same as the admittance of slot 1 because the two slots are identical (except for the fringing effects associate with the feed points on edge 1).

Assuming that there is no field variation along the direction which is parallel to the radiating edge, the characteristic admittance is given by [13]:

$$Y_0 = \frac{a\sqrt{\varepsilon_r}}{tz_0} \qquad (2.2)$$

where t is the substrate thickness. ε_r is the relative dielectric constant of the substrate.

To obtain the excitation of the slots 180° out of phase, the dimension b is set to be equal to slightly less than $\lambda_d/2$ where $\lambda_d = \frac{\lambda_0}{\sqrt{\varepsilon_r}}$

So $b = 0.48\lambda_d$ to $b = 0.49\lambda_d$

This slight reduction in resonant length is important due to the fringing fields at the radiation edges. After carefully choosing the length of reduction factor q, the admittance of slot 2 after transformation [13] [16] is equal to

$$G_2 + jB_2 = G_1 - jB_1 \qquad (2.3)$$

So that the total input admittance at resonance becomes

$$Y_{in} = (G_1 + jB_1) + (G_2 + jB_2) = (G_1 + jB_1) + (G_1 - jB_1) = 2G_1 \qquad (2.4)$$

In a typical design $a = \lambda_0 / 2$ so that $G_1 = 0.00417\ \Omega$

$$R_{in} = (1/2G_1) = 120\ \Omega \qquad (2.5)$$

The resonant frequency is equal to

$$f_r = \frac{c}{\lambda_d\sqrt{\varepsilon_r}} = q\frac{c}{2b\sqrt{\varepsilon_r}} \qquad (2.6)$$

The advantage of the transmission-line model is its simplicity, i.e., the resonant frequency and input resistance are expressed in a simple close form. The fringing factor q shows the accuracy of the resonant frequency; and in reality, the accuracy of resonant frequency is determined by f_r for a rectangular patch on given

substrate. Thus, it can be assumed that the same q value is for patches of other sizes on the same substrate and in the same frequency range [13].

2.2.2. Modal-Expansion Cavity Model

The above transmission-line model is simple and easy to use; however, the model also has many drawbacks. It is useful for rectangular patch antenna only. The fringing factor q must be established by empirical model. Moreover, the field variations are not accounted for radiation along the edge of patch. The transmission-line model is not adaptable to include the feed, etc. The drawbacks are solved in modal-expansion analysis whereby the pact is considered as a thin TM_z-mode cavity with magnetic walls [13]. The field in the substrate (between the patch and ground plan) is expanded as a function of a series of cavity resonant modes or eigenfunctions along with its eigenvalues or resonant frequency associated with each mode. The effect of radiation and other losses is analysed in term of either an artificially increase substrate loss tangent or by the more elegant method of an impedance boundary condition at the wall. In the cavity model, the formulation for input impedance, resonant frequency, ect, gives a much more accurate result for both rectangular patch and circular patch. However, it is good only at a modest increase in mathematical complexity.

2.2.2.1. Rectangular Patch Antenna

There is a rectangular patch antenna of width a and length b over a ground plane with a substrate with thickness t and a dielectric constant ε_r as shown in Figure2.3a and Figure2.3b. Since the substrate is electrically thin, the electric field will be considered as z-directed and the interior modes will be TM_{mn} to z [13] , so that :

$$E_z(x,y) = \sum_m \sum_n A_{mn} e_{mn}(x,y) \tag{2.7}$$

Where A_{mn} are the mode amplitude coefficients and e_{mn} are the z-directed orthonormal electric field mode vectors

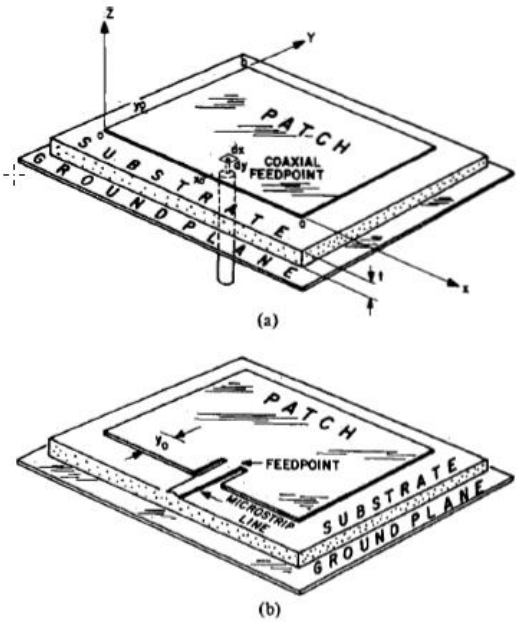

Figure 2.3 (a) Rectangular microstrip patch with inset coaxial feedpoint.
(b) Rectangular patch with inset microstrip transmission-line feed [9],[13].

For the elementary case of a non-radiating cavity with perfect open-circuit walls [13],

$$e_{mn}(x,y) = \frac{\chi_{mn}}{\sqrt{\varepsilon abt}} \cos k_n x \cos k_m y \tag{2.8}$$

With

$$\chi_{mn} = \begin{cases} 1, & m = 0 \quad and \quad n = 0 \\ \sqrt{2}, & m = 0 \quad or \quad n = 0 \\ 2, & m \neq 0 \quad and \quad n \neq 0 \end{cases} \tag{2.9}$$

The mode vectors satisfy the homogenous wave equation, and the eigenvalues satisfy the separation equation

$$k_{mn}{}^2 = \omega_{mn}{}^2 \mu\varepsilon = k_m{}^2 + k_n{}^2 \tag{2.10}$$

For the non-radiating cavity, $k_n = (n\pi / a) \quad and \quad k_m = (m\pi / b)$,

The magnetic field orthonormalized mode vector are found from Maxwell's equations as

$$\vec{\mathrm{h}}_{mn} = \frac{1}{j\omega\mu} \cdot \frac{\chi_{mn}}{\sqrt{\varepsilon abt}} \cdot \{\vec{\mathrm{x}} \cdot k_m \cos k_n x \sin k_m y - \vec{\mathrm{y}} \cdot k_n \sin k_n x \cos k_m y\} \tag{2.11}$$

For this non-radiating case it is seen that the boundary condition $\vec{n}\times\vec{h}_{mn}=0$ is satisfied on each perimeter wall.

When the field is allowed to radiate from the cavity, the eigenvalues turn to be complex, relating to complex resonant frequencies, so that $|k_n|$ is slightly smaller than $n\pi/a$ and $|k_m|$ is slightly smaller than $m\pi/b$. Thus, although the magnetic field mode vector h_{mn} has no longer a zero tangential component on the cavity sidewalls, a perturbation solution does show that the electric field mode vectors still have high accurate result from the formulation above (equation (2.8)).

For the effect of a z-directed current probe I_0 of small rectangular cross section $(d_x d_y)$ at (x_0, y_0) as shown in Figure 2.3(a), the coefficient of each electric mode vectors can be determined by the formula bellow [15] [13]:

$$A_{mn} = \frac{j\sqrt{\mu\varepsilon}k}{k^2 - k_{mn}{}^2} \iiint \vec{J}\cdot\vec{e}_{mn} * dv \tag{2.12}$$

which then becomes to:

$$A_{mn} = jI_0\sqrt{\frac{\mu t}{ab}}\frac{k\chi_{mn}}{k^2 - k_{mn}^2} G_{mn}\cos k_m y_0 \cos k_n x_0 \tag{2.13}$$

where

$$G_{mn} = \frac{\sin(n\pi d_x/2a)}{n\pi d_x/2a}\cdot\frac{\sin(m\pi d_y/2b)}{m\pi d_y/2b} \tag{2.14}$$

and

$$k_{mn} = \tilde{\omega}_{mn}\sqrt{\mu\varepsilon} \tag{2.15}$$

In (2.15) $\tilde{\omega}_{mn}$ is the complex resonant frequency of mn th mode as determined from (2.10). The formulation (2.12) for determining the coefficients is in term of the orthogonality of the mode vectors; however, the introduction of the radiation condition shows that these mode vectors are no longer orthogonal in the strict sense. For electrically thin substrates, the error due to this assumption is negligible.

The factor G_{mn} is to relate the formulation with width of feed line, for coaxial feeds $d_x = d_y$, and the cross-section area $d_x d_y$ is equal to the effective cross-section

area of probe. For microstrip line feeding, the feed point is at $y_0 = 0$, set $d_y = 0$, and use d_x equal to the feed line width as the zero order approximation ignoring junction capacitance effects.

Substitute (2.13) into (2.7) we obtain

$$E_z(x,y) = jI_0 Z_0 k \sum_{m=0}^{\infty}\sum_{n=0}^{\infty} \frac{\psi_{mn}(x,y)\psi_{mn}(x_0,y_0)}{k^2 - {k_{mn}}^2} G_{mn}\,, \tag{2.16}$$

where $k = \omega\sqrt{\mu\varepsilon}$, $Z_0 = \sqrt{\mu/\varepsilon}$, ${k_{mn}}^2 = {k_m}^2 + {k_n}^2$, and

$$\begin{aligned} \psi_{mn} &= \frac{\chi_{mn}}{\sqrt{ab}} \cos k_n x \cos k_m y \\ &\cong \frac{\chi_{mn}}{\sqrt{ab}} \cos\frac{n\pi x}{a} \cos\frac{m\pi y}{b} \end{aligned} \tag{2.17}$$

The voltage at the feed is now computed as

$$\begin{aligned} V_{in} &= -tE_z(x_0,y_0) \\ &= -jI_0 Z_0 kt \sum_{m=0}^{\infty}\sum_{n=0}^{\infty} \frac{{\psi_{mn}}^2(x_0,y_0)}{k^2 - {k_{mn}}^2} G_{mn} \end{aligned} \tag{2.18}$$

Therefore the input impedance is

$$Z_{in} = \frac{V_{in}}{I_0} = -jZ_0 kt \sum_{m=0}^{\infty}\sum_{n=0}^{\infty} \frac{{\psi_{mn}}^2(x_0,y_0)}{k^2 - {k_{mn}}^2} G_{mn} \tag{2.19}$$

The (0,0) term with $k_{00} = 0$ is the static capacitance term with a shunt resistance to stand for loss in the substrate. The (1,0) term stands for the domain RF mode and it is similar to the transmission-line model which is described in the section above. For (1,0) mode, equation (2.8) shows that the radiation field doesn't vary in the x direction and the variation of $a\cos(\pi y/b)$ is in the y direction. This mode is equivalent to a parallel *R-L-C* network where R stands for radiation, substrate, and copper losses. If the microstripo patch is square or almost square, the (1,0) mode can also be excited as degenerate losses and sum to form a net inductance *L*. Figure2.4(a) is a general network representation of the input impedance, and Figure 2.4(b) is a network model over a narrow band about an isolated TM_{10} mode, where the net series inductance is L_T. The feed probe diameter

as expressed by the factor G_{mn} is the main factor in determining L_T, since it controls the convergence of the series. Equation (2.19) can be written as :

$$Z_{in} = jX_L - \frac{j(\omega / C_{10})}{\omega^2 - (\omega_r + j\omega_i)^2} \tag{2.20}$$

Where

$$(\omega_r + j\omega_i)^2 = \omega_{10}{}^2 (1 + j/Q) \tag{2.21}$$

$$C_{10} = \frac{1}{2} C_{cd} \cos^{-2}(\pi y_0 / b) \tag{2.22}$$

With C_{dc} being the dc patch capacitance $(\varepsilon ab/t)$, Q the quality factor for the TM_{10} mode, and ω_{10} the radian frequency at resonance. A simple formulation for calculating both ω_{10} *and* Q will be shown in a subsequent paragraph. The series inductive reactance is given by

$$X_L = -\frac{1}{\omega C_{dc}} + \frac{\omega}{C_{dc}} \sum_{\substack{mn\neq 10 \\ mn\neq 00}}^{M} \sum^{N} \frac{\chi_{mn}{}^2 \cos^2\left(\frac{n\pi x_0}{a}\right) \cos^2\left(\frac{m\pi x_0}{b}\right)}{\omega_{mn}{}^2 - \omega^2} \cdot G_{mn} \tag{2.23}$$

The equation above shows that the series reactance is proportional to the substrate thickness.

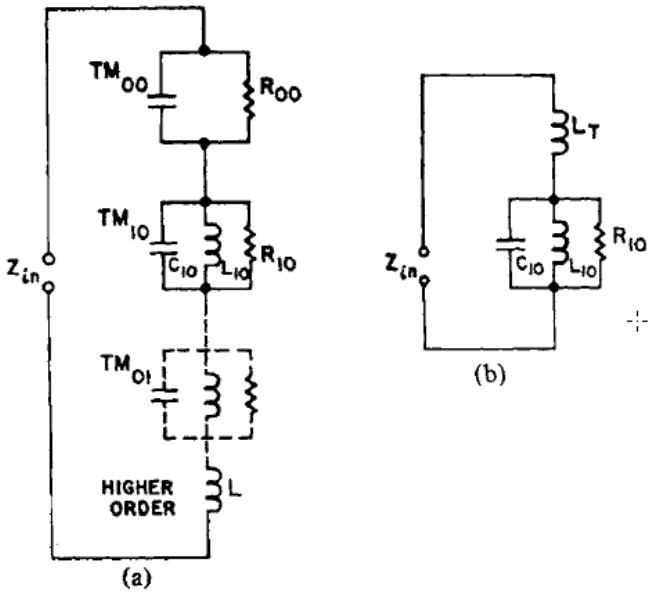

Figure 2.4 (a) General network model representing microstrip antenna
(b) Network model over narrowband about isolated TM_{01} mode[13].

2.2.3. Numerical Analysis Techniques

In recent decade, several numerical techniques, which are applied to microstrip antennas, have been proposed. Some favorable numerical techniques are Integral Equation, method of moments, finite-elements technique, and so on.

2.2.3.1 Integral Equation Formulation [17]

This technique is based on the Green's Function method which leads to the calculation of the total electric field $\vec{E}$ which is produced by the electric surface currents $\vec{\mathrm{J}}_S$ on the surface of microstrip patches antennas as follow:

$$\vec{E} = \vec{E}^{i} + \iint_{S} \overline{\overline{G}}.\vec{\mathrm{J}}_{\mathrm{S}}\, d\mathrm{s} \qquad (2.24)$$

Where $\vec{E}^{i}$ is the incident field excited by an impressed current source $\vec{J}_{\mathrm{i}}$

$\vec{J}_{\mathrm{i}}$ is current on the probe feed as shown in Figure 2.5

$\overline{\overline{G}}$ is an suitable dyadic Green's function which accounts for the grounded substrate

S is the surface of the patches

The boundary condition on the patches is that

$n \times \vec{E} = 0$ on the surface S

Where n is the unit vector normal to the surface of the patches

The equation above is the expression of the electric field integral equation for $\vec{\mathrm{J}}_{\mathrm{S}}$.

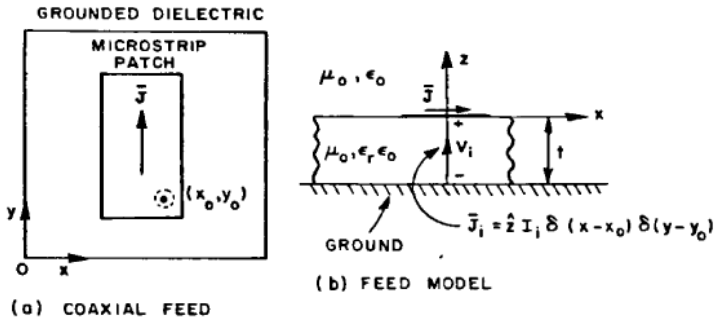

Figure 2.5 Configuration of Rectangular Microstrip with probe feed [17]

2.2.3.2 Moment Method Solution

The integral equation above (2.24) is solved by using the Galerkin form of the moment method where both the basis and testing functions are taken as a surface patch dipole mode. Thus, the unknown current $\vec{\mathrm{J}}_{\mathrm{S}}$ is expanded in to a set of N basis functions or modes

$$\vec{\mathrm{J}}_{\mathrm{S}} = \sum_{n=1}^{N} \mathrm{I}_n \vec{\mathrm{J}}_n \tag{2.25}$$

$\vec{\mathrm{J}}_n$ is the n^{th} mode and I_n is its unknown amplitude.

Using the same set of functions as testing functions to solves a system of linear algebraic equations for the unknown I_n

$$[Z][\mathrm{I}] = [\mathrm{V}] \tag{2.26}$$

$[Z]$ is the impedance matrix with elements

$$Z_{mn} = -\int_{S_n} \vec{E}_m \,.\, \vec{\mathrm{J}}_n \, d\mathrm{s} \tag{2.27}$$

$[\mathrm{V}]$ is the voltage vector whose elements are given by

$$\mathrm{V}_m = \int_{V_i} \vec{E}_m \,.\, \vec{\mathrm{J}}_i \, d\mathrm{v} \tag{2.28}$$

I_n are the elements of the current vector $[\mathrm{I}]$

$\vec{E}_m$ in the equation (27) and (28) is the electric field due to the mode current $\vec{\mathrm{J}}_m$ in the presence of the dielectric substrate and ground plane

S_n denotes the surface where current $\vec{\mathrm{J}}_n$ exists

V_i denotes the volume where current $\vec{\mathrm{J}}_i$ exists

2.2.3.3 Finite Element Technique

The interior field of the microstrip antenna can be calculated by using the numerical analysis which is a finite element approach [13]. Finite element method is a numerical method that is used for finding approximate answers to boundary-value problems of mathematical physics. To find the solutions of the boundary problems, two classic methods have been used. One method is the Rayliegh-Ritz method or

Ritz method, which is a variational method. By using the variational method, the boundary-value problem is formulated in term of a variational function. The approximate solution can be obtained by finding the minimum of the variational function. The other classic method is Galerkin's method, which is a weighted residual method. The solution of the problems can be obtained by weighting the residual of the differential equation. Therefore, the solution of the problems can be found by two ways, variational finite element and Galerkin finite element method. The difference between the variational finite element (Ritz method) and Galerkin method is the formulation of trail function.

By applying the variational finite element method (Ritz method) or Galerkin method, the boundary-value problems are in the form of a system of algebraic equations. The solution of the system of algebraic equation is that of the boundary-value problems. The system of algebraic are in the form of as fallowing:

$$[K]\{\phi\} = \{b\} \tag{2.29}$$

or

$$[A]\{\phi\} = \lambda[B]\{\phi\} \tag{2.30}$$

Equation (2.29) is a kind of deterministic system, which is because of an inhomogeneous differential equation or inhomogeneous boundary condition or both. In electromagnetic problems, deterministic systems are usually relating to scattering, radiation, and other problem where a source exists internally or externally.

Equation (2.30) is a kind of eigenvalue systems, which is because of homogenous differential equation and boundary condition. λ is an eigenvalue of the systems. In electromagnetic problems, the eigenvalue systems are usually relating to source-free problems such as wave propagation in wave guides and resonances in cavity.

When $\{\phi\}$ is solved from the above system of algebraic equation, the desired parameters can also be computed. The desired parameters can be capacitance, inductance, input impedance, and scattering or radiation pattern.

2.3. Mutual Coupling Between Two Antenna Element In Array

Assuming that the mutual coupling does not exist in an array, the input impedance of each antenna element would be the same, and it has the same value as a single isolated antenna element. The input impedance of each radiating element in the array would not be affected by the excitations of other elements. In addition, the pattern of the array can be realized by using the simple pattern of the multiplication and the array factor. However, in reality, the mutual coupling is unavoidable in the array. The effect of the mutual coupling is that it will make the input impedance depending on the excitation of the array elements, as well as the array pattern. Therefore, the real doubt of the antenna engineering is whether or not the mutual coupling effects should be concerned in the antenna array design. The mutual coupling can be analyzed by using the simple models [18] and the full-wave solution. The use of the full-wave solution is more accurate than the use of simple mode [18] since the full-wave solutions ensure that the surface wave and space wave coupling effects are properly accounted for. In addition, the mutual coupling can also be obtained by measurement. The knowledge of mutual coupling could help antenna design engineer to predict the performance of the array, or to design the feed network to balance its effects in the array. Instead of direct calculation of mutual couple, the mutual impedance will be analyzed. From the knowledge of the mutual impedance, the scattering parameters can be found and as well the mutual coupling. In the following chapter, the approximation model of mutual impedance will be discussed.

Chapter 3 MUTUAL IMPEDANCE BETWEEN TWO MICROSTRIP PATCH ANNTENAS (Simple model for approximation for mutual impedance)

Microstrip patch antennas are inherently low gain antenna, and this fact partially offsets the advantages which they offer in terms of costs and ease of fabrication. To overcome this disadvantage, many microstrip patch antennas are grouped in large arrays to obtain high gain. Linear array of microstrip antennas are popular candidates for multiple input multiple output (MIMO) systems and radar applications. Due to space limitation, the array antenna elements are placed in close proximity which becomes the main source of mutual coupling. In this case, mutual coupling is an unwanted phenomenon. However, the knowledge of the mutual coupling is important as describing chapter 2.

The ordinary of the mutual impedance between two antenna elements is defined when one antenna is in the transmitting mode with connecting to source while another antenna is in the receiving mode with open circuit [19] [20]. The mutual impedance can be calculated as the ratio of voltage, which is across the open circuit terminal and which is induced by the antenna 1, to current which is excited and flowing through the short circuit terminal of antenna 2 [19] [21]. The reciprocity theorem has been generally used to derive the voltage induced across the open circuit [22].

3.1. Basic Theory To Calculate Mutual Impedance Between Two Antenna Element

In this section, the mutual impedance will be examined in two ways which are circuit theory of mutual impedance and field theory of mutual impedance.

3.1.1. Circuit Theory Of Mutual Impedance

When two or more antennas are employed in an array, the driving-point impedance of each antenna depends upon the self-impedance of that antenna and in addition up on the mutual impedance between the given antenna and each of the others. For example, consider the two elements array of Figure3.1 in which base

currents I_1 and I_2 flow. As far as voltages and currents at the terminals (1) and terminal (2) are concerned, the two antennas of Figure3.1 can be represented by the general four-terminal network of Figure3.2.

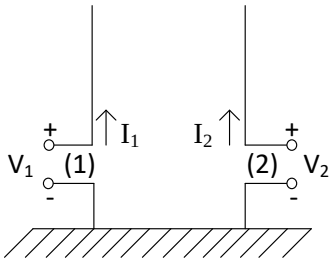

Figure 3.1 Two antennas

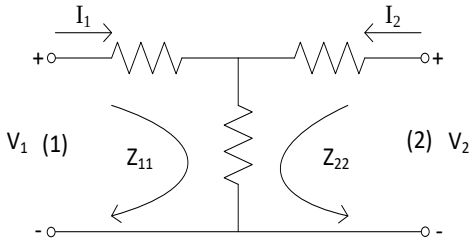

Figure 3.2 General four-terminal network

Z_{11} is the impedance measured at the terminals (1) when terminals (2) is an open circuit. Thus, Z_{11} is the mesh impedance of mesh (1). Z_{22} is the impedance measured at the terminals (2) when terminals (1) is an open circuit. Thus, Z_{22} is the mesh impedance of mesh (2). The mutual impedance between the antennas is Z_{12} and Z_{21}. From the reciprocity theory, we get $Z_{12} = Z_{21}$.

The mutual impedance can be calculated as following;

$$Z_{21} = \frac{V_{21}}{I_1} \quad ; \quad Z_{12} = \frac{V_{12}}{I_2}$$

where V_{21} is the open-circuit voltage induced across terminals (2) of antenna (2) owing to current I_1, flowing (at the base) in antenna (1)

V_{21} is the open circuit voltage induced across the terminals (1) of antenna (1) owing to current I_2, flowing (at the base) in antenna (2).

The self-impedance of an antenna is the input impedance of that antenna when all other antennas are entirely removed. However, when the length antenna (2) is very near a resonant length (that is, $h \approx \lambda/2$, h is the length of the antenna (2)) or when it is very close to antenna (1), the input impedance of antenna (1) will be nearly the same, when the antenna (2) is an open circuit, as input impedance of antenna (1) when antenna (2) is entirely removed from the field of antenna (1).

The mesh equations for the Figure3.1 are:

$$\begin{cases} V_1 = I_1 Z_{11} + I_2 Z_{12} \\ V_2 = I_1 Z_{21} + I_2 Z_{22} \end{cases}$$

Let $r = \frac{I_1}{I_2}$, where in general r is the complex number. Then we get:

$$\begin{cases} \frac{V_1}{I_1} = Z_{11} + \frac{1}{r} Z_{12} \\ \frac{V_2}{I_2} = r Z_{21} + Z_{22} \end{cases}$$

From the equation above, it is seen that input impedances, $\frac{V_1}{I_1}$ and $\frac{V_2}{I_2}$ are dependent up on the ratio r. These are the impedances that any impedance transforming networks must be designed to feed, and in order to calculate those input impedance, the mutual impedance must be known.

3.1.2. Field Theory Of Mutual Impedance

From [22], two antennas A and B are considered and placed near each other. The two antennas are assumed to have an electrically small feeding terminal. From the Reciprocity Theorem, when antenna A and B are located at different original point and near each other, the power is sent from A and received by B is equal to the average power which is sent by B and received by A. The equation can be represented by the equation (3.1a) and (3.1b) as following:

$$\iint_{S_{A+B}} \left(\vec{E}_A \times \vec{H}_B \right) \hat{n}.ds = \iint_{S_{A+B}} \left(\vec{E}_B \times \vec{H}_A \right) \hat{n}.ds \qquad (3.1a)$$

$$\iint_{S_{A+B}} \left(\vec{E}_A \times \vec{H}_B - \vec{E}_B \times \vec{H}_A \right) \hat{n}.ds = 0 \qquad (3.1b)$$

The two antennas A and B can be equivalent to two-ports network. The circuit can be shown as follow:

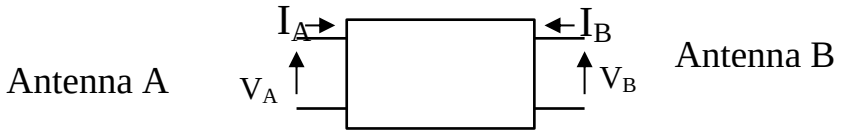

Figure 3.3 Diagram of two-ports network representing two antennas systems

$$\begin{cases} V_A = Z_{AA}.I_A + Z_{AB}.I_B & (3.2a) \\ V_B = Z_{BA}.I_A + Z_{BB}.I_B & (3.2b) \end{cases}$$

when antenna A is an open circuit, from equation (3.2a) we get:

$$Z_{AB} = \frac{V_A^{oc}}{I_B} \tag{3.3a}$$

when antenna B is an open circuit, from equation (3.2b) we get:

$$Z_{BA} = \frac{V_B^{oc}}{I_A} \tag{3.3b}$$

From the reciprocity theorem, we can see that (from Appendix B)

$$V_A^{oc} = \frac{1}{I_A} \oiint_{S_A} \left(\vec{E}_B . \vec{J}_A \right) . \hat{n} ds \tag{3.4a}$$

And

$$V_B^{oc} = \frac{1}{I_B} \oiint_{S_B} \left(\vec{E}_A . \vec{J}_B \right) . \hat{n} ds \tag{3.4b}$$

From equation (3.3) and (3.4) we get the formulation of mutual impedance as follow:

$$Z_{AB} = \frac{1}{I_B I_A} \oiint_{S_A} \left(\vec{E}_B . \vec{J}_A \right) . \hat{n} ds \tag{3.5a}$$

And

$$Z_{BA} = \frac{1}{I_A I_B} \oiint_{S_B} \left(\vec{E}_A . \vec{J}_B \right) . \hat{n} ds \tag{3.5b}$$

From equation 3.5a, we can see that the integration term is the coupling power that E_A exerts on H_B. The same as (3.5a), in equation (3.5b), the integration term shows the coupling power that E_B exerts on H_A.

From the appendix C, we can see that $Z_{AB} = Z_{BA}$.

Applying the formula in equation (3.5a) and (3.5b) to a pair of patch antennas, which are printed on the same plan of the grounded substrate. The length of the substrate is assumed to be infinity.

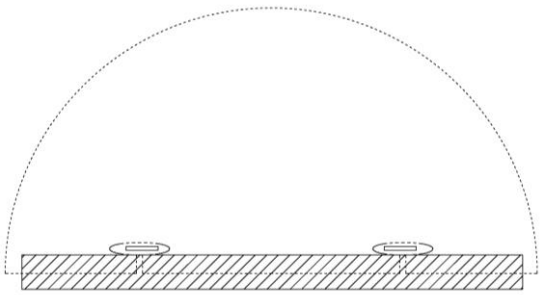

Figure 3.4 Symbol of two patches printed on the same substrate

From the equation (3.5a) we get:

$$Z_{AB} = \frac{1}{I_B I_A} \oiint_{S_A} \left(\vec{E}_B . \vec{J}_A \right) . \hat{n} ds \tag{3.6}$$

The surface of antenna A and antenna B is divided into:

$$S_A = S_A^{+} + S_A^{-} \tag{3.7}$$

Where S_A^{+} is the surface area of antenna A on the top

S_A^{-} is the surface area of antenna A on the bottom

$$S_B = S_B^{+} + S_B^{-} \tag{3.8}$$

Where S_B^{+} is the surface area of antenna A on the top

S_B^{-} is the surface area of antenna A on the bottom

The normal vector to surface of the patch is subdivided into:

$\hat{n}^{+}$ which is the outward vector normal to top surface

$\hat{n}^{-}$ which is the outward vector normal to bottom surface

So we get $\hat{n}^{-} = -\hat{n}^{+}$

From (3.6) $Z_{AB} = \frac{1}{I_B I_A} \oiint_{S_A} \left(\vec{E}_B . \vec{J}_A \right) . \hat{n} ds$

$$\vec{J}_A = \left(\vec{H}_A \Big|_{S_A^{+}} - \vec{H}_A \Big|_{S_A^{-}} \right) \times \hat{n}^{+} \tag{3.8}$$

$\vec{J}_A$ is the surface current on the thin surface of the patch antenna A.

The electric field $\vec{E}_B$ can be expressed in term of a substrate dyadic Green's function:

$$\vec{E}_B(\rho) = \iint_{S_{B(\text{patch})}} \overline{\overline{G}}_\rho(\rho \mid \rho').\vec{J}_B(\rho')ds' \tag{3.9}$$

$\overline{\overline{G}}_\rho(\rho \mid \rho')$ is the electric dyadic green function of the substrate

$\vec{J}_B(\rho')$ is the surface current on the thin substrate of patch B

ρ is the position vector to any points on patch A

ρ' is the position vector to any point on patch B

$$Z_{AB} = \frac{1}{I_A I_B} \iint_{S_{B(\text{patch})}} \iint_{S_{A(\text{patch})}} ds' \ \overline{\overline{G}}_\rho(\rho \mid \rho').\vec{J}_B(\rho')ds'\vec{J}_A(\rho)ds$$

$$Z_{AB} = \frac{1}{I_A I_B} \iint_{S_{A(\text{patch})}} ds \iint_{S_{B(\text{patch})}} ds' \ \overline{\overline{G}}_\rho(\rho \mid \rho').\vec{J}_B(\rho')\vec{J}_A(\rho) \tag{3.10}$$

In the above formula, the mutual impedance Z_{AB} is in the form of integral equation. To get the solution of the integral equation, we need to use numerical method.

3.2. Proposed Method

Mutual coupling is an undesired and unavoidable phenomenon; however, the knowledge of mutual coupling is important. From the previous chapters, the mutual coupling can be calculated by using the full-wave analysis numerical techniques. In addition to those full-wave numerical techniques, the approximation model of the mutual coupling between two microstrip patch antennas is going to be proposed in this research.

Firstly, the numerical technique will be used to calculate the mutual coupling between the two microstrip patch antennas. Secondly, find the approximation model that is suitable for physical characteristic of microstrip antennas. The model must contain some coefficients which can be found in next steps. Thirdly, Least-square optimization technique and the numerical data will be used to define the coefficients of the proposed model.

This research will focus only on the relation between the mutual coupling and the position of patch element. The position of patch antenna is divided into two

variables which are the spacing from center between two patch antennas and the azimuth angle of the two patches. Therefore, the proposed function will be a function of two variables which is $f(\rho,\phi)$. ρ is the spacing from center to center between the patches, and ϕ is the azimuth angle between the two patches as shown in Figure 3.5.

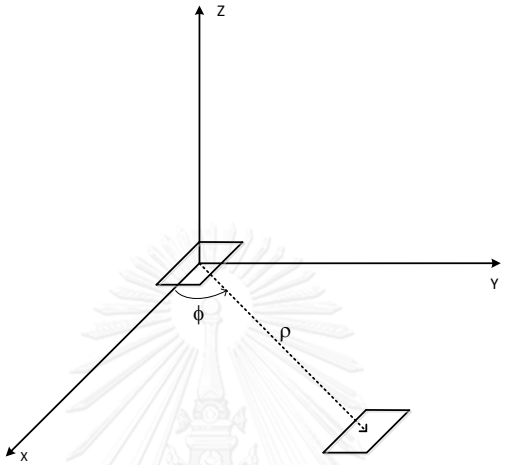

Figure 3.5 Coordinates of two coupling microstrip patches

3.2.1. Numerical Simulation

To calculate the numerical data of mutual coupling between two patch antennas, the EM simulation software will be used in this research. To calculate the numerical data, some parameters of the patch antenna element must be defined. The values of the parameters are as the following (the parameters are taken from EM simulation software manual):

1. The frequency that is used for model is f = 3GHz (wavelength λ_0 = 10cm)
2. The width of the patch antenna is W = 2.7 cm
3. The length of the patch antenna is L = 3 cm
4. The thickness of the substrate is h = 1mm
5. The shape of the patch element is rectangular

The configuration of the patch element is the same the figure below:

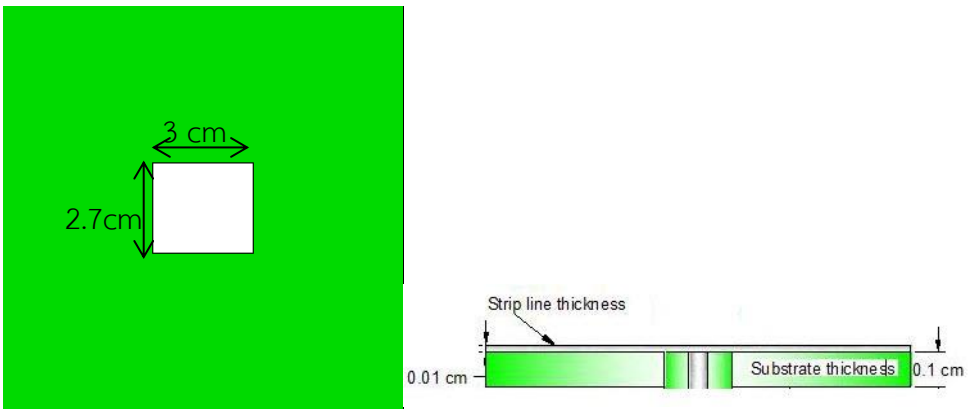

Figure 3.6 Thickness of substrate

Figure 3.7 Top view of patch antenna

From the above description, the approximation model of the mutual coupling is the function of two variables which the spacing and the angle. Therefore, to get the numerical data for the function of two variables, the distance between two patches and the angle when position of patch is changed along the azimuth angular direction, must be varied for each simulation.

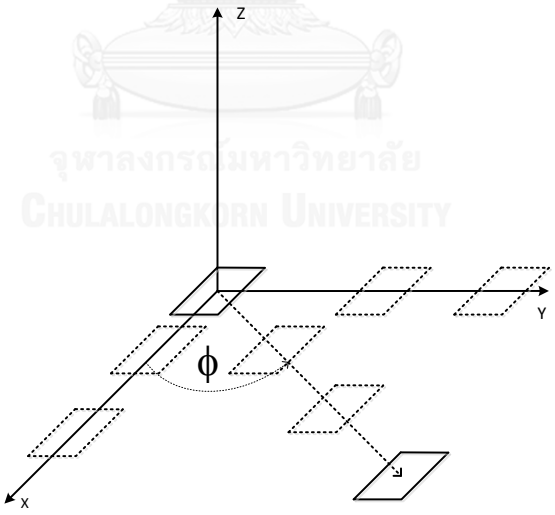

Figure 3.8 Coordinate of two antenna array

3.2.2 Proposed Model

From the previous section of 3.1.2 Field Theory Of The Mutual Impedance, The mutual impedance can be expressed in the form of the integration between the

electric field and the surface current on the antenna. The formulation can be expressed as the following (From 3.6):

$$Z_{AB} = \frac{1}{I_B I_A} \oiint_{S_A} \left(\vec{E}_B . \vec{J}_A \right) . \hat{n} ds$$

The patch antenna on a ground substrate is considered to the TM to z (TM_Z) direction. Consider a point source on the microstrip patch antenna with the moment of p, the electric field of that point source can be expressed as the following [23] (assuming $e^{-j\omega t}$ is the time dependence):

$$E_z = j \frac{p}{8\pi\omega\varepsilon} \int_{-\infty}^{\infty} dk_\rho \left[k_\rho^2 \cos\phi \left(1 - R^{TM}\right) H_1^{(1)}\left(k_\rho \rho\right) e^{jk_z z} \right] \tag{3.11}$$

Supposed that: $E_z\left(k_\rho\right) = j \frac{p}{8\pi\omega\varepsilon} \left[k_\rho^2 \cos\phi \left(1 - R^{TM}\right) H_1^{(1)}\left(k_\rho \rho\right) e^{jk_z z} \right]$ (3.12)

R^{TM} is the reflection coefficient

$H_1^{(1)}\left(k_\rho \rho\right)$ is the first order of the first kind of Hankel function

The tangential (transfers) components of the electric field can be found as the following [23]:

$$\vec{E}_t\left(k_\rho\right) = \frac{1}{k_\rho} \left[\vec{\nabla}_t \frac{\partial E_z\left(k_\rho\right)}{\partial z} - j\omega\varepsilon \vec{\nabla}_t \times \vec{H}_z\left(k_\rho\right) \right] \tag{3.13}$$

$$\vec{\nabla}_t = \hat{\rho} \frac{\partial}{\partial \rho} + \hat{\phi} \frac{1}{\rho} \frac{\partial}{\partial \phi} \tag{3.14}$$

The electromagnetic waves that propagate from the patch antenna are considered in the form of the cylindrical wave; thus, the coordinates in the electric field above are written in the form of cylindrical coordinate. The patch antenna is TM to z, thus the component H_z is zero, and we electric field as following:

$$\vec{E}_t\left(k_\rho\right) = \frac{1}{k_\rho} \left[\vec{\nabla}_t \frac{\partial E_z\left(k_\rho\right)}{\partial z} \right] \tag{3.15}$$

From (3.14) and (3.15), we get the transfers component of the electric field as following:

$$\vec{E}_t\left(k_\rho\rho\right)=\frac{1}{k_\rho^2}\begin{bmatrix}\hat{\rho}\left\{-\dfrac{p}{8\pi\omega\varepsilon}k_\rho^3k_z\cos\phi\left(1-R^{TM}\right)H_1^{(1)\prime}\left(k_\rho\rho\right)\right\}\\+\hat{\phi}\left\{\dfrac{p}{8\pi\omega\varepsilon\rho}k_\rho^2k_z\sin\phi\left(1-R^{TM}\right)H_1^{(1)}\left(k_\rho\rho\right)\right\}\end{bmatrix}.e^{jk_zz} \qquad (3.16)$$

From equation (3.6) and (3.16), the mutual impedance can be expressed as following:

$$Z_{AB}=\frac{1}{I_BI_A}\oiint_{S_A}\left(\int_{-\infty}^{\infty}\left(\frac{1}{k_\rho^2}\begin{bmatrix}\hat{\rho}\left\{-\dfrac{p}{8\pi\omega\varepsilon}k_\rho^3k_z\cos\phi\left(1-R^{TM}\right)H_1^{(1)\prime}\left(k_\rho\rho\right)\right\}\\+\hat{\phi}\left\{\dfrac{p}{8\pi\omega\varepsilon\rho}k_\rho^2k_z\sin\phi\left(1-R^{TM}\right)H_1^{(1)}\left(k_\rho\rho\right)\right\}\end{bmatrix}.e^{jk_zz}dk_\rho\right).\vec{J}_A\right).\hat{n}ds \quad (3.17)$$

From the equation (3.17), we can see that the mutual impedance is the function of the Hankel function, which is a combination of Bessel's function.

3.2.2.1 Element Spacing Variable (ρ/λ)

In this research, the mutual impedance is written into the form of resistance (Real Part) and reactance (Imaginary Part) as following:

$$Z=R+jX \quad (3.18)$$

Instead of finding the model to represent the whole formulation, the formulation of mutual resistance R and mutual reactance X will be found separately. From equation (3.18), the mutual impedance is in term of Hankel function. In [23], from the wave concept, the cylindrical wave can be represented by the superposition of the Hankel functions. However, Hankel function is the combination of the Bessel's functions. Therefore, the formula with Bessel's functions will be proposed to find the approximation model of the mutual impedance. The Hankel function in equation (3.18) is the first kind and the first order with argument $k_\rho\rho$ which present the element spacing between the two antennas; therefore the Bessel's function in the proposed model will also be in the first kind and the first order with argument $k_\rho\rho$. The proposed model with the element spacing variable will be in form as following:

$$R=\sum_{m=1}^{M}\mathrm{A}_mJ_1\left(\mathrm{B}_m\left(\frac{\rho}{\lambda}\right)+\mathrm{C}_m\right) \qquad (3.19)$$

$$X = \sum_{n=1}^{N} \mathrm{E}_n J_1\left(\mathrm{F}_n\left(\frac{\rho}{\lambda}\right) + \mathrm{G}_n\right) \tag{3.20}$$

From the equation (3.19) and (3.20), $\mathrm{A_m}$, $\mathrm{B_m}$, $\mathrm{C_m}$, $\mathrm{E_n}$, $\mathrm{F_n}$, $\mathrm{G_n}$ are the coefficients will be determined by using least-square optimization.

3.2.2.2 Azimuthal Angle Variable (ϕ)

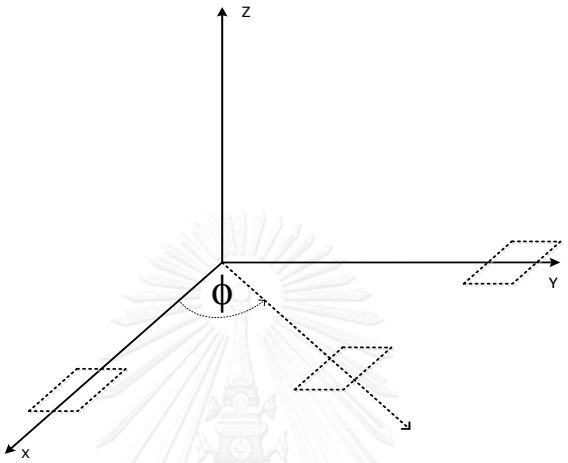

Figure 3.9 Coordinate of ϕ variation

The Azimuth angle between the two patches contains the periodic behavior, therefore, the angle ϕ should be put as the phase sift inside the equation (3.19) and (3.20). Thus, after inserting the azimuth angle ϕ inside the equation (3.19) and (3.20) the approximation model of the mutual resistance R and mutual reactance X will be as the following:

$$R = \sum_{m=1}^{M} \mathrm{A}_m J_1\left(\mathrm{B}_m\left(\frac{\rho}{\lambda}\right) + \mathrm{C}_m\phi + \mathrm{D}_m\right) \tag{3.21}$$

$$X = \sum_{n=1}^{N} \mathrm{E}_n J_1\left(\mathrm{F}_n\left(\frac{\rho}{\lambda}\right) + \mathrm{G}_n\phi + \mathrm{H}_n\right) \tag{3.22}$$

where $\mathrm{D_m}$, $\mathrm{H_n}$ are also determined by the least-square optimization method.

3.2.3 Coefficients Determination

From the propose formulation above, there are some unknown coefficient which are required to define in order to use the completed model to calculate the mutual impedance between two rectangular patch antennas. To determine those

unknown coefficients, the numerical data from the EM simulation software along with the least-square optimization technique will be used.

The concept of least-square optimization is a method that is used to find the unknown parameters which give the smallest total value of error square. In this research, the unknown parameters are the unknown coefficients in the proposed model. The total value of error is sum of error between the numerical values and the empirical values. To find the unknown coefficients which give the minimum value of the error, the Nelder-Mead minimization technique will be used. In this optimization procedure, there are some procedures which must be followed. To find the point that gives a minimum value of a function, one guessing point must be provides. Thus, one guessing set of the unknown coefficients must be put in the optimization technique. However, every guessing point can give different optimum results which are local and global minimum results. The local optimum point is a point that is optimum for one guessing point. The global optimum point is a point that is optimum for the whole system. Since the guessing point can be any points, in this research, the guessing point is set to be random. However, those random points are not guarantee that they will give the global minimum point, so the constraint of the minimum error is set. In addition, the total value of error also depends on the number of terms inside the proposed model. The more terms of functions inside the proposed model has given better result. Although the number of terms can be increased as many, the total value of error is limited. The total value of error will not be improved much. To avoid this trade off, the number of terms in the proposed model will be increased in accordance with the rigorous result of the model. To find a set of coefficients that optimize total error, Nelder-Mead Method will be used in this research.

Nelder-Mead Method is a simplex method for finding a local minimum of a multi-variable function. In case of the two variables function, a simplex is a triangle, and the method is a pattern search that compares function values at the three vertices of a triangle. The worst vertex, where $f(x, \mathrm{y})$ is the largest, is rejected and replaced with a new vertex. A new triangle is formed and the searching is continued.

The process will generate a lot of triangle sequentially (that triangles might have different shapes), for which the values of function at the vertices is getting smaller and smaller.

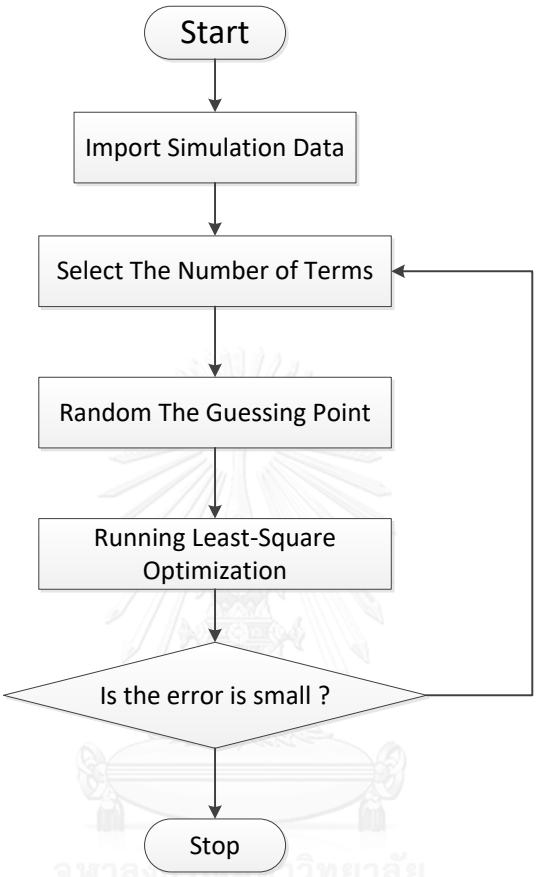

Figure 3.10 Flow chat of least-square optimization

The size of the angles is being reduced and the coordinates of the minimum point are found. The algorithm is stated using the term of simplex (a generalized triangle in N dimensions) and will find the minimum of a function of N variables. Using Nelder-Mead Method is effective and computationally compact. The algorithm of the Nelder-Mead Method can be found in [24] [25] [26].

Approximation model for both mutual resistance R and mutual reactance X will be found by using the same procedure of least-square optimization method. Either model of mutual resistance or mutual reactance will be explained in the following. The least-square function can be expressed as below:

$$L(\beta)=\sum_{\rho}\sum_{\phi}\left[\bar{R}_{\rho,\phi}-R_{\rho,\phi}(\beta)\right]^2 \tag{3.23}$$

where $\bar{R}_{\rho,\phi}$ is the mutual resistance from EM simulation software

$R_{\rho,\phi}(\beta)$ is the mutual resistance from the proposed model

β represents a set of coefficients $\mathrm{A_m}$, $\mathrm{B_m}$, $\mathrm{C_m}$, $\mathrm{D_m}$

The parameter β will be determined to get a minimum value of $L(\beta)$, so that the values of $\bar{R}_{\rho,\phi}$ and $R_{\rho,\phi}(\beta)$ are approximately equal. Nelder-Mead Method is applied to find $\beta_{\min}$. The procedure to find $\beta_{\min}$ is as the following:

1. Randomly generate 'n' sets of β (n= dimension of β plus 1)
2. Order β according to the value of $L(\beta)$ from smallest $L(\beta)$ to biggest $L(\beta)$:

$$L(\beta_1)\le L(\beta_2)\le L(\beta_3)\le\cdots\le L(\beta_n)$$

3. Calculate β_c which is the centroid value of all β except β_n
4. Compute reflected point $\beta_r=\beta_c+\alpha(\beta_c-\beta_n)$ (α is refection coefficient α=1). If the reflected point is better than the second worst, not better than the best, i.e. $L(\beta_1)\le L(\beta_r)<L(\beta_{n-1})$, then a new simplex is obtained by replacing the worst point β_n with the reflected point β_r and go to step 2.
5. If the reflected point is the best point so far, $L(\beta_r)<L(\beta_1)$, then compute the expanded point $\beta_e=\beta_c+\gamma(\beta_r-\beta_c)$, ($\gamma$ is an expansion coefficient γ=2), then if the expanded point is better than the reflected point, i.e. $L(\beta_e)<L(\beta_r)$, then a new simplex is obtained by replacing the worst point β_n with the expanded point β_e, and go to step 2. Else obtain a new simplex by replacing the worst point β_n with the reflected point β_r, and go to step 2. Else (i.e. reflected point is not better than second worst) continue to step 6.

6. Here, it is certain that $L(\beta_r) \geq L(\beta_n)$, then compute contracted point $\beta_x = \beta_c + \chi(\beta_n - \beta_c)$(0<χ<0.5 χ is the contraction coefficient). If the contracted point is better than the worst point, i.e. $L(\beta_x) < L(\beta_n)$, then obtain a new simplex by replacing the worst point β_n with the contracted β_x , and then go to step 2. Else go to step 7.
7. For all but the best point, replace the point with $\beta_i = \beta_1 + \eta(\beta_i - \beta_1)$ for all $i \in \{2, \cdots, n\}$ then go to step 2.

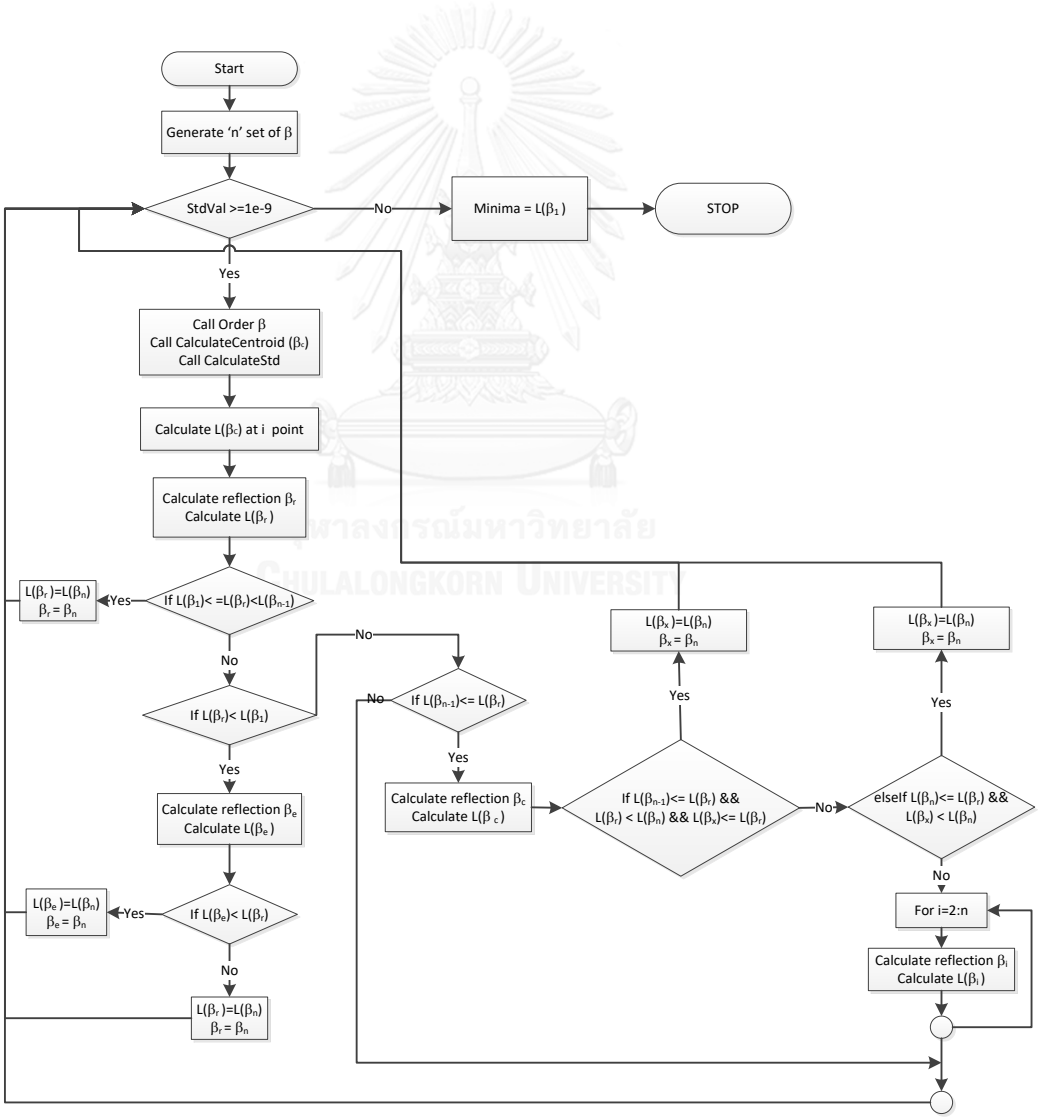

Figure 3.11 Coefficients Determination Diagrams

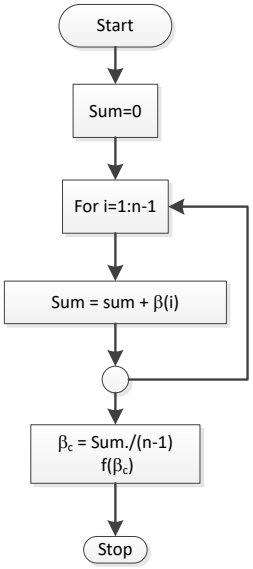

Figure 3.13 Centroid Calculation

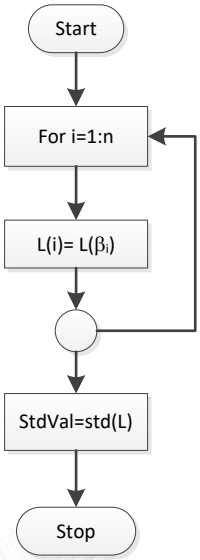

Figure 3.14 Tolerance Calculation

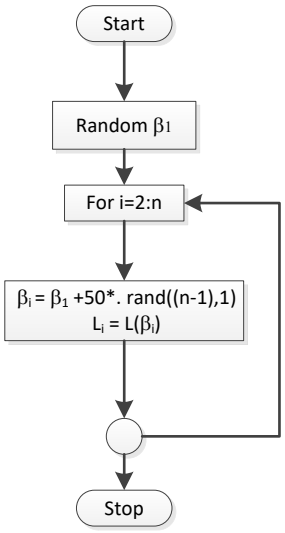

Figure 3.12 Generate 'n' set of β

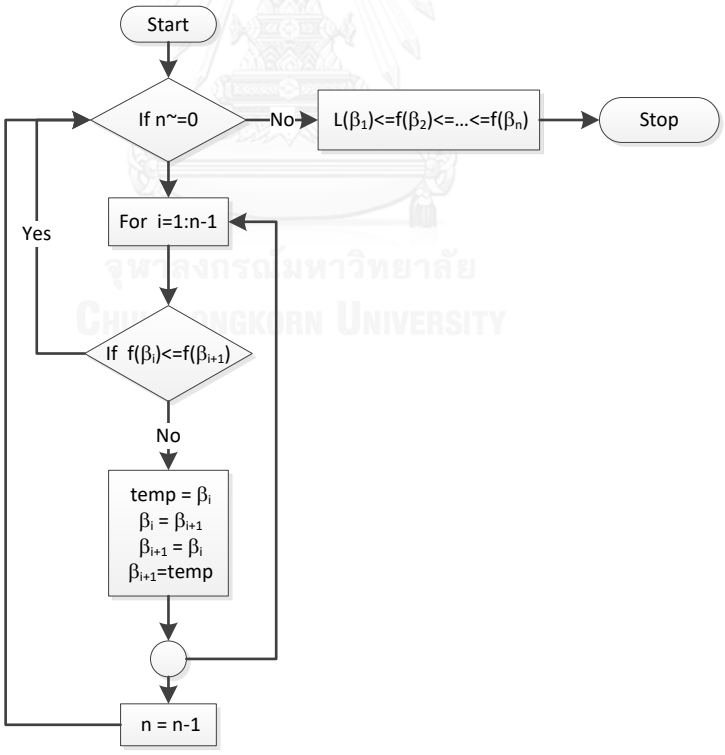

Figure 3.15 Ordering value of $L(\beta_i)$

Chapter 4 RESULT AND DISCUSSION

From the previous chapter, the proposed function ($f(\rho,\phi)$) is a function of two variables which are element spacing (ρ) and azimuth angle (ϕ). In addition, the proposed function ($f(\rho,\phi)$) is in the form of a summation of Bessel's function, so that if the number of terms of Bessel's function are increased, the approximation models will give a better results. However, the number of terms can be increased as many as wanted since the total value of error is constrained. Moreover, the total value of error will not be improved much when the error is getting close to the constrained boundary, and the proposed formulations are looked more complex when there are more terms of Bessel's function. Therefore, there is a tradeoff between the number of terms and the total value of error.

In addition to the tradeoff of the number of terms, the accuracy of the proposed models also depends on the number of numerical data points which will be employed in the least-square optimization technique. Theoretically, if many data points are going to be used in the optimization process, the accuracy of the proposed models is also good, although more time and resources are needed to get more data points. As the proposed model is the function of two variables, the data points must have 2 dimensions, and they must be sampled along the element spacing and azimuth angle. If the sampling rate is small along each dimension, there will be a lot of data points. However, the time for simulating the numerical data is also long. If the data points can be reduced as many as possible with a good accuracy, time consumption problems can be also solved and more resource can be also saved.

From chapter 3, when the mutual impedance is studied in term of the element spacing, the proposed models are in the form of Bessel's functions which are sinusoidal periodic function. In order to plot or to find the function of a sinusoidal characteristic, only peak points and zeros crossing point are needed. Therefore, the required points along element spacing variable can be reduces. For the azimuth angle dimension, the characteristic of this variable is periodic, and these

are symmetric between the four quadrants of the circle, so that this research will study within 0 to $\pi/2$ rad only for ϕ . For the sampling rate along the ϕ dimension, there will be some discussions.

4.1. Selection Of The Number Of Terms

In order to solve the tradeoff between the total value of error and the complexity of the proposed models, the selection of the number of terms must be optimized. For the element spacing variable, the range of variable ρ will be studied within 0.5λ to 2.48λ. Within this range, only peak points and zero crossing points are taken to use for determining the proposed models. For variable ϕ , the sampling rate is $\pi/36$ rad (5°) within the range of 0 to $\pi/2$ rad. In this research, mutual impedance is written in term of mutual resistance (real part) and mutual reactance (imaginary part). Therefore, the mutual resistance and mutual reactance will be studied separately. The results bellow will show the relation between mean-square error and the number of terms of Bessel's function in the approximation model of mutual resistance.

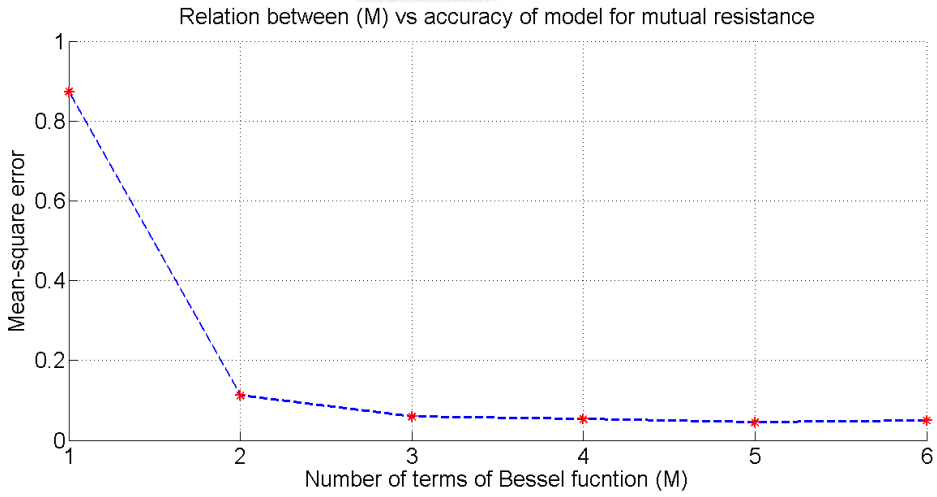

Figure 4.1 Relation between mean-square error Vs number of terms of Bessel function in model of mutual resistance

Figure 4.1 shows that when the number of Bessel terms is increased, the mean-square error of the proposed model is decreasing. However, starting from M=3 the mean-square error is slightly decreasing and the curve is almost constant.

Therefore the number of Bessel terms which are proposed for mutual resistance is three terms (M=3).

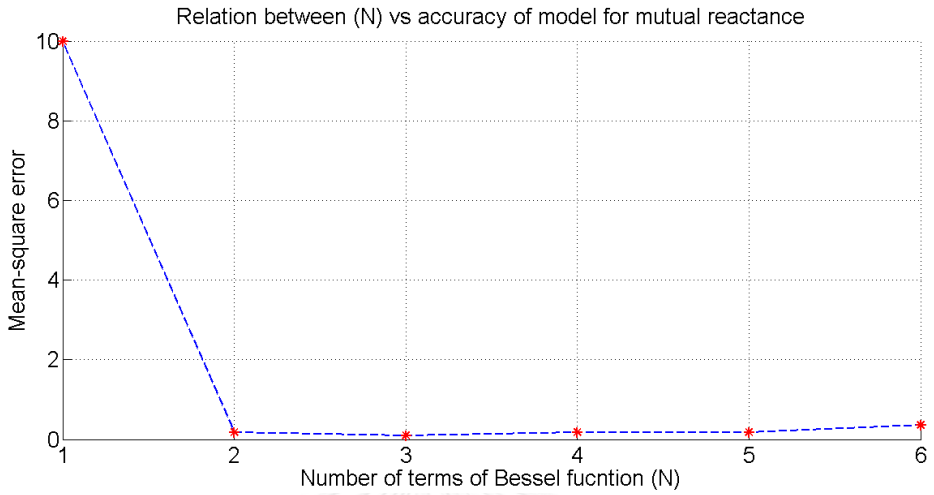

Figure 4.2 Relation between mean-square errors Vs Bessel terms in proposed model for mutual reactance

The Figure 4.2 above shows that mean-square error decreases to smallest values when the number of Bessel terms is equal to 3. From N=3 to N=6, the mean-square slightly increase. Therefore, the number of Bessel terms that is used in proposed model for mutual reactance is equal to 3. For more clear, Appendix C will show the result in 2D, so that the result can be easily observed for the accuracy.

4.2. Sampling Point A Long Azimuth Angle ϕ

The Figures in section 4.1, the azimuth angle ϕ is sampled at the rate of $\pi/36$ rad (5°) with the range 0 to $\pi/2$rad (90°). Therefore, there are a lot of points to be simulated in order to get the approximation model. In this section, the sampling rate along the azimuth angle will be discussed. The accuracy of the approximation model will be compared when the sampling rate along the azimuth angle ϕ is changed.

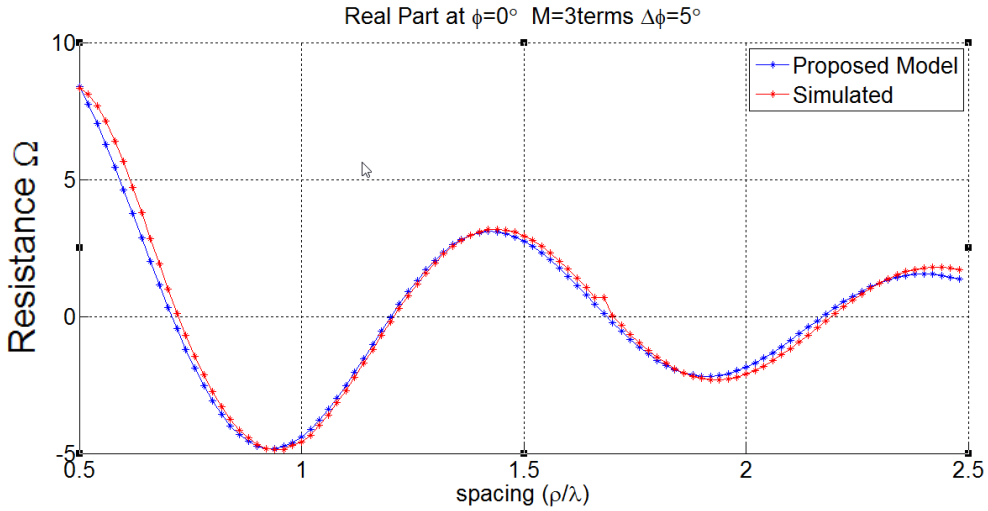

Figure 4.3 Comparison between proposed model and simulation at ϕ=0° with $\Delta\phi$=5°

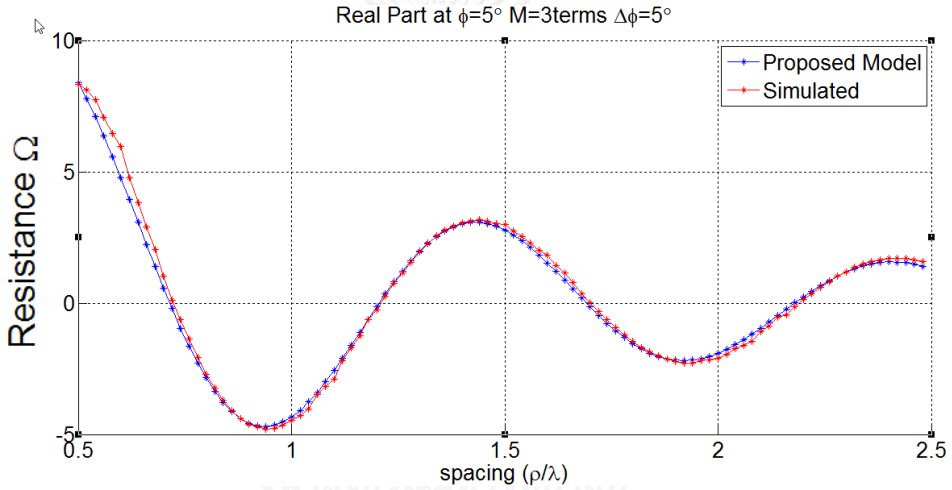

Figure 4.4 Comparison between proposed model and simulation at ϕ=5° with $\Delta\phi$=5°

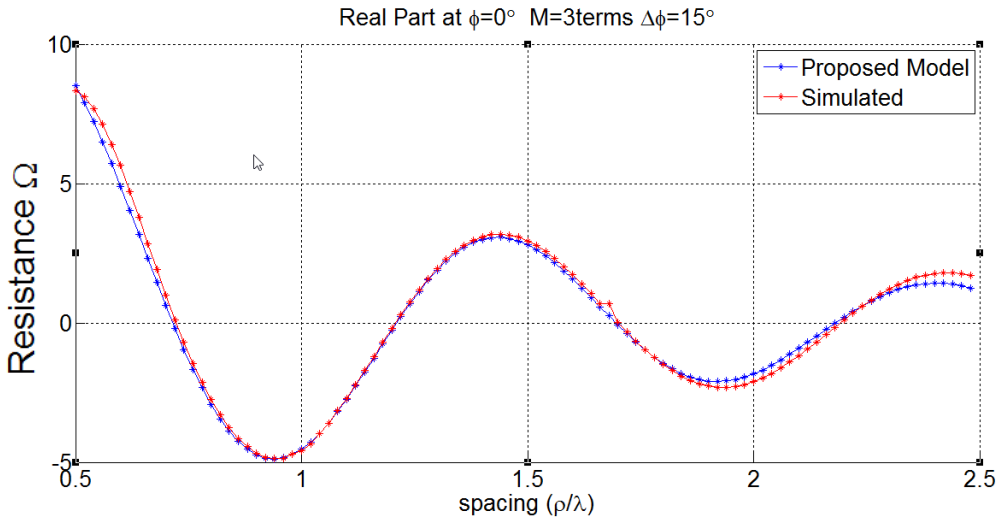

Figure 4.5 Comparison between proposed model and simulation at ϕ=0° with $\Delta\phi$=15°

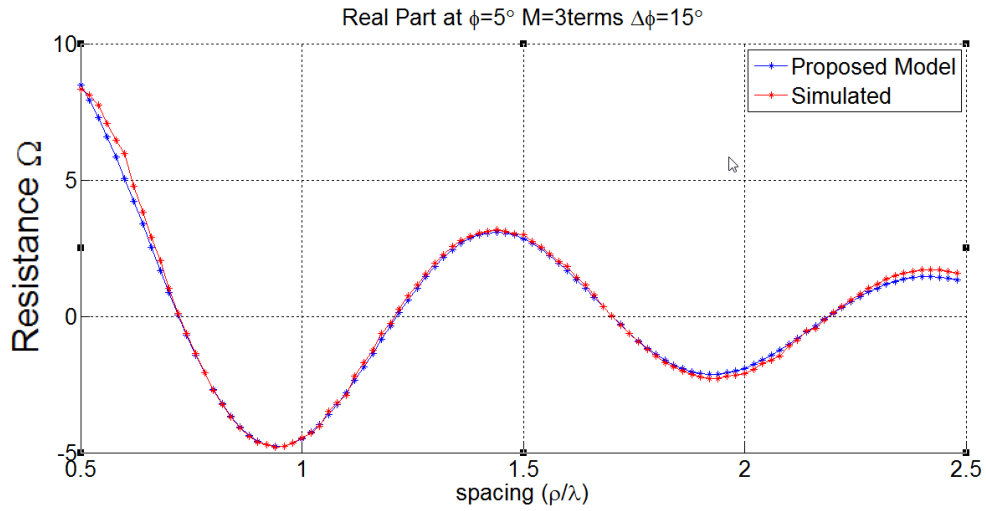

Figure 4.6 Comparison between proposed model Vs simulation at ϕ=0° with $\Delta\phi$=15°

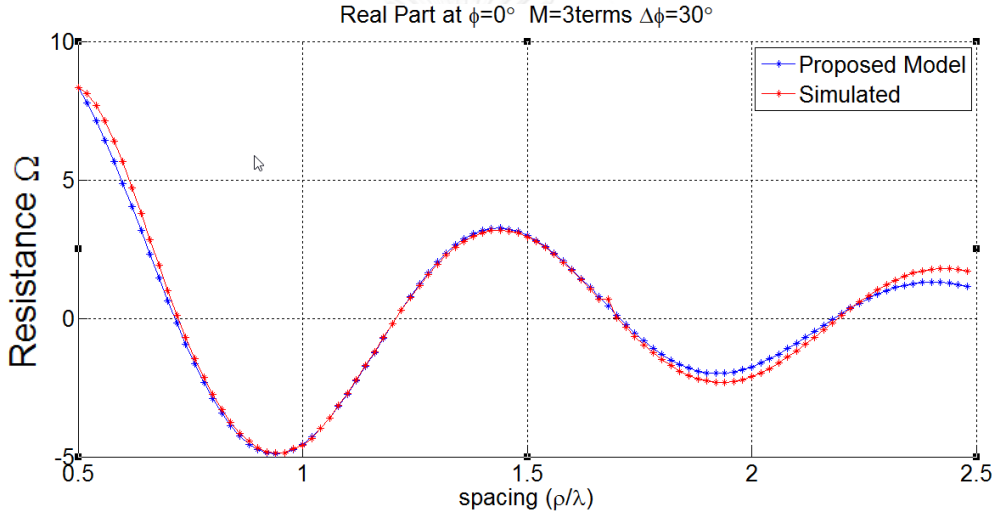

Figure 4.7 Comparison between proposed model and simulation at ϕ=0° with $\Delta\phi$=30°

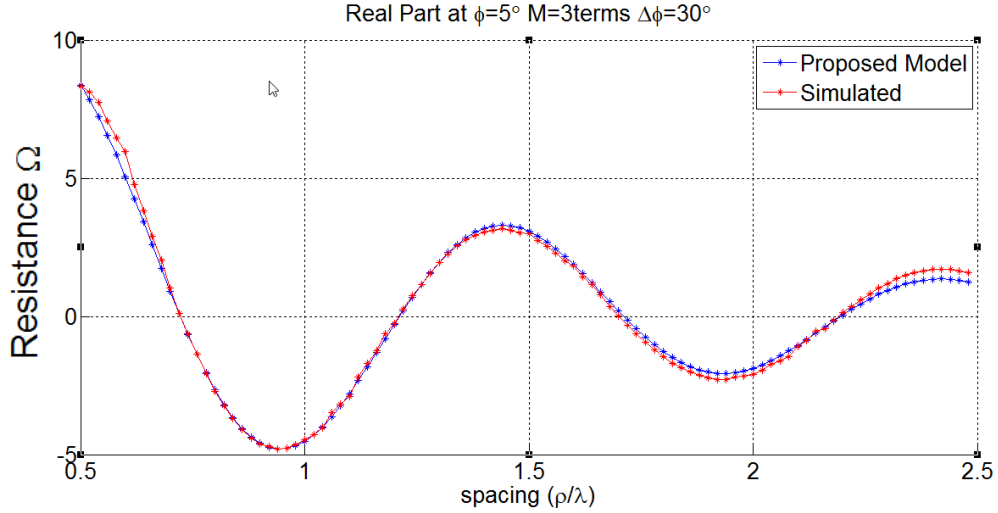

Figure 4.8 Comparison between proposed model Vs simulation at ϕ=0° with $\Delta\phi$=30°

The Figure 4.5, 4.6, 4.7, 4.8, 4.9, 4.10 above show mutual resistance results from the approximation model and from the simulation. The difference between Figure 4.5, 4.7 and Figure 4.9 is the sampling rate along azimuth variable, but the number of terms of Bessel function is used the same (three terms of Bessel's function). Figure 4.5 shows results when the azimuth angle ϕ is incremented every π/36rad (5°). Figure 4.7 shows results when the azimuth angle ϕ is incremented every π/12rad (15°). Figure 4.9 shows results when the azimuth angle ϕ is incremented every π/6 (30°). Therefore, the number of points of Figure 4.7 which must be calculated by numerical method (full-wave analysis) is less than that of Figure 4.5. For Figure 4.9, the number of numerical data points which are required is the least. However, from Figure 4.5 to Figure 4.10 show that the accuracy in Figure 4.9 and Figure 4.10 is almost the same as or even better than the accuracy in Figure 4.5 and Figure 4.6 and also the same as accuracy in Figure 4.7 and 4.8, to be clear the more numerical can be verified in the appendix D. In order to save time and resource as well as to have a good accuracy, the sampling rate along angle ϕ can be at π/6 rad (30°).

The Figure 4.8, 4.9, 4.10 below show mutual reactance results from the approximation models comparing with results from the simulation. The difference between this Figure4.8 to Figure 4.10 is the sampling rate along azimuth variable, but the number of terms of Bessel function is used the same (three terms of Bessel's function).

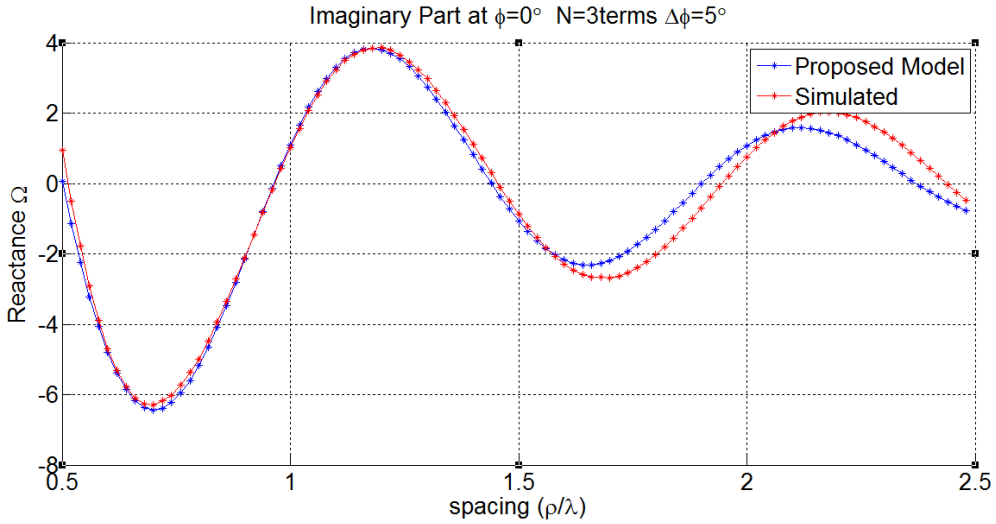

Figure 4.9 Comparison between proposed model Vs simulation at $\phi=0^{\circ}$ with $\Delta\phi=5^{\circ}$

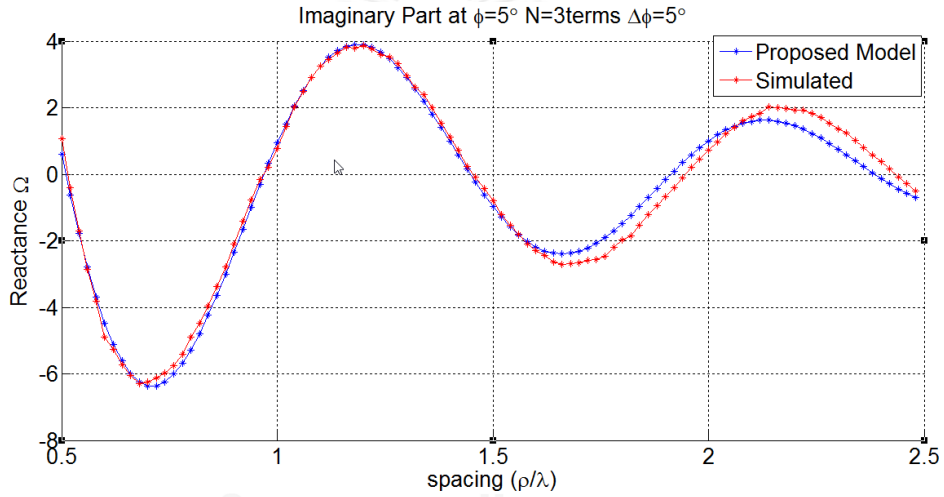

Figure 4.10 Comparison between proposed model Vs simulation at $\phi=5^{\circ}$ with $\Delta\phi=5^{\circ}$

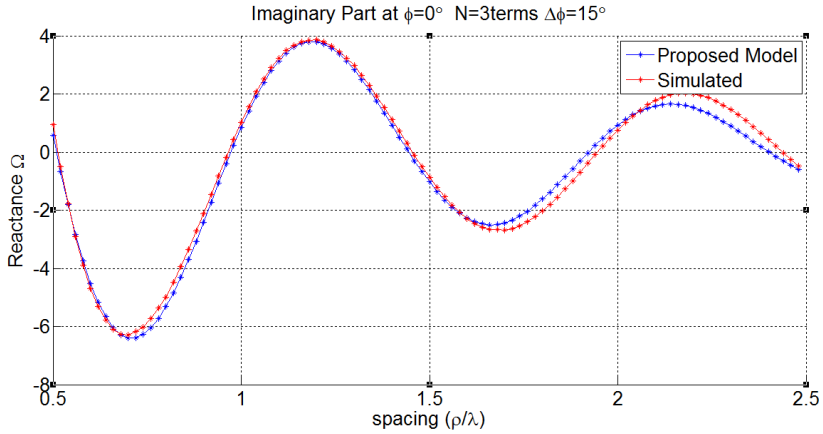

Figure 4.11 Comparison between proposed model Vs simulation at $\phi=0^{\circ}$ with $\Delta\phi=15^{\circ}$

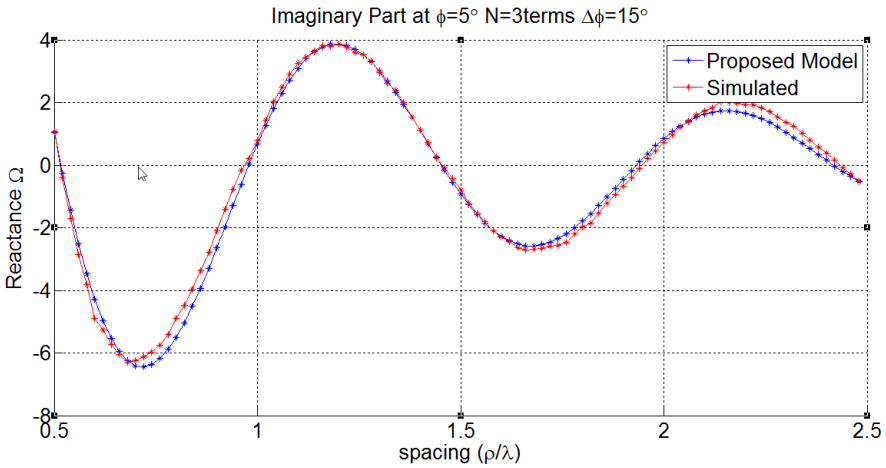

Figure 4.12 Comparison between proposed model Vs simulation at ϕ=5° with $\Delta\phi$=15°

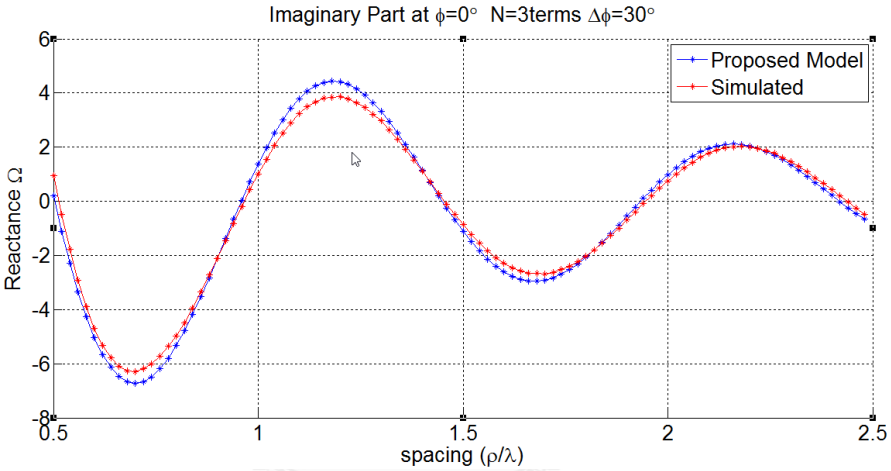

Figure 4.13 Comparison between proposed model Vs simulation at ϕ=0° with $\Delta\phi$=30°

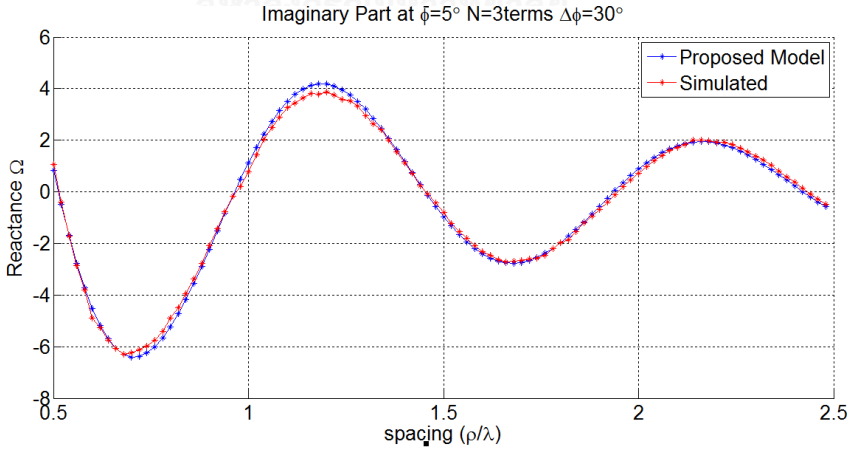

Figure 4.14 Comparison between proposed model Vs simulation at ϕ=5° with $\Delta\phi$=30°

Figure 4.11 and 4.12 show results when the azimuth angle ϕ is incremented every π/36 rad (5°). Figure 4.13 and 4.14 show results when the azimuth angle ϕ is incremented every π/12 rad (15°). Figure 4.15 and 4.16 show results when the

azimuth angle ϕ is incremented every $\pi/6$ rad (30°). Therefore, the number of points of Figure 4.13 and 4.14, which must be calculated by numerical method (full-wave analysis), is less than that of Figure 4.11 and 4.12. For Figure 4.15 and 4.16, the number of numerical data points which are required is the least. However, from Figure 4.11 to Figure 4.14 show that the accuracy in Figure 4.13 and 4.14 is almost the same as the accuracy in Figure 4.11 and 4.12, and the accuracy in Figure 4.15 and 4.16 is more better than in Figure 4.11 to 4.14. Moreover, Figure 4.15 and 4.16 require less point than in Figure 4.11 to 4.14, since the increment of angle ϕ is greater. Therefore, the increment of angle ϕ should be 30°. At this increment rate, the accuracy is acceptable and the needed data points can also be reduced.

From the discussion above, the number of terms that is suitable for the approximation of mutual impedance is 3; therefore, equation (3.20) and (3.21) become as the following expression:

$$R = \sum_{m=1}^{3} \mathrm{A}_m J_1\left(\mathrm{B}_m\left(\frac{\rho}{\lambda}\right) + \mathrm{C}_m\phi + \mathrm{D}_m\right) \tag{4.1}$$

$$X = \sum_{n=1}^{3} \mathrm{E}_n J_1\left(\mathrm{F}_n\left(\frac{\rho}{\lambda}\right) + \mathrm{G}_n\phi + \mathrm{H}_n\right) \tag{4.2}$$

Where $\frac{\rho}{\lambda}$ is unit less

ϕ is in radian

The set of the equation (4.1) are

$$\left\{\begin{array}{l} \mathrm{A}_1\text{=-1.2462}\,,\,\mathrm{B}_1\text{=5.9247},\,\mathrm{C}_1\text{=3.4502}\,,\,\mathrm{D}_1\text{ =3.8665}\,;\,\mathrm{A}_2\text{=13.3664}\,,\,\mathrm{B}_2\text{=6.4472},\\ \mathrm{C}_2\text{=-0.897}\ \,,\mathrm{D}_2\text{ =1.5937}\,;\,\mathrm{A}_3\text{=13.0411}\,,\,\mathrm{B}_3\text{=6.6776}\,,\,\mathrm{C}_3\text{=-0.5416}\,,\mathrm{D}_3 = -0.4498 \end{array}\right\}$$

The set of the equation (4.2) are

$$\left\{\begin{array}{l} \mathrm{E}_1\text{=1.1496}\,,\,\mathrm{F}_1\text{=6.5234}\,,\,\mathrm{G}_1\text{=4.2742}\ \,\mathrm{H}_1 = 7.1200\,;\,\mathrm{E}_2\text{=46.8053}\,,\,\mathrm{F}_2\text{=6.5576}\,,\\ \mathrm{G}_2\text{=-0.7851}\,,\mathrm{H}_2 = 0.2179\,;\,\mathrm{E}_3\text{=50.1531}\,,\,\mathrm{F}_3\text{=6.6397}\,,\,\mathrm{G}_3\text{=-0.6653}\,,\mathrm{H}_3 = -2.5871 \end{array}\right\}$$

4.3. The Effect Of The Orientation Of Patch Elements

The magnitude of mutual impedance between two rectangular patch antennas also depends on the orientation of the two patches antenna. The mutual

coupling is the phenomenon that is occurred by the effect of the fringing field between edges of the two patch antennas which face to each other. When the area of the facing edges or surface is large, the magnitude of the mutual coupling is also large. When the area of the facing edge or surface is small, the magnitude of the mutual coupling is also small. For the rectangular patch antenna, the mutual impedance is strong when the two rectangular patches are parallel to each other. When the two rectangular patches are parallel to each other, the area of facing edge is the big. The area is getting small when orientation of either antenna is changed, or when both of the two patch antenna rotate. Figure 4.11, Figure 4.12 and Figure 4.13 show the orientation geometries of two patch antennas on the horizontal plan. Figure 4.11 is when orientation of an antenna is changed, Figure 4.12 is when two patch antennas are parallel to each other, and Figure 4.13 is when orientation of both antennas are changed at the same angle. Thus, the mutual impedance between the two antennas is also getting smaller in Fugure 4.11 and Figure 4.13.

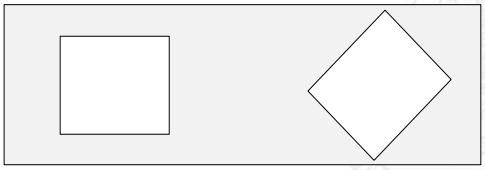

Figure 4.15 One antenna is tilted

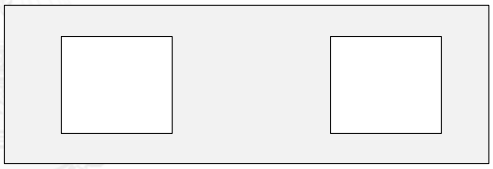

Figure 4.16 both antennas are parralel

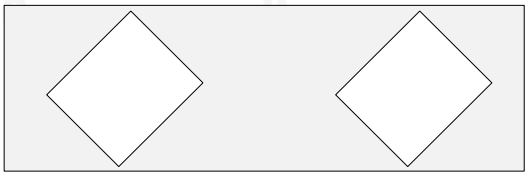

Figure 4.17 Both antennas are titled

Figure 4.14 shows results of magnitude of mutual impedance between two patch antennas when the orientation of one antenna is changed. The Figure 4.14 can be concluded that the magnitude of mutual impedance is getting smaller when the orientation angle of one antenna is at 75° or 90°.

Figure 4.15 shows result of magnitude of mutual impedance between two patch antennas when the orientation of both antennas is changed at the same angle.

The Figure 4.15 can be assumed that the magnitude of mutual impedance is getting smaller when the orientation angle of both antennas is at 45°.

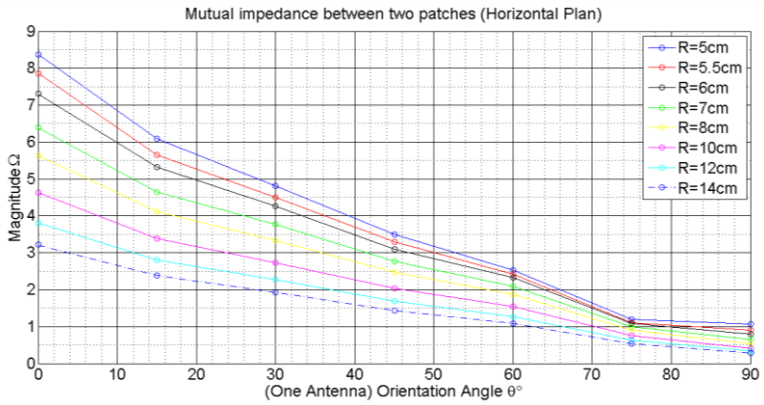

Figure 4.18 Magnitude of one tilted antenna

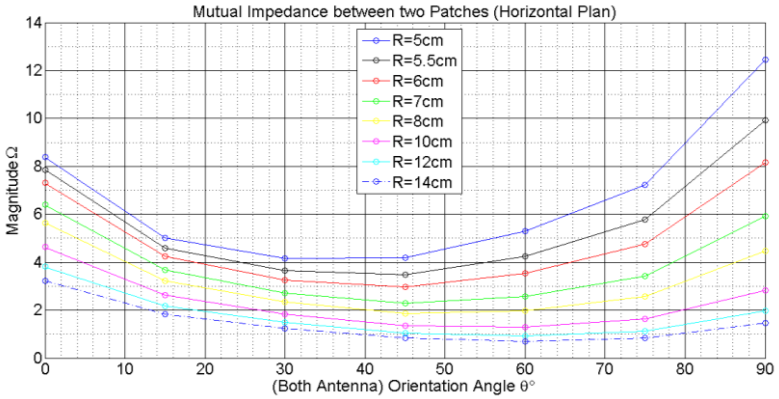

Figure 4.19 Magnitude of both tilted antennas

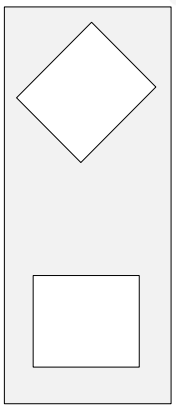

Figure 4.20 One tilted antenna

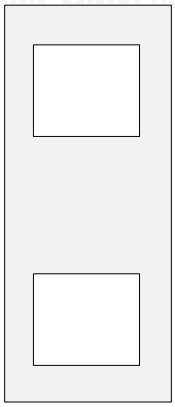

Figure 4.21 Two parallel

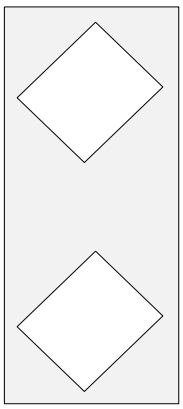

Figure 4.22 Two tilted

Figure 4.16, Figure 4.17, and Figure 4.18 show the orientation geometries of two patch antennas on the vertical plan. Figure 4.16 is when orientation of an antenna is changed, Figure 4.17 is when two patch antennas are parallel to each othe, and Figure 4.18 is when orientation of both antennas are changed at the same angle. Thus, the mutual impedance between the two antennas is also getting smaller in Figure 4.16 and Figure 4.18.

The results bellow show the effect of the orientation between two patch antennas on the magnitude of mutual impedance, when the two patch antennas are on the vertical geometry as shown in Figure 4.16 and Figure 4.18.

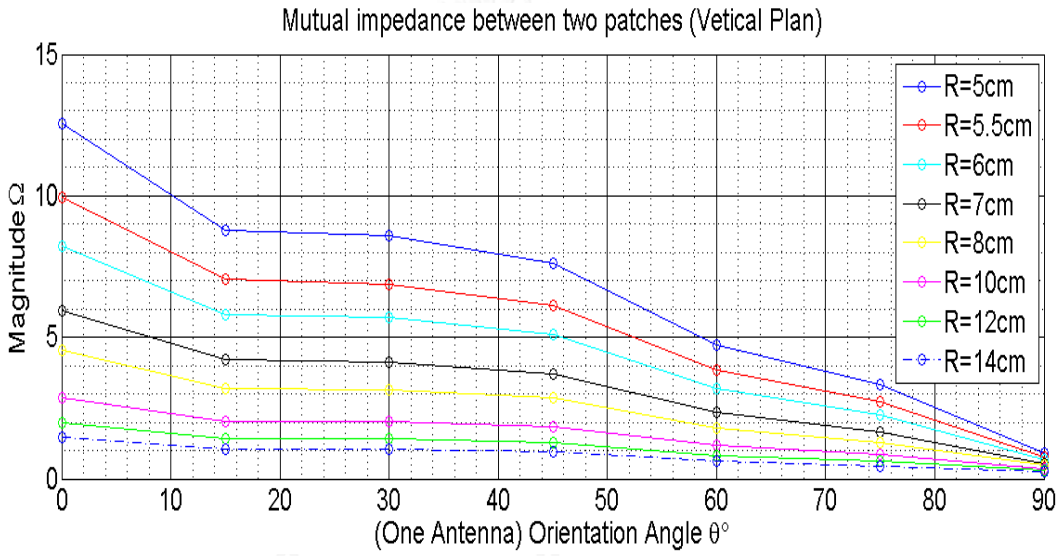

Figure 4.23 Magnitude of one tilted antenna

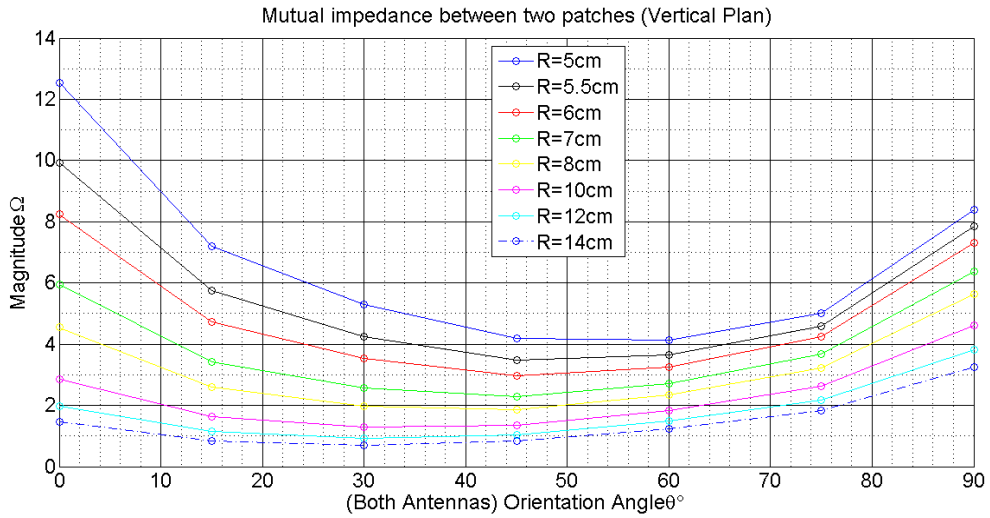

Figure 4.24 Magnitude of both tilted antennas

Figure 4.19 shows the results of magnitude of mutual impedance, when orientation angle of one antenna is changed. From the results, the magnitude of mutual impedance is getting the smallest when the orientation angle of one antenna is at 90°. Figure 4.20 shows the results of magnitude of mutual impedance, when the orientation angle of both antennas is changed. From the results, the magnitude of mutual impedance is getting small when the orientation angle of both antennas is at 45°.

4.4 Extrapolation Comparison

The approximation models, which are found in this research, are capable to calculate the mutual impedance within the interval of spacing that is used in the research only. However, the extrapolation comparison will show the accuracy of the approximation models when the element spacing is out of the domain which is used in this research. The results of the comparison will be shown as the following Figures 4.21 to 4.28:

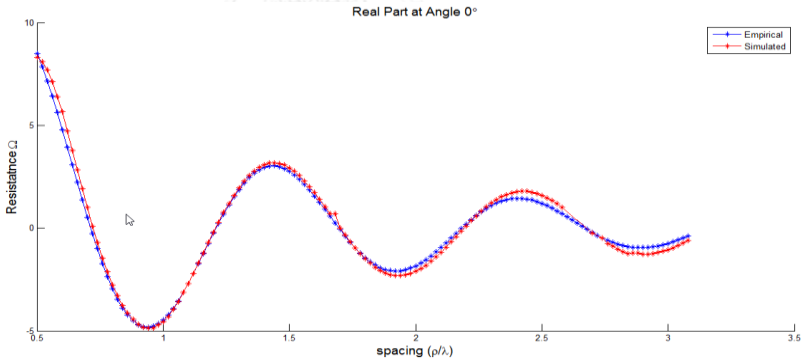

Figure 4.25 Real part at ϕ 0°

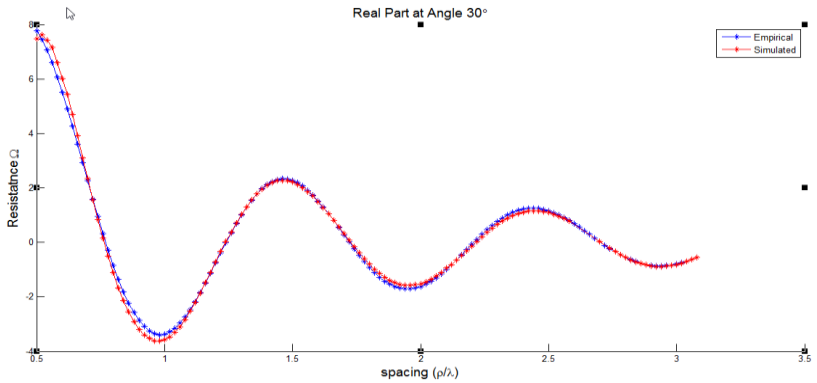

Figure 4.26 Real Part at ϕ 30°

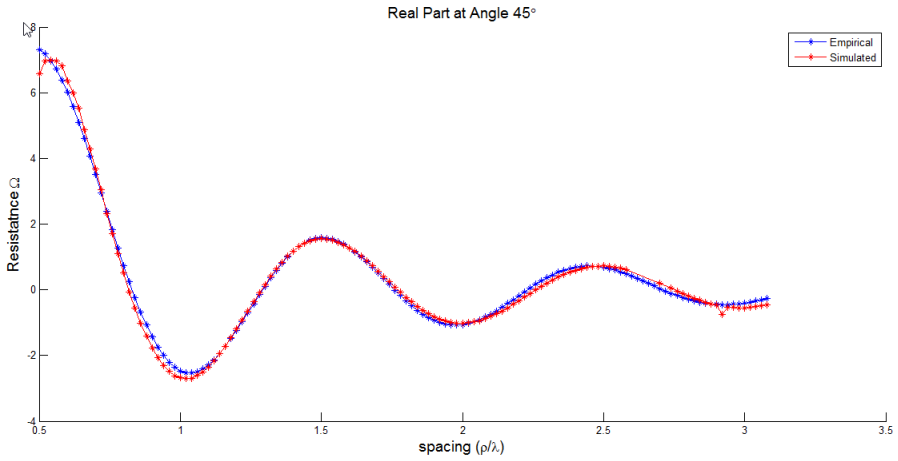

Figure 4.27 Real part at ϕ 45°

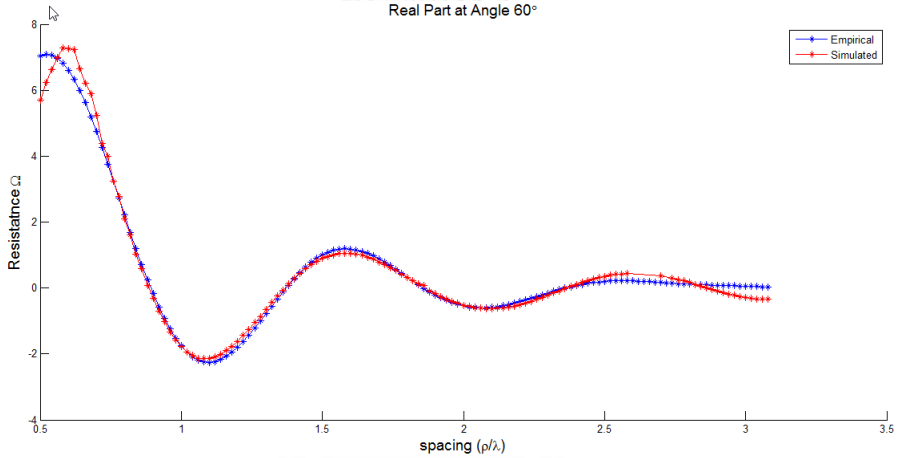

Figure 4.28 Real part at ϕ 60°

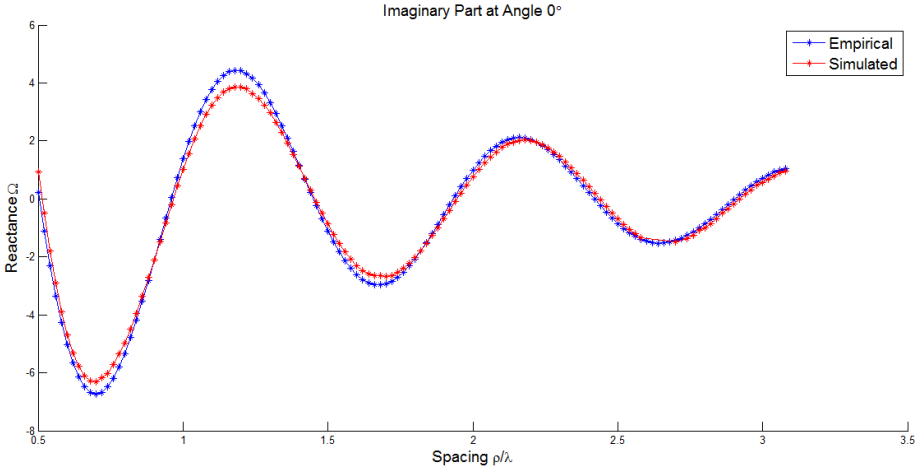

Figure 4.29 Imaginary part at ϕ 0°

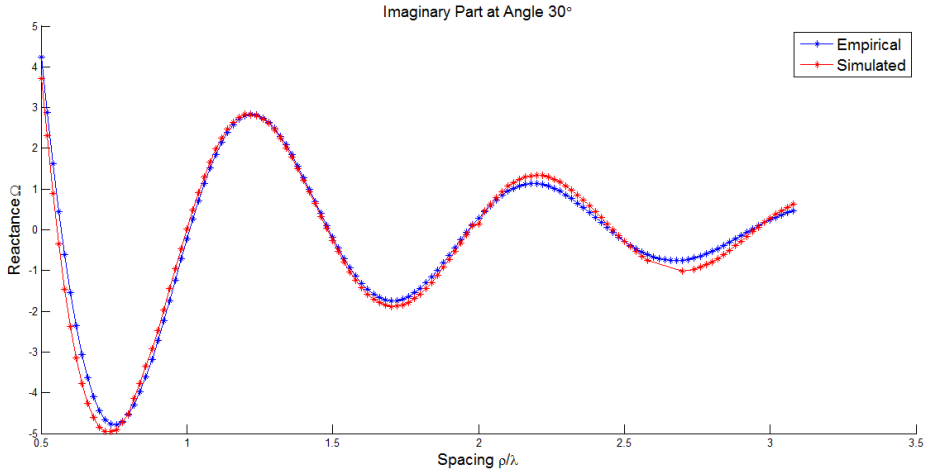

Figure 4.30 Imaginary part at ϕ 30°

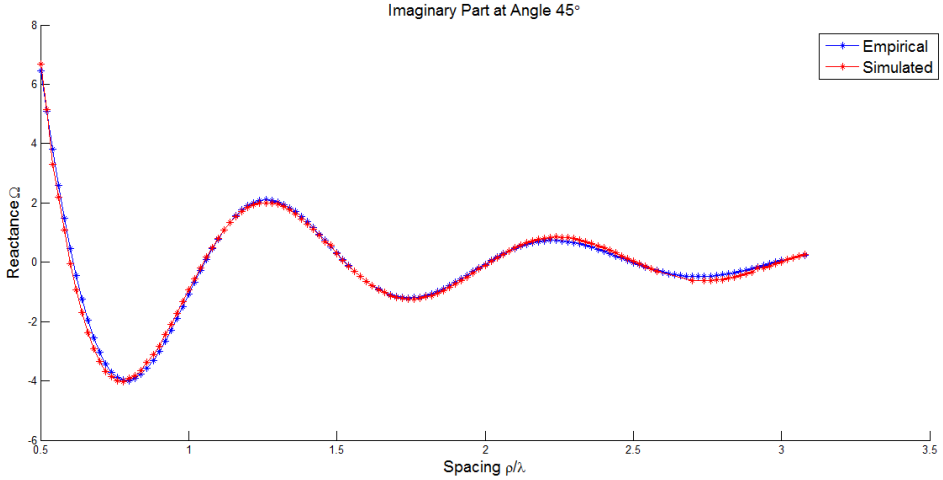

Figure 4.31 Imaginary part at ϕ 45°

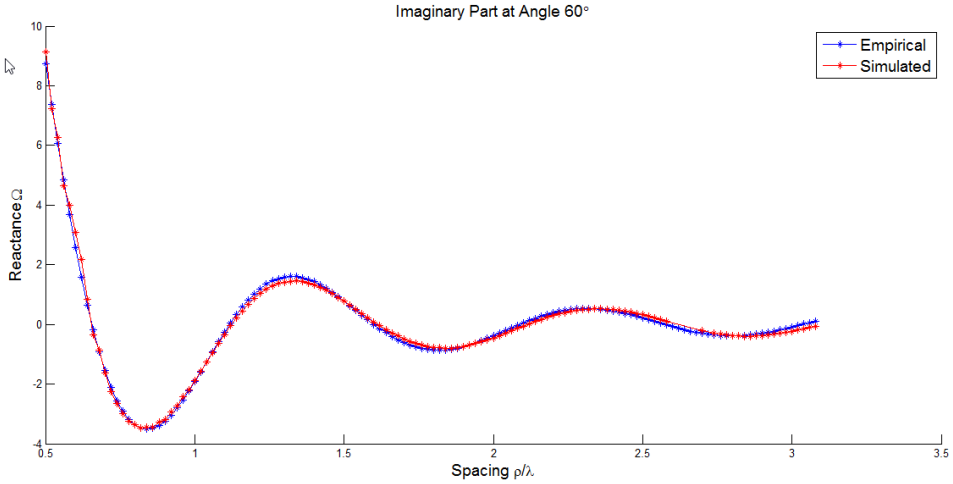

Figure 4.32 Imaginary part at ϕ 60°

As describing above, the range of the element spacing that is used to find sets of coefficients of approximation model is from $0.5\lambda_0$ to $2.48\lambda_0$, and within this range, the approximation model can be effectively used to calculate the mutual resistance and reactance between two patch antennas with a good accuracy (be aware that the characteristic of the microstrip patch antennas must be the same as in the research). From Figure4.21 to Figure4.24 show the comparison of the mutual resistance. From Figure4.25 to Figure4.28 is the comparison of the mutual reactance. From Figures4.21 to Figures4.28, the accuracy of the approximation is very high when the element spacing is within the interval of $0.5\lambda_0$ to $2.48\lambda_0$, but there are discrepancies when the element spacing is greater than $2.48\lambda_0$ or is outside the interval of $0.5\lambda_0$ to $2.48\lambda_0$. However, when element spacing is greater than $2.48\lambda_0$, the discrepancies are not so high that it could affect approximation model and value of mutual impedance. On the one hand, the mutual impedance between the two patch antennas, when the element spacing is getting father, is so small that it could not affect the antenna systems and that it can be neglected. For more clear about the extrapolation comparison, the appendix E will show more results. Therefore, from the extrapolation comparison above, the approximation model is accountable to calculate the mutual impedance between two patch antennas which are in the condition that the two patch antennas have parameters (thickness, relative permittivity, patch size, and frequency) the same as those of the patch antennas in this research. In case the patch antenna has different parameters from those in this research, the model of equation 4.1 and 4.2 could be kept; however the number of terms and sets of new coefficients must be changed consistently.

4.5 Comparison with Existing Experiment

The equation (4.1) and (4.2) can be used to calculate the mutual impedance only in the same conditions of parameters that have been used in this research. However, the existing experiment has different parameters which have been used in this research. From [27], the parameters of the microstrip patch antenna are as the following:

- Size of patch $10.57cm \times 6.55cm$

- Frequency $f = 1410MHz$
- Relative permittivity $\varepsilon_r = 2.5$
- Thickness of the substrate $\mathrm{h} = 0.1575cm$

Since the parameters of microstrip patch above are different from which are used in this research, the equation (4.1) and (4.2) with the provided sets of coefficients cannot be used to calculate the mutual impedance to compare with result in [27]. In addition, the results in [27] are from the two parallel patches with the same orientation, so that the coefficients of azimuth angle ϕ in both equation (4.1) and equation (4.2) are zero. The function in (4.1) and (4.2) becomes a one variable function, so that the number of terms also can be reduced from three terms to two terms. The equation 4.1 and 4.2 will become:

$$R = \sum_{m=1}^{2} \mathrm{A}_m J_1\left(\mathrm{B}_m\left(\frac{\rho}{\lambda}\right) + \mathrm{D}_m\right) \tag{4.3}$$

$$X = \sum_{n=1}^{2} \mathrm{E}_n J_1\left(\mathrm{F}_n\left(\frac{\rho}{\lambda}\right) + \mathrm{H}_n\right) \tag{4.4}$$

Nevertheless, new sets of coefficients will be determined to use with the equation (4.3) and (4.4). The ways to determine the new sets of coefficients are the same as in section 3.2.3. From whole process, the new sets of coefficients are as in the following value:

$$\left\{\begin{array}{l} \mathrm{A}_1 = 5.3881\,,\ \mathrm{B}_1 = 6.3456,\ \mathrm{C}_1 = 1.2353\,; \\ \mathrm{A}_2 = 5.2784,\ \mathrm{B}_2 = 6.5176\,,\ \mathrm{D}_2 = -1.1052 \end{array}\right\}$$

$$\left\{\begin{array}{l} \mathrm{E}_1 = 5.3881,\ \mathrm{F}_1 = 6.3456\,,\ \mathrm{H}_1 = 1.2353\,; \\ \mathrm{E}_2 = 5.2784\,,\ \mathrm{F}_2 = 6.5176\,,\ \mathrm{H}_2 = -1.1052 \end{array}\right\}$$

By using the equation (4.1) and (4.2) with the new sets of coefficient, the comparing results will be shown as above:

The mutual coupling between two microstrip patch antennas S_{12} can be calculated by using the following formulation:

$$S_{12} = \frac{4Z_0 Z_{12}}{\left(Z_{11} + Z_0\right)^2 - {Z_{12}}^2} \quad \left(Z_0 = 50\Omega\right)$$

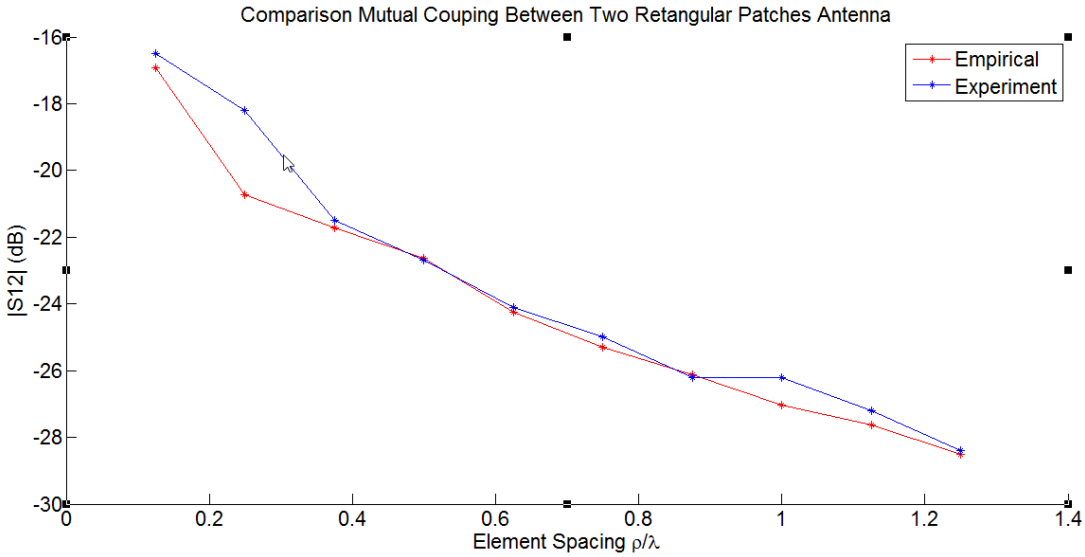

Figure 4.33 Comparison between approximation model and Experiment [27]

From Figure 4.29, the discrepancy is big for the spacing which is smaller than $0.4\lambda_0$, and it is small when the spacing is greater than $0.4\lambda_0$. As mention above, the approximation model with the Bessel's function is effectively used to represent the cylindrical wave for the far field region. Therefore, the approximation is good when the spacing between two patches antenna is greater $0.5\lambda_0$.

4.6 Application Of The Approximation Model In Array Antenna

In array antenna, each microstrip patch elements must get power from a feed network which is designed to divide power from source and to supply to each antenna element. The feed network is normally as microstrip line which is design to operate well with corresponding antenna array in order to achieve desirable performance.

A finite array can be analyzed rigorously if the mutual coupling between the elements in the array environment is known. The present of patch elements together with feeding network on a grounded plane is a problem to analyze the electromagnetic radiation and receiving. Therefore, the array systems can be decomposed into two main parts; one is dealing with antenna array a lone, and the other dealing with feed network alone. Results from the two parts above are combined by using a generalized Thevenin's theorem [28]. The approximation model can be used to find the mutual impedance between each element in the case of the

array antenna alone. The feed network alone can be analyzed by using EM simulation software. After applying the generalized Thevenin's theorem, the radiation pattern and the receiving can be efficiently analyzed.

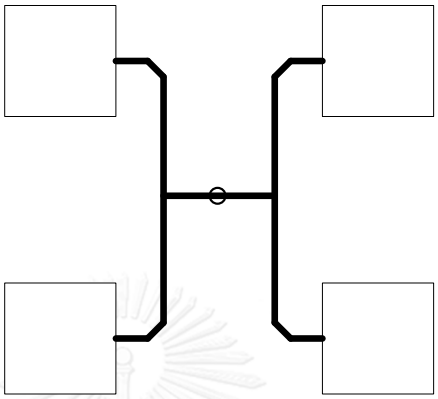

Figure 4.34 4 patches array

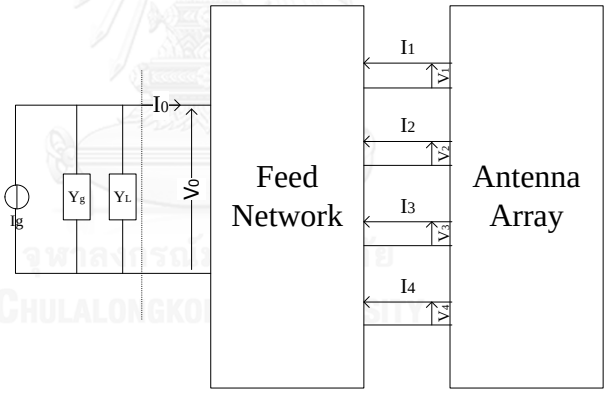

Figure 4.35 4 patches array-feed network configuration

Chapter 5 CONCLUSIONS

5.1 Conclusions

This research has proposed to find an approximation model of mutual impedance between two patches antennas. As the result, the approximation model has in the form of a superposition of Bessel's function which is used to represent the characteristic of the cylindrical wave in the far field region. However, the application of the proposed formulation is still having a limitation. The first limitation is that the model can only be used when the element spacing is within the interval $0.5\lambda_0$ to $2.48\lambda_0$ (f_0=2.98GHz). Although the proposed model cannot be used when element spacing is greater than $2.48\lambda_0$, the mutual impedance can be neglected with element spacing is greater than $2.48\lambda_0$ (See Appendix E). On the other hand, the full wave analysis is needed, when the element spacing is smaller than $0.5\lambda_0$. Moreover, the parameters of the microstrip patch antenna are also limitations of the approximation model. In case the microstrip patch has different relative permittivity ($\varepsilon_r \neq 2.3$) with thickness ($h \neq 0.01\lambda_0$), patch size ($\neq 0.3\lambda_0 \times 0.27\lambda_0$), or frequency ($f_0 \neq$ 2.98GHz), the approximation models cannot be used to calculate the mutual impedance between those two patch antennas. In addition to parameters of patch antennas, orientation of each patch antenna must also in the same orientation as in this research. The approximation model can be concluded that it can only be used when the frequency is equal to 2.98GHz (f_0=2.98GHz), and the patch size is equal to $0.3\lambda_0 \times 0.27\lambda_0$ with dielectric thickness $h_t=0.01\lambda_0$. The model can be effectively used when patch antenna has the same parameters as in the research.

5.2 Future Work

From section 5.1, the approximation model has a lot of limitation regarding to parameters of microstrip antenna. To make the proposed model to be more applicable, those limited parameters must be examined to include into the approximation model. Firstly, the frequency scalability should be examined since one antenna system can be operated at variety of frequency depending on the

systems requirement. In addition, the size of each patch antenna should be included in the approximation models since the resonance frequency of each patch antenna does depend on the size of the patch. Moreover, the size of antenna is a continuous quantity; the size of the patch antenna is suitable to be a variable of the formulation. Furthermore, dielectric thickness is also an important parameter to be included in the approximation model due to the extreme of effect of thickness of dielectric. After the inclusion of those important parameters above, the approximation model would be widely applicable. In case of relative permittivity, the value of the relative permittivity depends on the dielectric material which is fabricated by the factory. Thus, many cases of dielectric material should be examined in combination with those parameters above. Besides, the approximation model should be examined in array structure in order to investigate the accuracy of the models as well as the effect of multiple elements (array factor) on the approximation model for two patch elements. Finally, if all the parameter above were included in, the approximation models would be very useful and helpful for antenna design engineer to deal with mutual impedance between patch antenna elements in array systems.

REFERENCES

[1] Balanis, C.A., *Antenna theory: analysis and design*. 2016: John Wiley & Sons.

[2] Deschamps, G.A. *Microstrip microwave antennas*. in *3rd USAF Symposium on Antennas*. 1953.

[3] Gutton, H. and G. Baissinot, *Flat aerial for ultra high frequencies.* French patent, 1955. **703113**.

[4] Pozar, D.M. and D.H. Schaubert, *Microstrip antennas: the analysis and design of microstrip antennas and arrays*. 1995: John Wiley & Sons.

[5] Wong, K.-L., *Compact and broadband microstrip antennas*. Vol. 168. 2004: John Wiley & Sons.

[6] Chen, Z.N. and M.Y.W. Chia, *Broadband planar antennas: design and applications*. 2006: John Wiley & Sons.

[7] Uzunoglu, N., N. Alexopoulos, and J. Fikioris, *Radiation properties of microstrip dipoles.* IEEE Transactions on Antennas and Propagation, 1979. **27**(6): p. 853-858.

[8] Rana, I. and N. Alexopoulos, *Current distribution and input impedance of printed dipoles.* IEEE Transactions on Antennas and Propagation, 1981. **29**(1): p. 99-105.

[9] Barrett, R.M., *Microwave Printed Circuits - The Early Years.* IEEE Transactions on Microwave Theory and Techniques, 1984. **32**(9): p. 983-990.

[10] Howe, H., *Microwave Integrated Circuits - An Historical Perspective.* IEEE Transactions on Microwave Theory and Techniques, 1984. **32**(9): p. 991-996.

[11] Denlinger, E.J., *Radiation from Microstrip Resonators (Correspondence).* IEEE Transactions on Microwave Theory and Techniques, 1969. **17**(4): p. 235-236.

[12] Lil, E.V. and A.V.D. Capelle, *Transmission line model for mutual coupling between microstrip antennas.* IEEE Transactions on Antennas and Propagation, 1984. **32**(8): p. 816-821.

[13] Carver, K. and J. Mink, *Microstrip antenna technology.* IEEE Transactions on Antennas and Propagation, 1981. **29**(1): p. 2-24.

[14] Munson, R., *Conformal microstrip antennas and microstrip phased arrays.* Antennas and Propagation, IEEE Transactions on, 1974. **22**(1): p. 74-78.

[15] Harrington, R.F., *Time-harmonic electromagnetic fields*. 1961: McGraw-Hill.

[16] Derneryd, A., *A theoretical investigation of the rectangular microstrip antenna element.* IEEE Transactions on Antennas and Propagation, 1978. **26**(4): p. 532-535.

[17] KWAN, B.W., *MUTUAL COUPLING ANALYSIS FOR CONFORMAL MICROSTRIP ANTENNAS (DYADIC, EIGENFUNCTION, ASYMPTOTIC).* in *ProQuest Dissertations and Theses,*. (1984). (Order No. 8504042, The Ohio State University). p. 279.

[18] Penard, E. and J.P. Daniel, *Mutual coupling between microstrip antennas.* Electronics Letters, 1982. **18**(14): p. 605-607.

[19] Hui, H.T., *A new definition of mutual impedance for application in dipole receiving antenna arrays.* IEEE Antennas and Wireless Propagation Letters, 2004. **3**(1): p. 364-367.

[20] Jordan, E.C., *Electromagnetic waves and radiating systems.* 1964.

[21] Kraus, J.D., *Antennas.* 1988.

[22] Carson, J.R., *Reciprocal Theorems in Radio Communication.* Proceedings of the Institute of Radio Engineers, 1929. **17**(6): p. 952-956.

[23] Kong, J.A., *Theory of electromagnetic waves.* New York, Wiley-Interscience, 1975. 348 p., 1975. **1**.

[24] Nelder, J.A. and R. Mead, *A simplex method for function minimization.* The computer journal, 1965. **7**(4): p. 308-313.

[25] Lagarias, J.C., et al., *Convergence properties of the Nelder--Mead simplex method in low dimensions.* SIAM Journal on optimization, 1998. **9**(1): p. 112-147.

[26] Gao, F. and L. Han, *Implementing the Nelder-Mead simplex algorithm with adaptive parameters.* Computational Optimization and Applications, 2012. **51**(1): p. 259-277.

[27] Jedlicka, R., M. Poe, and K. Carver, *Measured mutual coupling between microstrip antennas.* IEEE Transactions on Antennas and Propagation, 1981. **29**(1): p. 147-149.

[28] Mahachoklertwattana, P., et al. *A hybrid MoM-asymptotic and circuit based analysis of the radiation/receiving by large finite patch antenna arrays with a printed feed network*. in *IEEE Antennas and Propagation Society Symposium, 2004.* 2004.

[29] Balanis, C.A., *{Advanced Engineering Electromagnetics.* Wiley, 2012.

[30] Richmond, J., *A reaction theorem and its application to antenna impedance calculations.* IRE Transactions on Antennas and Propagation, 1961. **9**(6): p. 515-520.

Appendix A

Reciprocity Theorem

$$\iiint_V \left(\vec{E}_A.\vec{J}_B - \vec{H}_A\vec{M}_B\right)dv' = \iiint_V \left(\vec{E}_B.\vec{J}_A - \vec{H}_B\vec{M}_A\right)dv'$$

$$\langle A,B\rangle = \iiint_V \left(\vec{E}_A.\vec{J}_B - \vec{H}_A\vec{M}_B\right)dv'$$

$\langle A,B\rangle$ is the relation to the reaction (coupling) that antenna A, having source $\vec{J}_A$ and $\vec{M}_A$, and inducing $\vec{E}_A$ and $\vec{H}_A$ on the antenna B having source $\vec{J}_B$ and $\vec{M}_B$.

$$\langle B,A\rangle = \iiint_V \left(\vec{E}_B.\vec{J}_A - \vec{H}_B\vec{M}_A\right)dv'$$

$\langle B,A\rangle$ is the relation to the reaction (coupling) that antenna B, having source $\vec{J}_B$ and $\vec{M}_B$, and inducing $\vec{E}_B$ and $\vec{H}_B$ on the antenna A having source $\vec{J}_A$ and $\vec{M}_A$.

Therefore, the formula can be written in the form as following

$$\langle A,B\rangle = \langle B,A\rangle$$

The reaction theorem can be written in the form of current and voltage which is induced by one antenna to another antenna [29] [30].

$\langle A,B\rangle = I_B V_{BA}$ $\langle B,A\rangle = I_A V_{AB}$

I_B is current on the antenna B I_B is current on the antenna B

V_{BA} is voltage on antenna B due to A V_{AB} is voltage on antenna A due to B

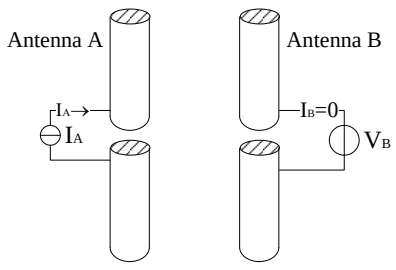

Assuming that the current flowing through the antenna B is zero; therefore the voltage at the antenna B open circuit V_B^{oc} is the voltage that is due to antenna A. From the expression of reaction theorem above, we can see that:

$$V_B^{oc} = V_{BA}$$

$$I_B V_{BA} = \langle B, A \rangle = \iiint_V \left(\vec{E}_A . \vec{J}_B - \vec{H}_A . \vec{\mathrm{M}}_B \right) dv'$$

$$I_B V_{BA} = \iiint_V \left(\vec{E}_A . \vec{J}_B - \vec{H}_A . \vec{\mathrm{M}}_B \right) dv'$$

$$V_{BA} = \frac{1}{I_B} \iiint_V \left(\vec{E}_A . \vec{J}_B - \vec{H}_A . \vec{\mathrm{M}}_B \right) dv'$$

Covert the volume integral to the surface integral we get:

$$V_{BA} = \frac{1}{I_B} \oiint_{S_B} \left(\vec{E}_A . \vec{J}_B - \vec{H}_A . \vec{\mathrm{M}}_B \right) ds'$$

The antenna can be represented by the electric current density:

$$\vec{J}_B = -\hat{n} \times \vec{H}_B$$

$$\vec{M}_B = \vec{0}$$

$$V_B^{oc} = V_{BA} = \frac{1}{I_B} \oiint_{S_B} \left(\vec{E}_A . \vec{J}_B \right) ds'$$

In the same way, we get the open-circuit voltage at antenna A:

$$V_A^{oc} = V_{AB} = \frac{1}{I_A} \oiint_{S_A} \left(\vec{E}_B . \vec{J}_A \right) ds'$$

$$\vec{J}_A = -\hat{n} \times \vec{H}_A$$

$$\vec{M}_A = \vec{0}$$

Appendix B

The mutual impedance in equation 3.5a and 3.5b are:

$$Z_{AB} = \frac{1}{I_B I_A} \oiint_{S_A} \left(\vec{E}_B . \vec{J}_A \right) ds$$

$$Z_{AB} = \frac{1}{I_B I_A} \oiint_{S_A} \left(\vec{E}_B \times \vec{H}_A \right) . \hat{n} ds$$

$$Z_{BA} = \frac{1}{I_A I_B} \oiint_{S_B} \left(\vec{E}_A . \vec{J}_B \right) ds$$

$$Z_{BA} = \frac{1}{I_A I_B} \oiint_{S_B} \left(\vec{E}_A \times \vec{H}_B \right) . \hat{n} ds$$

From the reciprocity theorem

$$\oiint_{S_A + S_B} \left(\vec{E}_A \times \vec{H}_B - \vec{E}_B \times \vec{H}_A \right) . \hat{n} ds = 0$$

$$\oiint_{S_A} \left(\vec{E}_A \times \vec{H}_B - \vec{E}_B \times \vec{H}_A \right) . \hat{n} ds = \oiint_{S_B} \left(\vec{E}_B \times \vec{H}_A - \vec{E}_A \times \vec{H}_B \right) . \hat{n} ds$$

$$\oiint_{S_A} \left(\vec{E}_A \times \vec{H}_B \right) . \hat{n} ds - \oiint_{S_A} \left(\vec{E}_B \times \vec{H}_A \right) . \hat{n} ds = \oiint_{S_B} \left(\vec{E}_B \times \vec{H}_A \right) . \hat{n} ds - \oiint_{S_B} \left(\vec{E}_A \times \vec{H}_B \right) . \hat{n} ds$$

$$\oiint_{S_A} \left(\vec{E}_A \times \vec{H}_B \right) . \hat{n} ds = 0$$

$$\oiint_{S_B} \left(\vec{E}_B \times \vec{H}_A \right) . \hat{n} ds = 0$$

$$-\oiint_{S_A} \left(\vec{E}_B \times \vec{H}_A \right) . \hat{n} ds = -\oiint_{S_B} \left(\vec{E}_A \times \vec{H}_B \right) . \hat{n} ds$$

$$\oiint_{S_A} \left(\vec{E}_B \times \vec{H}_A \right) . \hat{n} ds = \oiint_{S_B} \left(\vec{E}_A \times \vec{H}_B \right) . \hat{n} ds$$

So we get: $Z_{AB} = Z_{BA}$

Appendix C

Mutual Resistance (Approximation Vs Simulation)

When 2 terms of Bessel function are used in the approximation model.

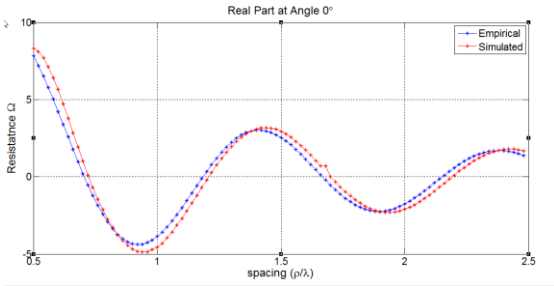

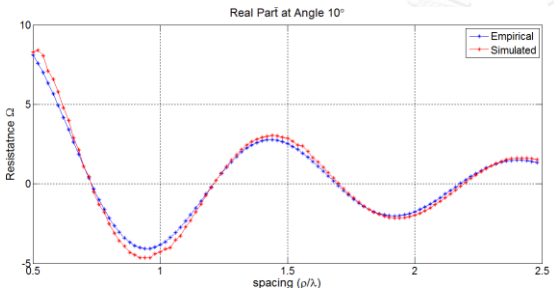

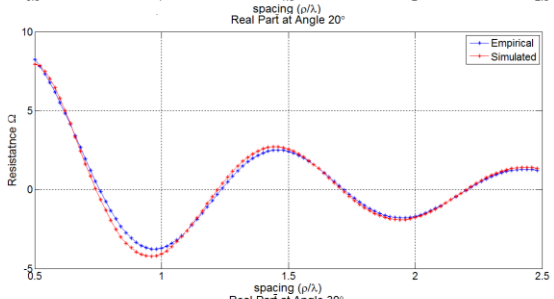

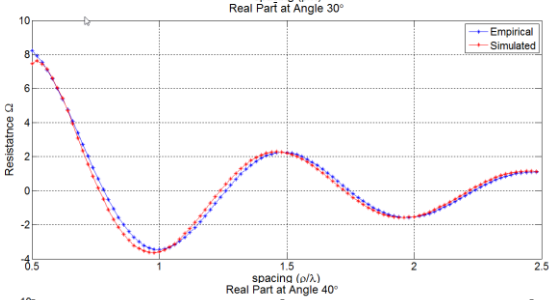

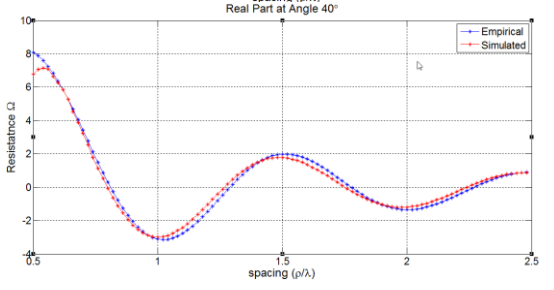

When 3 terms of Bessel function are used in the approximation model.

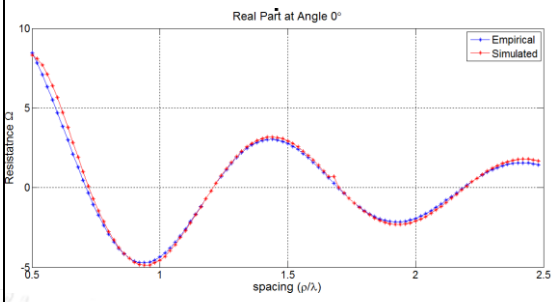

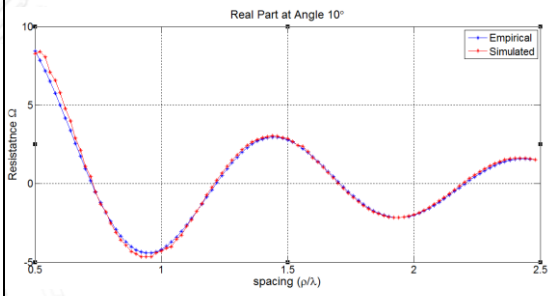

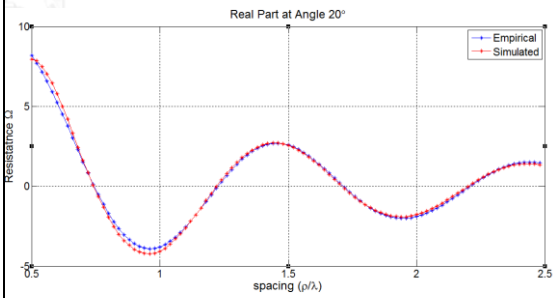

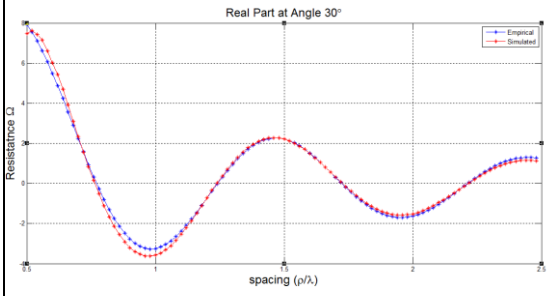

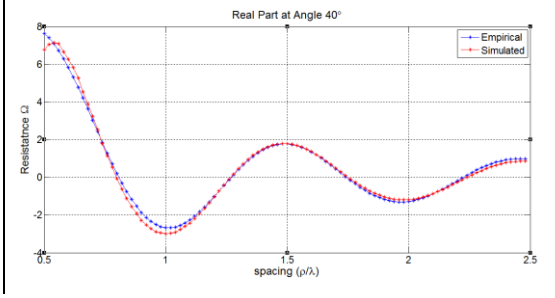

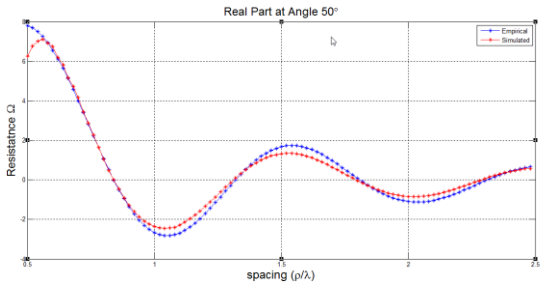
Real Part at Angle 50°
Empirical
Simulated
Resistatnce Ω
spacing (ρ/λ)

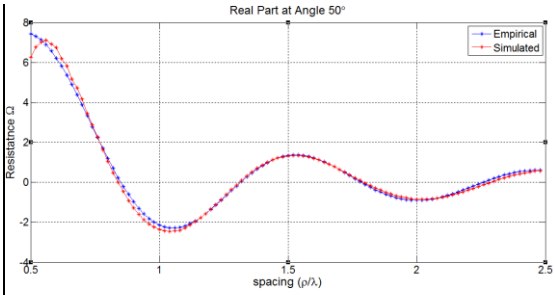
Real Part at Angle 50°
Empirical
Simulated
Resistatnce Ω
spacing (ρ/λ)

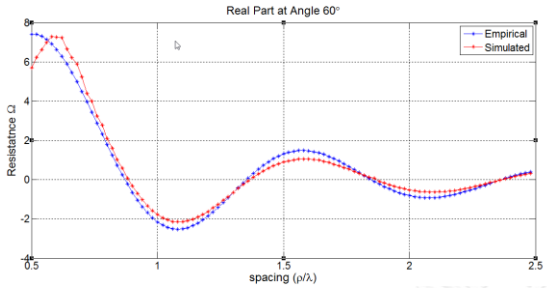
Real Part at Angle 60°
Empirical
Simulated
Resistatnce Ω
spacing (ρ/λ)

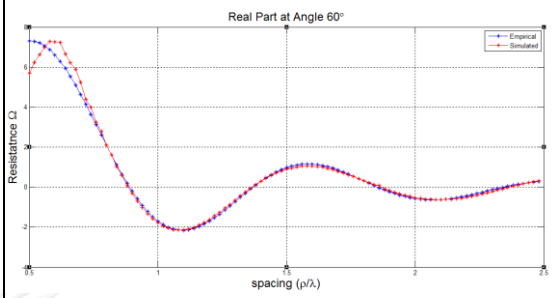
Real Part at Angle 60°
Empirical
Simulated
Resistatnce Ω
spacing (ρ/λ)

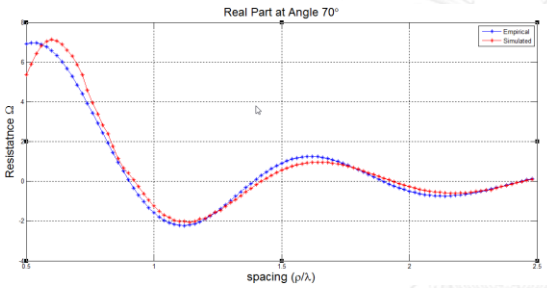
Real Part at Angle 70°
Empirical
Simulated
Resistatnce Ω
spacing (ρ/λ)

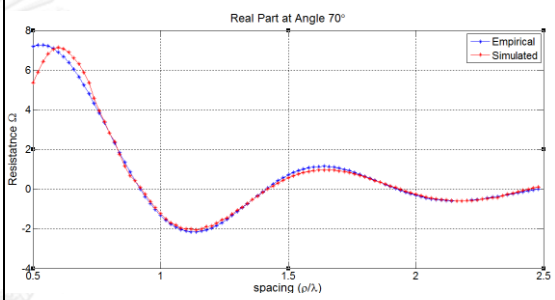
Real Part at Angle 70°
Empirical
Simulated
Resistatnce Ω
spacing (ρ/λ)

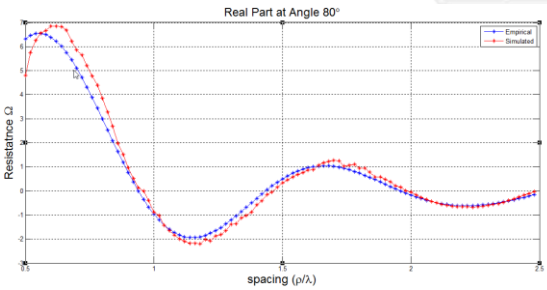
Real Part at Angle 80°
Empirical
Simulated
Resistatnce Ω
spacing (ρ/λ)

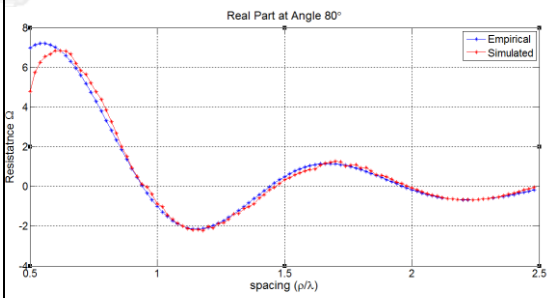
Real Part at Angle 80°
Empirical
Simulated
Resistatnce Ω
spacing (ρ/λ)

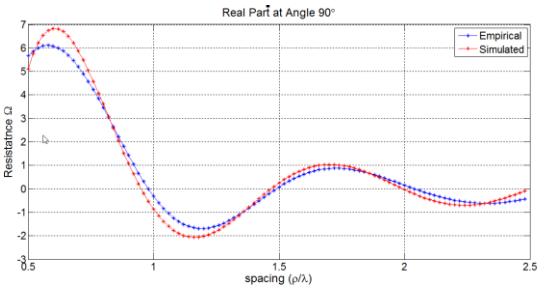
Real Part at Angle 90°
Empirical
Simulated
Resistatnce Ω
spacing (ρ/λ)

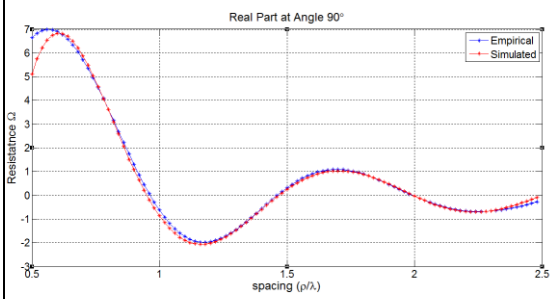
Real Part at Angle 90°
Empirical
Simulated
Resistatnce Ω
spacing (ρ/λ)

Mutual Reactance (Approximation Vs Simulation)

When 2 terms of Bessel function are used in the approximation model.

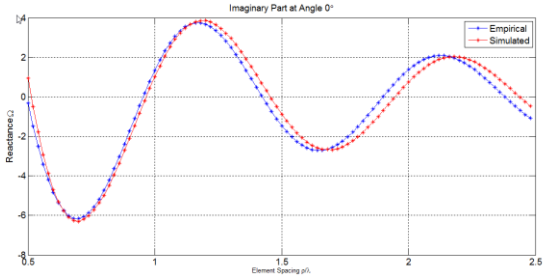

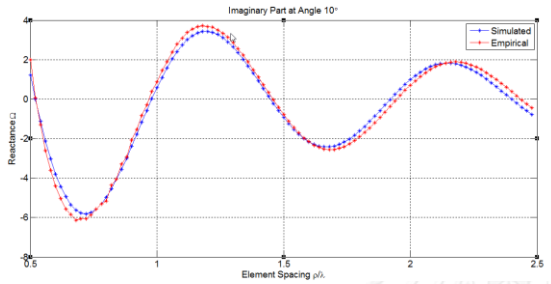

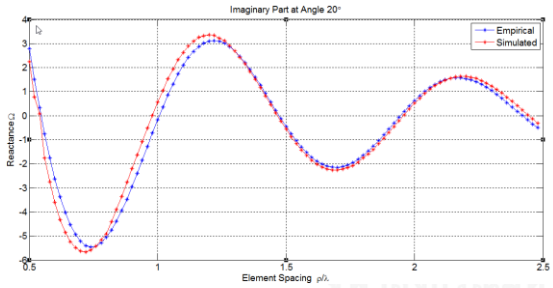

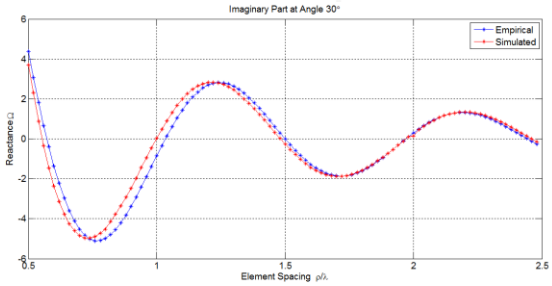

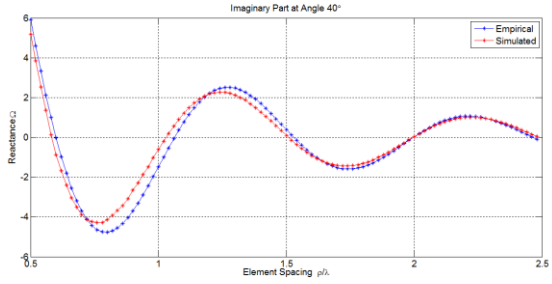

When 3 terms of Bessel function are used in the approximation model.

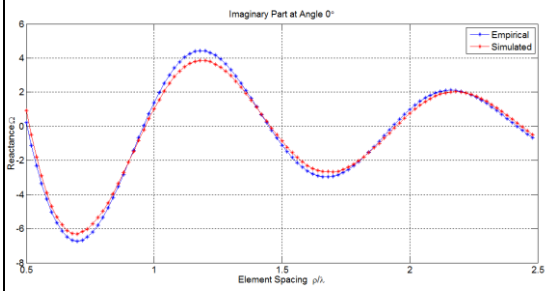

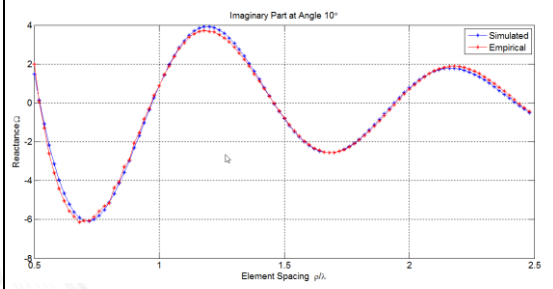

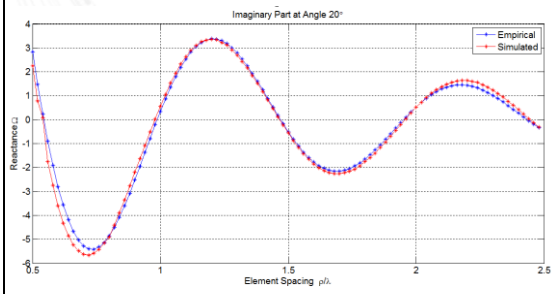

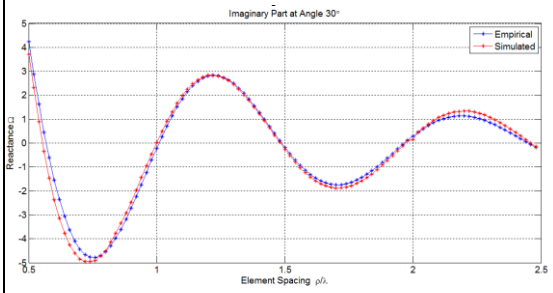

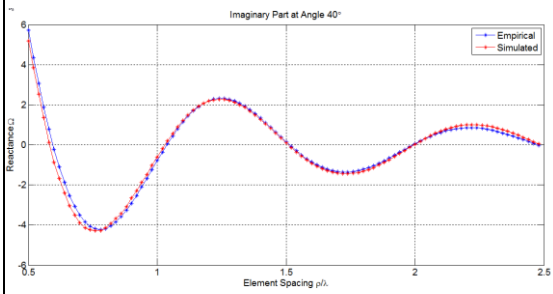

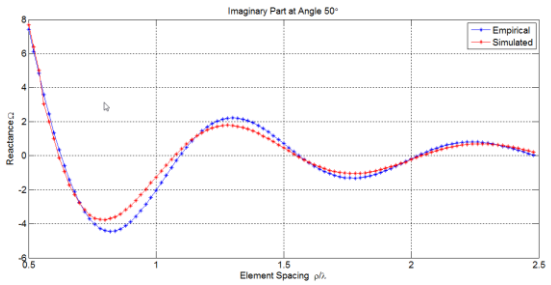
Imaginary Part at Angle 50°
Empirical
Simulated
Reactance Ω
Element Spacing ρ/λ

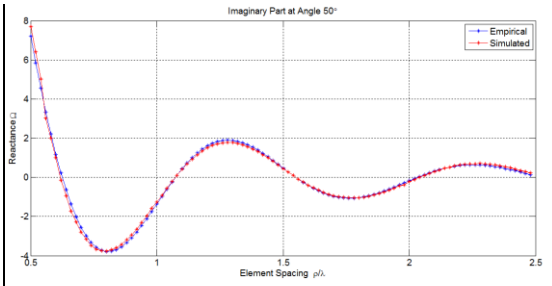
Imaginary Part at Angle 50°
Empirical
Simulated
Reactance Ω
Element Spacing ρ/λ

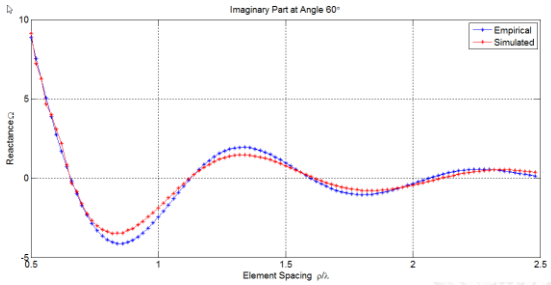
Imaginary Part at Angle 60°
Empirical
Simulated
Reactance Ω
Element Spacing ρ/λ

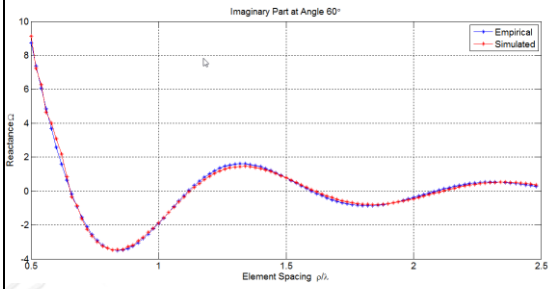
Imaginary Part at Angle 60°
Empirical
Simulated
Reactance Ω
Element Spacing ρ/λ

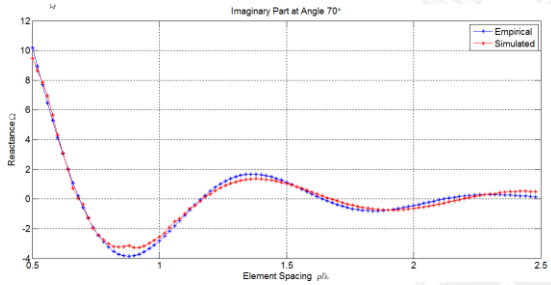
Imaginary Part at Angle 70°
Empirical
Simulated
Reactance Ω
Element Spacing ρ/λ

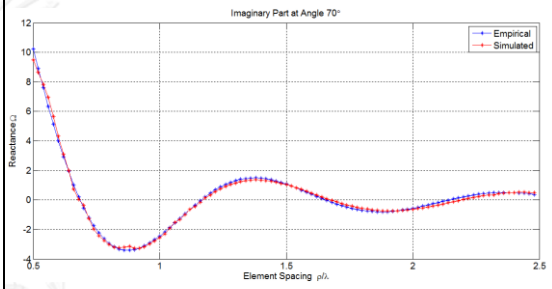
Imaginary Part at Angle 70°
Empirical
Simulated
Reactance Ω
Element Spacing ρ/λ

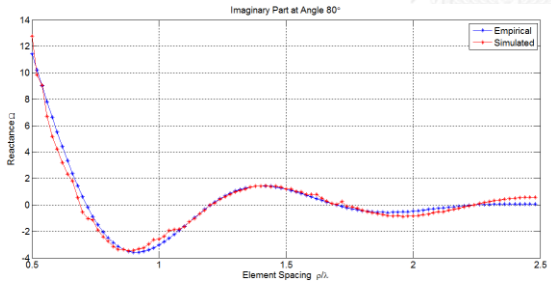
Imaginary Part at Angle 80°
Empirical
Simulated
Reactance Ω
Element Spacing ρ/λ

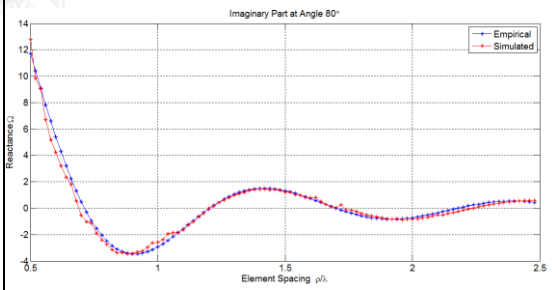
Imaginary Part at Angle 80°
Empirical
Simulated
Reactance Ω
Element Spacing ρ/λ

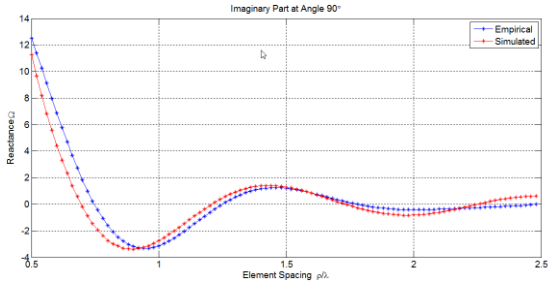
Imaginary Part at Angle 90°
Empirical
Simulated
Reactance Ω
Element Spacing ρ/λ

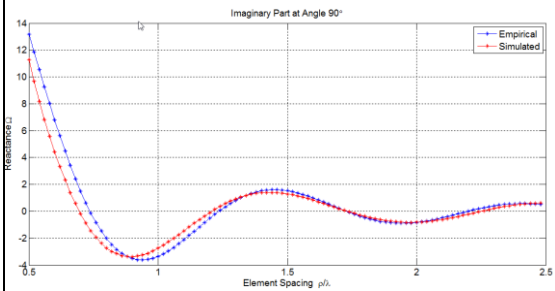
Imaginary Part at Angle 90°
Empirical
Simulated
Reactance Ω
Element Spacing ρ/λ

Appendix D

Mutual Resistance (Approximation Vs Simulation | sampling angle ϕ)

Angle ϕ is incremented every 5°

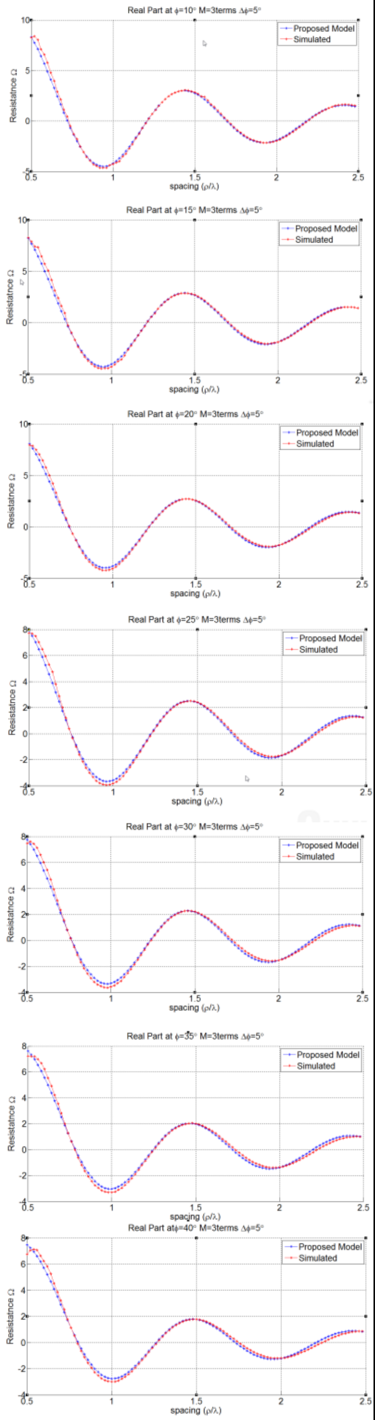

Angle ϕ is incremented every 15°

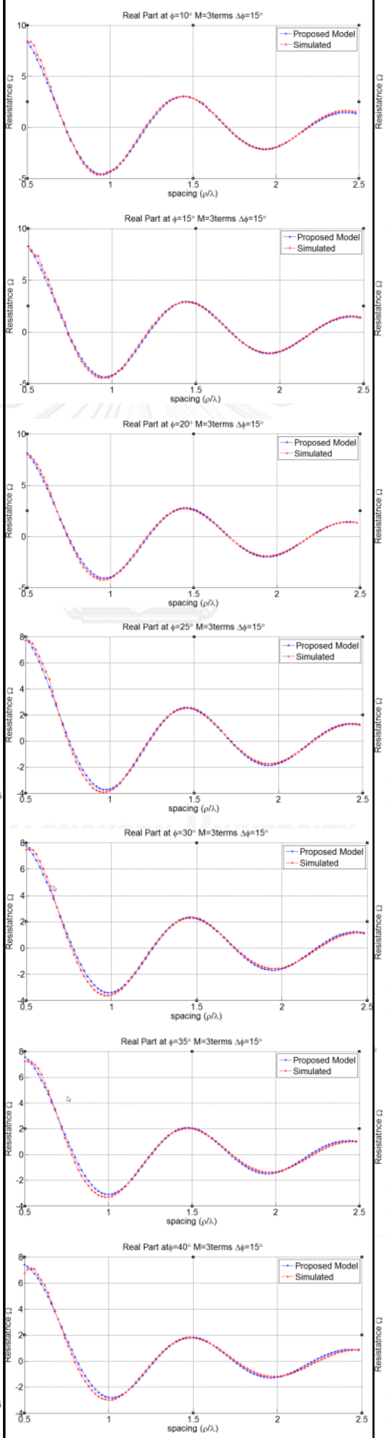

Angle ϕ is incremented every 30°

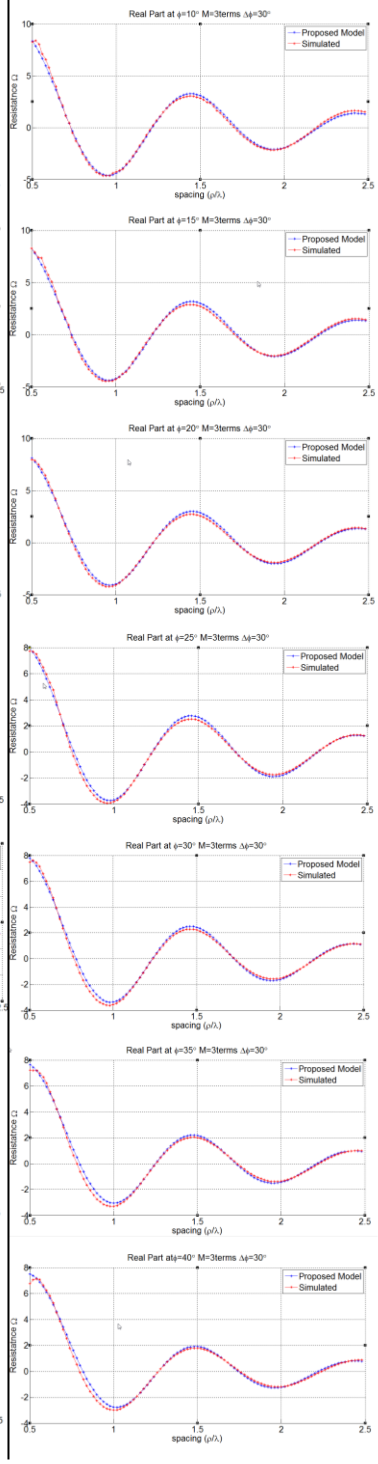

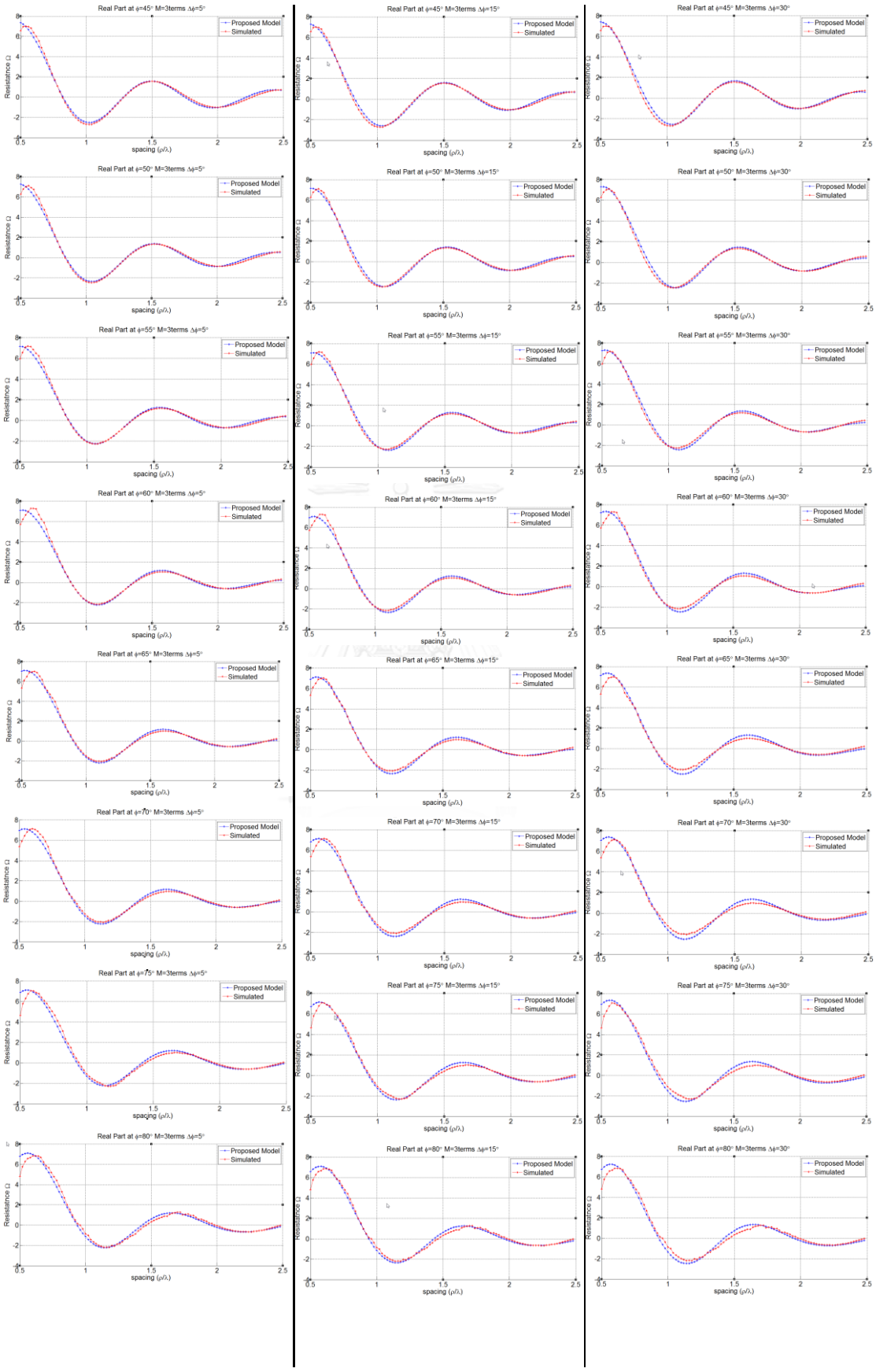
Real Part at ϕ=45° M=3terms Δϕ=5°
Real Part at ϕ=45° M=3terms Δϕ=15°
Real Part at ϕ=45° M=3terms Δϕ=30°
Real Part at ϕ=50° M=3terms Δϕ=5°
Real Part at ϕ=50° M=3terms Δϕ=15°
Real Part at ϕ=50° M=3terms Δϕ=30°
Real Part at ϕ=55° M=3terms Δϕ=5°
Real Part at ϕ=55° M=3terms Δϕ=15°
Real Part at ϕ=55° M=3terms Δϕ=30°
Real Part at ϕ=60° M=3terms Δϕ=5°
Real Part at ϕ=60° M=3terms Δϕ=15°
Real Part at ϕ=60° M=3terms Δϕ=30°
Real Part at ϕ=65° M=3terms Δϕ=5°
Real Part at ϕ=65° M=3terms Δϕ=15°
Real Part at ϕ=65° M=3terms Δϕ=30°
Real Part at ϕ=70° M=3terms Δϕ=5°
Real Part at ϕ=70° M=3terms Δϕ=15°
Real Part at ϕ=70° M=3terms Δϕ=30°
Real Part at ϕ=75° M=3terms Δϕ=5°
Real Part at ϕ=75° M=3terms Δϕ=15°
Real Part at ϕ=75° M=3terms Δϕ=30°
Real Part at ϕ=80° M=3terms Δϕ=5°
Real Part at ϕ=80° M=3terms Δϕ=15°
Real Part at ϕ=80° M=3terms Δϕ=30°
Proposed Model
Simulated
Resistance Ω
spacing (ρ/λ)

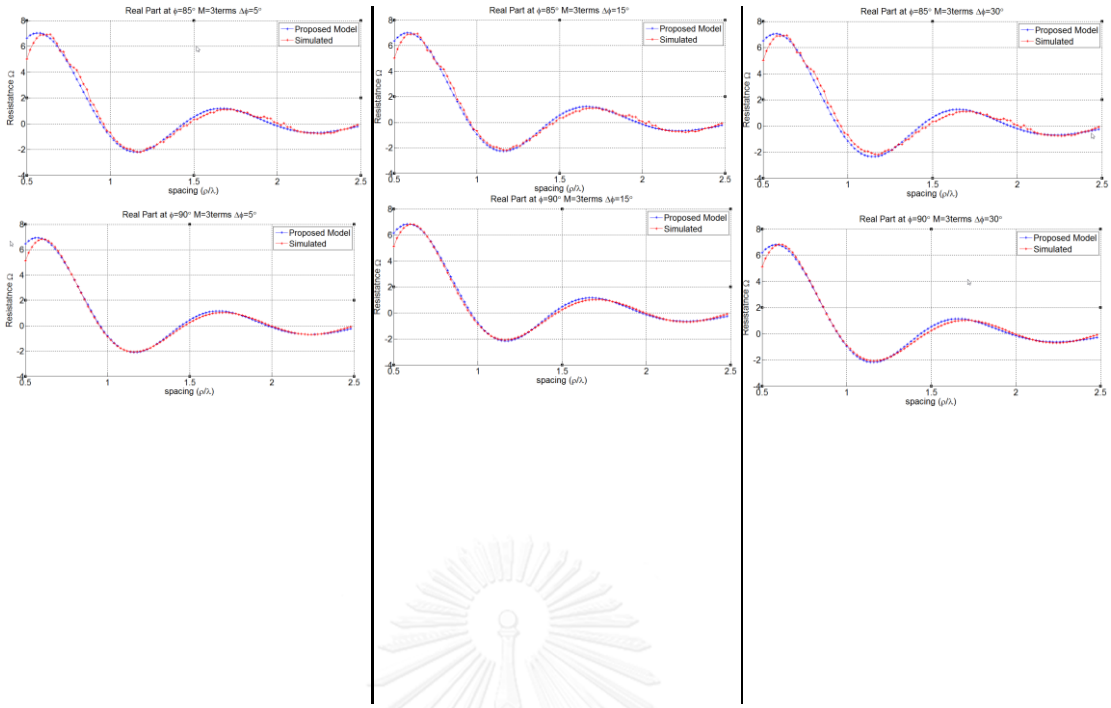

Mutual Reactance (Approximation Vs Simulation | sampling angleϕ)

Angle ϕ is incremented every 5°	Angle ϕ is incremented every 15°	Angle ϕ is incremented every 30°

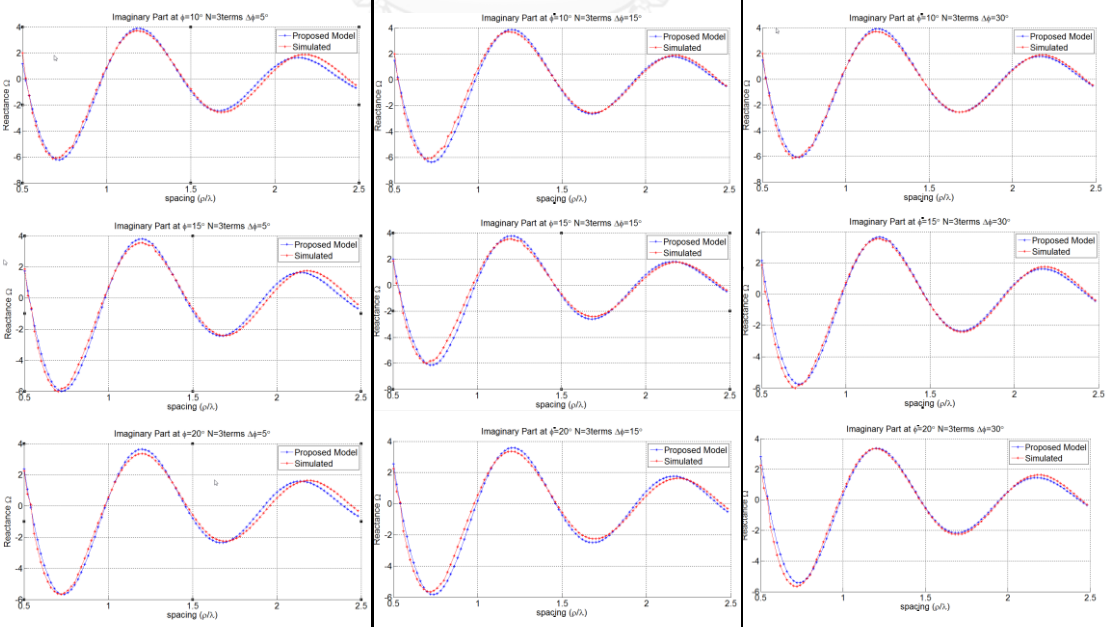

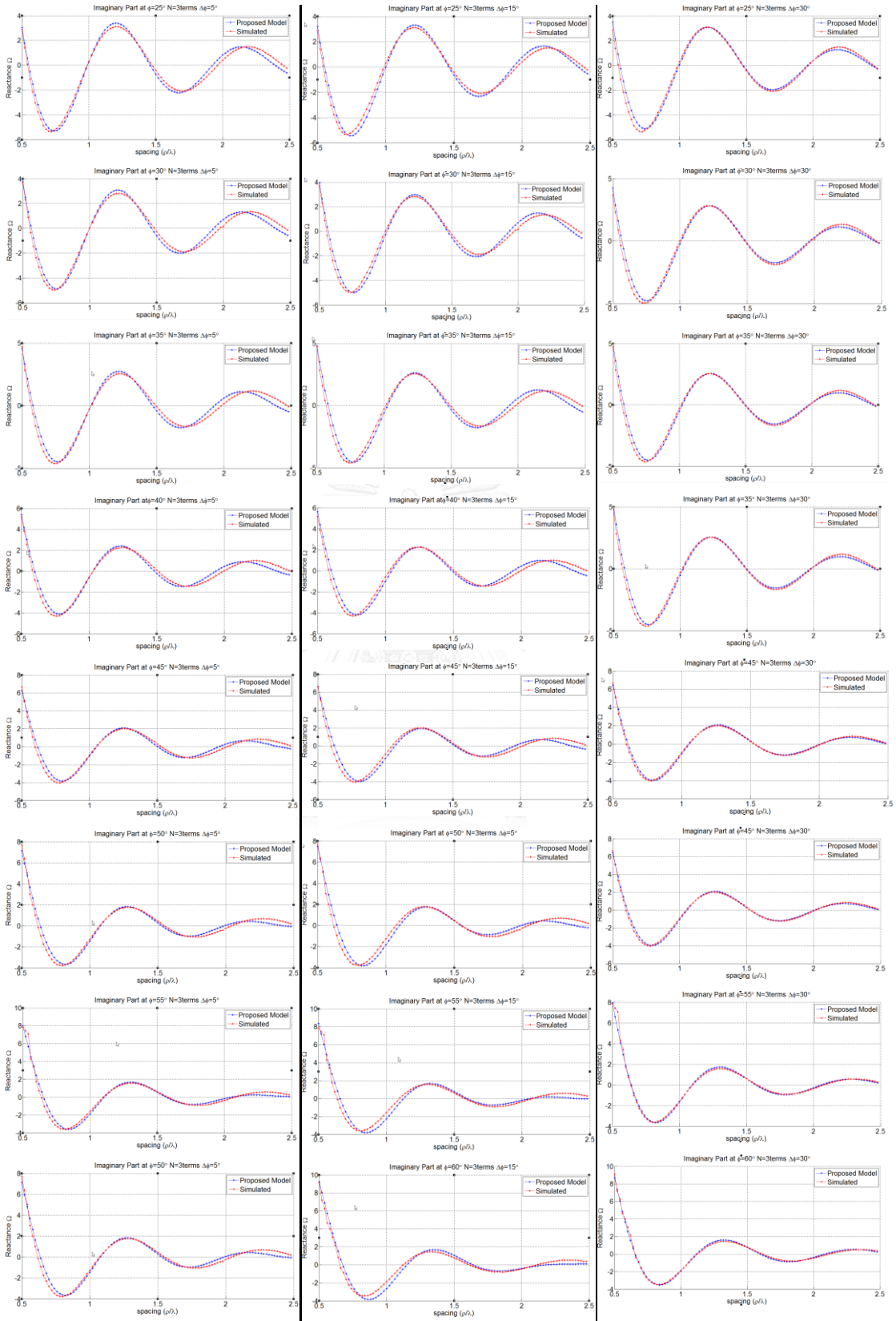
Imaginary Part at ϕ=25° N=3terms Δϕ=5°
Imaginary Part at ϕ=25° N=3terms Δϕ=15°
Imaginary Part at ϕ=25° N=3terms Δϕ=30°
Imaginary Part at ϕ=30° N=3terms Δϕ=5°
Imaginary Part at ϕ=30° N=3terms Δϕ=15°
Imaginary Part at ϕ=30° N=3terms Δϕ=30°
Imaginary Part at ϕ=35° N=3terms Δϕ=5°
Imaginary Part at ϕ=35° N=3terms Δϕ=15°
Imaginary Part at ϕ=35° N=3terms Δϕ=30°
Imaginary Part at ϕ=40° N=3terms Δϕ=5°
Imaginary Part at ϕ=40° N=3terms Δϕ=15°
Imaginary Part at ϕ=35° N=3terms Δϕ=30°
Imaginary Part at ϕ=45° N=3terms Δϕ=5°
Imaginary Part at ϕ=45° N=3terms Δϕ=15°
Imaginary Part at ϕ=45° N=3terms Δϕ=30°
Imaginary Part at ϕ=50° N=3terms Δϕ=5°
Imaginary Part at ϕ=50° N=3terms Δϕ=5°
Imaginary Part at ϕ=45° N=3terms Δϕ=30°
Imaginary Part at ϕ=55° N=3terms Δϕ=5°
Imaginary Part at ϕ=55° N=3terms Δϕ=15°
Imaginary Part at ϕ=55° N=3terms Δϕ=30°
Imaginary Part at ϕ=50° N=3terms Δϕ=5°
Imaginary Part at ϕ=60° N=3terms Δϕ=15°
Imaginary Part at ϕ=60° N=3terms Δϕ=30°
Proposed Model
Simulated
Reactance Ω
spacing (ρ/λ)

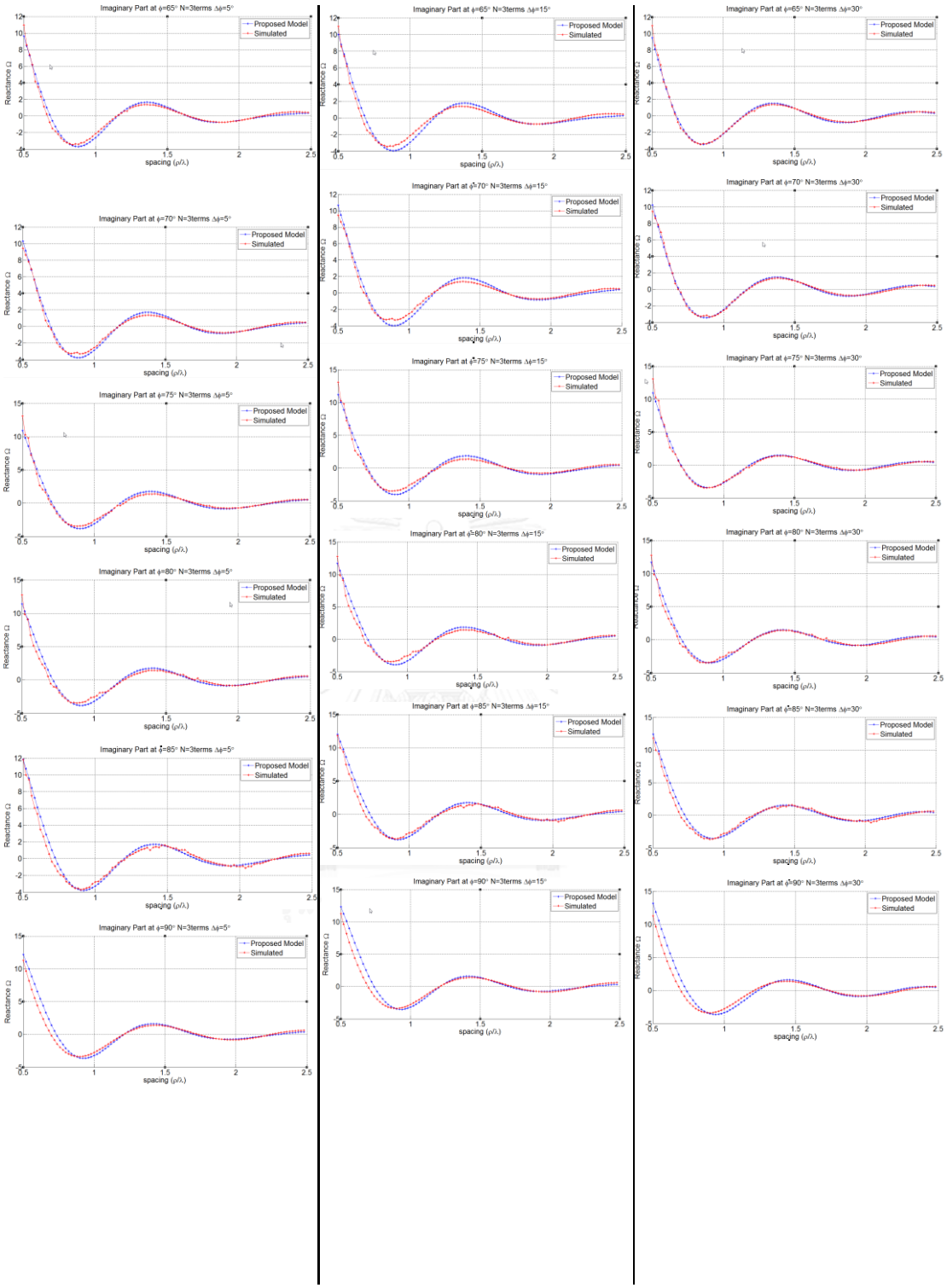
Imaginary Part at ϕ=65° N=3terms Δϕ=5°
Imaginary Part at ϕ=65° N=3terms Δϕ=15°
Imaginary Part at ϕ=65° N=3terms Δϕ=30°
Imaginary Part at ϕ=70° N=3terms Δϕ=5°
Imaginary Part at ϕ=70° N=3terms Δϕ=15°
Imaginary Part at ϕ=70° N=3terms Δϕ=30°
Imaginary Part at ϕ=75° N=3terms Δϕ=5°
Imaginary Part at ϕ=75° N=3terms Δϕ=15°
Imaginary Part at ϕ=75° N=3terms Δϕ=30°
Imaginary Part at ϕ=80° N=3terms Δϕ=5°
Imaginary Part at ϕ=80° N=3terms Δϕ=15°
Imaginary Part at ϕ=80° N=3terms Δϕ=30°
Imaginary Part at ϕ=85° N=3terms Δϕ=5°
Imaginary Part at ϕ=85° N=3terms Δϕ=15°
Imaginary Part at ϕ=85° N=3terms Δϕ=30°
Imaginary Part at ϕ=90° N=3terms Δϕ=5°
Imaginary Part at ϕ=90° N=3terms Δϕ=15°
Imaginary Part at ϕ=90° N=3terms Δϕ=30°
Proposed Model
Simulated
Reactance Ω
spacing (ρ/λ)

Appendix E

Extrapolation Comparison

Extrapolation comparison of mutual resistance

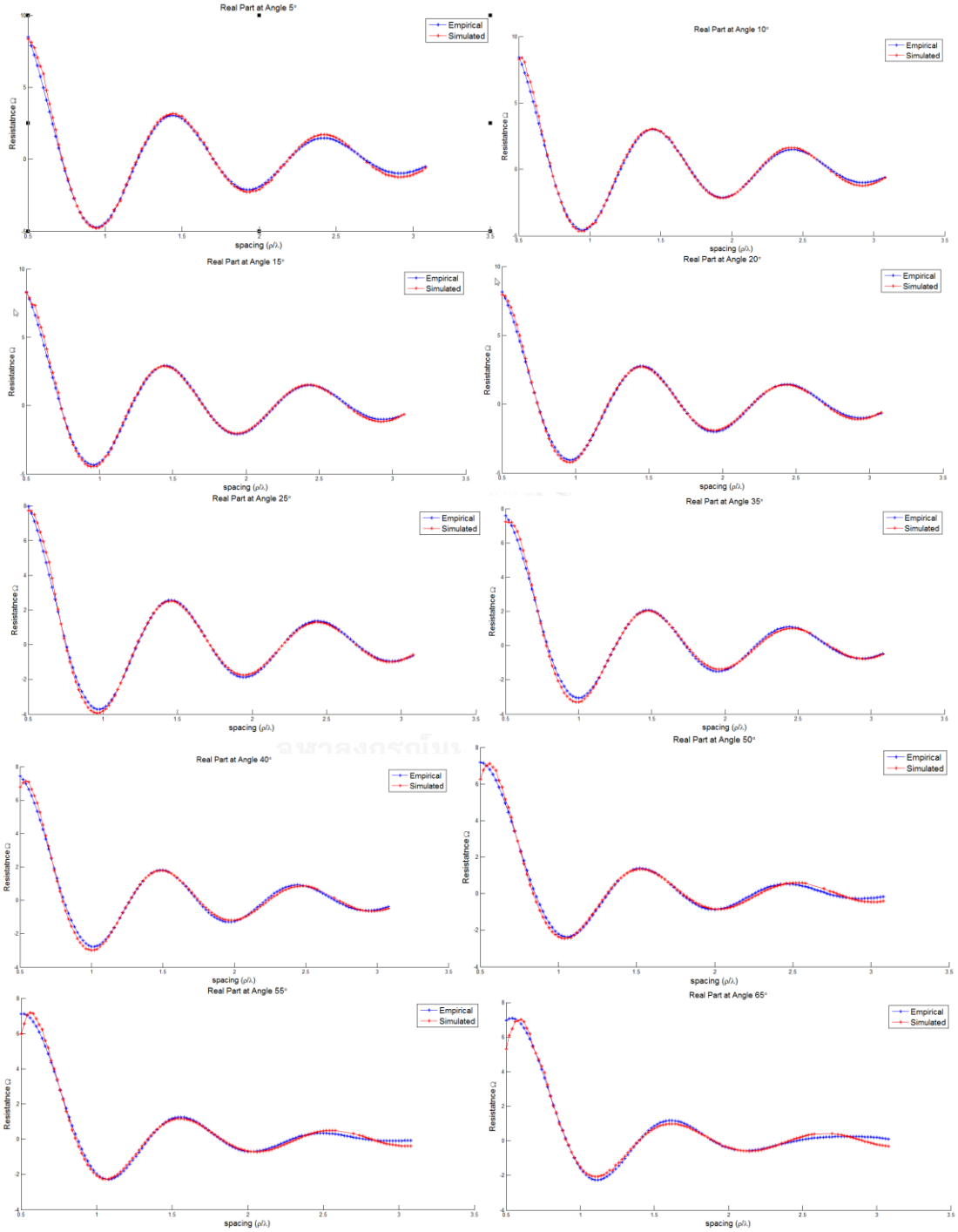

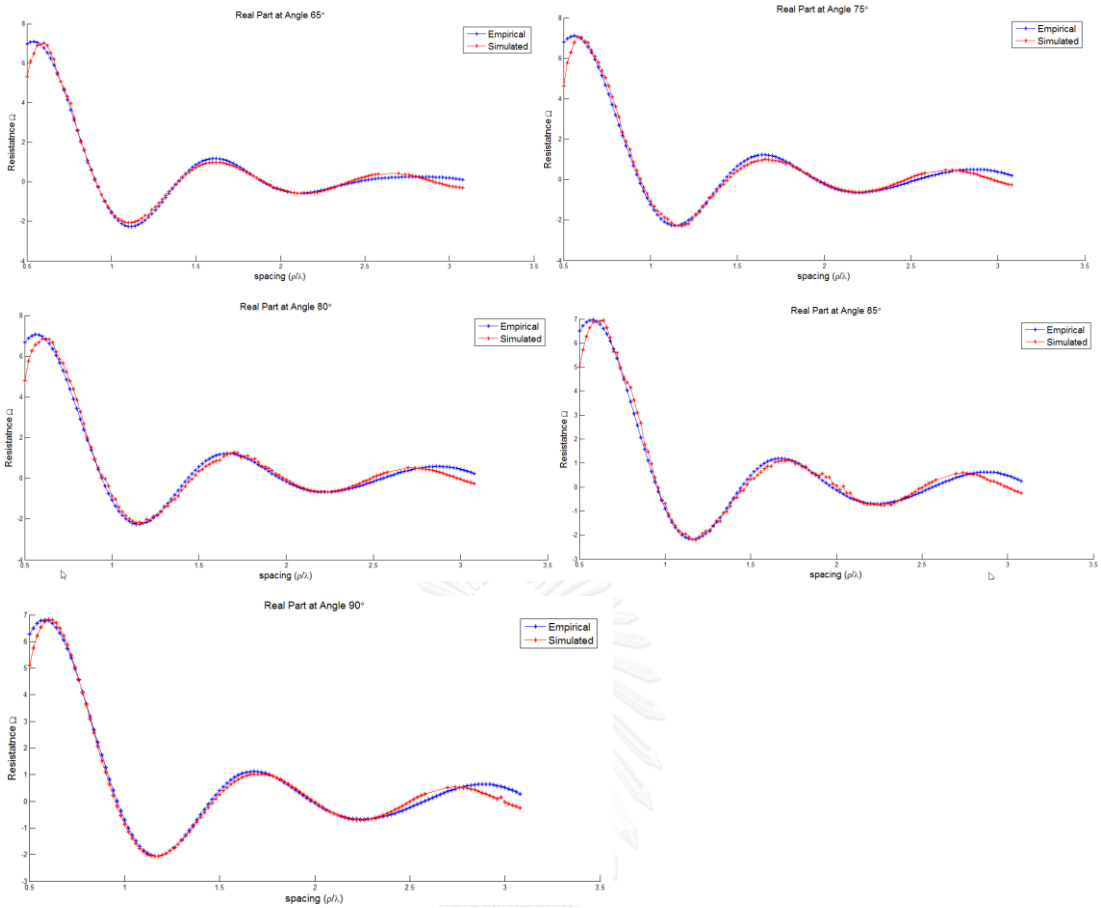

Extrapolation Comparison of mutual reactance

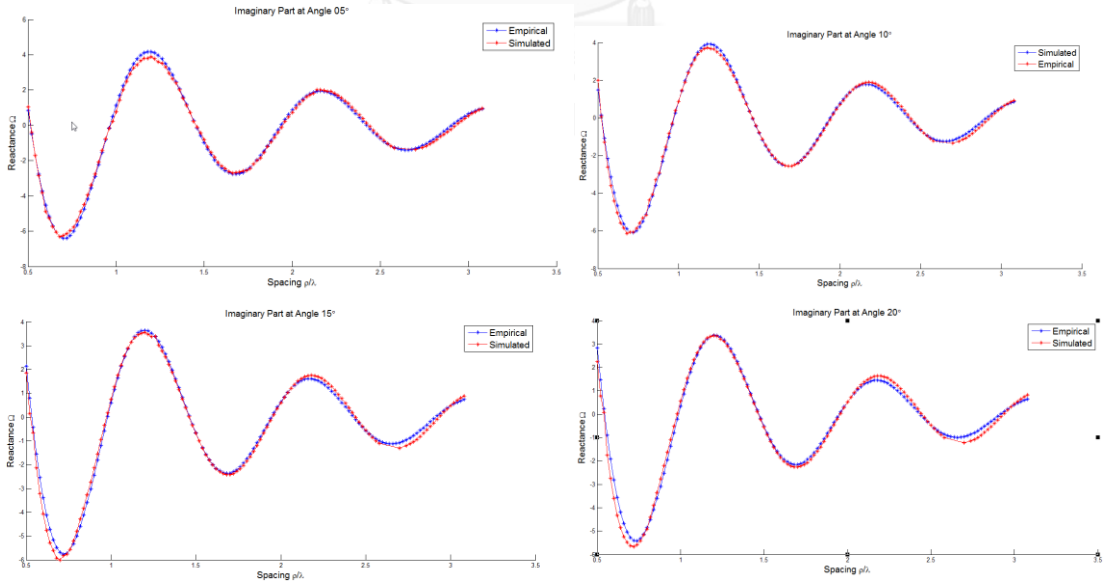

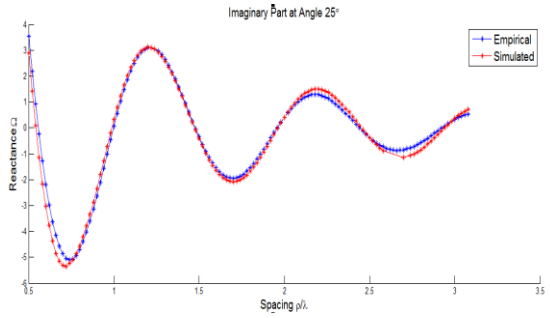
Imaginary Part at Angle 25°
Empirical
Simulated
Reactance Ω
Spacing ρ/λ

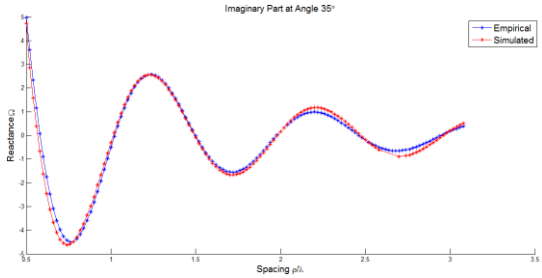
Imaginary Part at Angle 35°
Empirical
Simulated
Reactance Ω
Spacing ρ/λ

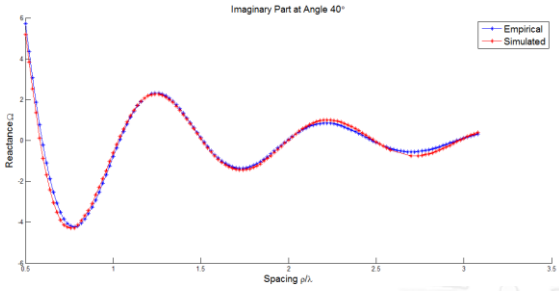
Imaginary Part at Angle 40°
Empirical
Simulated
Reactance Ω
Spacing ρ/λ

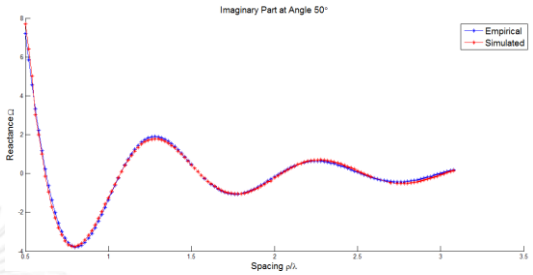
Imaginary Part at Angle 50°
Empirical
Simulated
Reactance Ω
Spacing ρ/λ

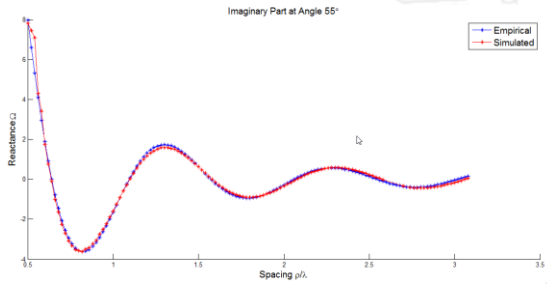
Imaginary Part at Angle 55°
Empirical
Simulated
Reactance Ω
Spacing ρ/λ

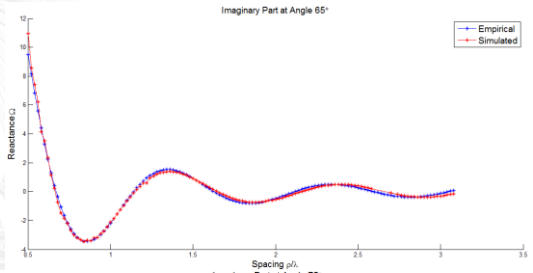
Imaginary Part at Angle 65°
Empirical
Simulated
Reactance Ω
Spacing ρ/λ

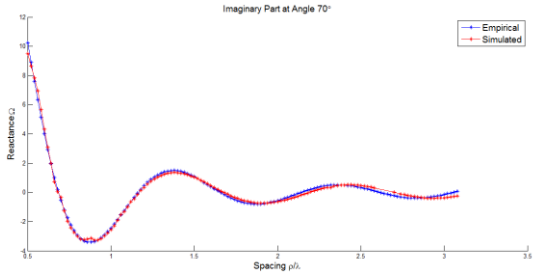
Imaginary Part at Angle 70°
Empirical
Simulated
Reactance Ω
Spacing ρ/λ

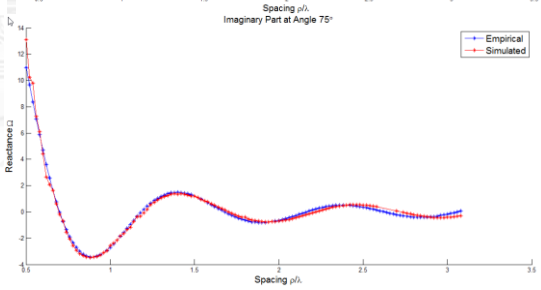
Imaginary Part at Angle 75°
Empirical
Simulated
Reactance Ω
Spacing ρ/λ

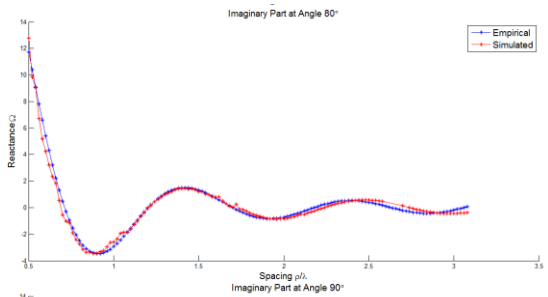
Imaginary Part at Angle 80°
Empirical
Simulated
Reactance Ω
Spacing ρ/λ

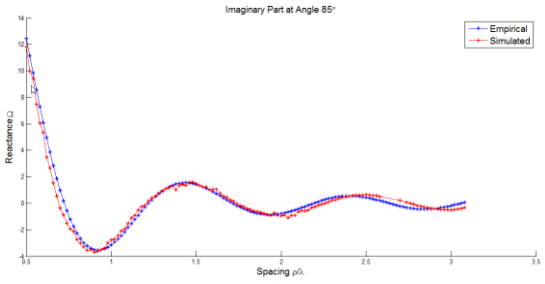
Imaginary Part at Angle 85°
Empirical
Simulated
Reactance Ω
Spacing ρ/λ

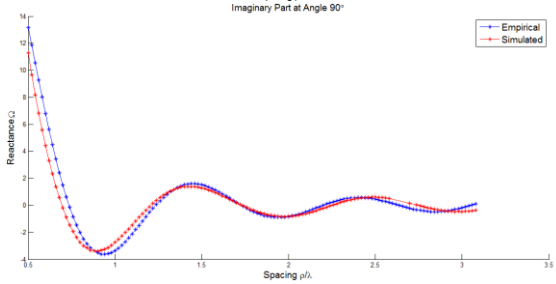
Imaginary Part at Angle 90°
Empirical
Simulated
Reactance Ω
Spacing ρ/λ

VITA

Mangseang Hor was born in Kratie Province, Cambodia in 1991. He received the Bachelor's Degree of Electrical Engineering from Institute of Technology of Cambodia in 2014. He has been granted a scholarship by Graduate School of Chulalongkorn University (ASEAN Scholarship) to pursue the master's Degree at Chulalongkorn University,Thailand since 2014. He has conducted his research with Microwave Communication, Telecommunication Research Laboratory at Department of Electrical Engineering, Faculty of Engineering, Chulalongkorn University. His main research interests in on array antennas and radar systems.